Distribution of phthalates in the indoor environment

– Application and evaluation of indoor air models –

Von der Fakultät für Lebenswissenschaften

der Technischen Universität Carolo-Wilhelmina

zu Braunschweig

zur Erlangung des Grads eines

Doktors der Naturwissenschaften

(Dr. rer. nat.)

genehmigte

D i s s e r t a t i o n

von Tobias Schripp

aus Braunschweig

1. Referent:	Professor Dr. Karl-Heinz Gericke
2. Referent:	Professor Dr. Tunga Salthammer
eingereicht am:	04.05.2009
mündliche Prüfung (Disputation) am:	03.07.2009

Druckjahr 2009

Vorveröffentlichungen der Dissertation

Teilergebnisse aus dieser Arbeit wurden mit Genehmigung der Fakultät für Lebenswissenschaften, vertreten durch den Mentor der Arbeit, in folgenden Beiträgen vorab veröffentlicht.

Tagungsbeiträge

Schripp T. and Salthammer T. (2007) Distribution of semi volatile organic compounds in the indoor environment. In: *Proceedings of the 17th Annual Conference of the International Society of Exposure Analysis (ISEA), Durham, NC*, Paper ID 27.

Schripp T., Salthammer T., Clausen P. A., Little J. C. (2008) Gas-particle partitioning of plasticizers in emission test chambers with minimized sink effect. In: *Proceedings of the 11th International Conference on Indoor Air Quality and Climate, Copenhagen*, Paper ID 76.

Schripp T., Fauck C., Meinlschmidt P., Wensing M., Moriske H. J.,Salthammer T. (2008) Relationship between indoor air particle pollution and the phenomenon of “Black Magic Dust” in housings. In: *Proceedings of the 11th International Conference on Indoor Air Quality and Climate, Copenhagen*, Paper ID 122.

Danksagung

Die vorliegende Arbeit entstand zwischen April 2006 und März 2009 am Fraunhofer Wilhelm-Klauditz Institut unter der Leitung von Prof. Dr. T. Salthammer, dem ich für die interessante Themenstellung und engagierte Betreuung danken möchte. Für die finanzielle Förderung des Projekts danke ich dem Verband PlasticsEurope und hier insbesondere Herrn Dr. R. Baunemann.

Für die Betreuung auf universitärer Seite danke ich Prof. Dr. K.-H. Gericke für seine Diskussionsbereitschaft und seine Ideen zur Bearbeitung der gegebenen Fragestellung.

Ich danke der Fa. Caparol für die Bereitstellung der dotierten Farben. Des Weiteren danke ich der Fa. Byk Additives & Instruments, insbesondere Herrn Dr. W. Pettau und Herrn M. Fischer, für die Herstellung der dotierten PVC-Materialien.

Ich danke allen Mitarbeitern des Fachbereichs Materialanalytik und Innenluftchemie für Unterstützung oder Hilfestellung bei der Durchführung dieser Arbeit. Besonders möchte ich Herrn C. Fauck danken für die umfangreiche Hilfe beim Aufbau und Durchführung der Experimente, die in diesem Umfang sonst nicht möglich gewesen wären.

Ich danke Frau M. Lignau vom Fraunhofer Wilhelm-Klauditz Institut für die Erstellung der technischen Zeichnungen.

Ich danke außerdem allen Mitarbeitern des Fachbereichs Air Quality Engineering im Departement of Civil and Environmental Engineering der VirginaTech University und hier insbesondere Prof. Dr. J.C. Little, Prof. Dr. L.C. Marr, Frau Y. Xu, und Frau A. Tiwari für die vielfältigen Diskussionen über die Modellierung von Innenraumemissionen und für die außergewöhnliche Gastfreundschaft während meines Aufenthalts.

Ein ganz besonderer Dank gilt Herrn Dr. E. Uhde für seine äußerst geduldige Beantwortung bzw. Diskussion fachlicher Fragen.
Ich danke meinen Freunden für die tatkräftige Unterstützung während der Erstellung dieser Arbeit und besonders Frau C. Odin für ihre Hilfe während der sprachlichen Überarbeitung des Manuskripts.

Abschließend möchte ich meinen Eltern für die moralische und finanzielle Unterstützung während meines Studiums danken.

Essentially, all models are wrong, but some are useful.

(George Edward Pelham Box, 1987)

Table of contents

List of abbreviations

AGD	Anogenital distance
AGI	Anogential index
amu	Atomic mass unit
ATSDR	Agency for Toxic Substances and Disease Registry
BBP	Butylbenzylphthalate
BET	Brunauer, Emmett, Teller-model
BL	Boundary layer
BLDC	Boundary layer diffusion controlled adsorption model
BMD	Black Magic Dust
BPA	Bisphenol A
CAS	Chemical Abstract Service
CERHR	Center for the Evaluation of Risks to Human Reproduction (EU)
CFD	Computational fluid dynamics
CIS	Cold injection system
CLIMPAQ	Chamber for Laboratory Investigations of Materials, Pollution, and Air Quality
CPC	Condensation particle counter
DBP	Di-n-butylphthalate
DEHP	Bis(2-ethyhexyl)phthalate
DEP	Diethylphthalate
DHHS	US-Departement of Health and Human Services
DiBP	Diisobutylphthalate
DIDP	Diisodecylphthalate
DINP	Diisononylphthalate
DIOP	Diisooctylphthalate
DKK	Large double climate chamber (Doppelklimakammer)
DMP	Dimethylphthalate
DnOP	Di-n-octylphthalate
EA	Equilibrium adsorption model
ECA	European Collaborative Action
EPA	Environmental Protection Agency (US)
ETS	Environmental Tobacco Smoke
FID	Flame ionisation detector
FLEC	Field and laboratory emission cell
FMPS	Fast mobility particle sizer
GC	Gas chromatography
HS	Headspace
hsPTR-MS	High-sensitivity proton transfer reaction mass spectrometer
IAQ	Indoor air quality
IARC	International Agency for Research on Cancer
LOQ	Limit of quantitation
m/z	Mass-to-charge ratio
MS	Mass spectrometry
n.d.	Not determined

NDIR	Non-dispersive infrared
NIEHS	National Institute of Environmental Health Science (US)
OSB	Oriented strand board
PAH	Polyaromatic hydrocarbons
PMMA	Polymethyl-methacrylate
ppm	Parts per million, 10^{-6}
ppt	Parts per trillion, 10^{-12}
PTFE	Polytetrafluoroethylene
PVC	Polyvinylchloride
SEV	Secondary electron multiplier
SMPS	Scanning mobility particle sizer
SPR	Structure property relationship
SVOC	Semi-volatile organic compound
TD	Thermal desorption
TDI	Total Daily Intake
TVOC	Total volatile organic compounds
VDI	Association of German Engineers (Verein Deutscher Ingenieure)
VOC	Volatile organic compound
WHO	World Health Organization
WKI	Fraunhofer Wilhelm-Klauditz-Institut

Symbols

A	Area [m^2]
A_A	Parameter of the Antoine equation [ ]
a_n	Solutions of a transcendent equation [ ]
a_{TSP}	Particle specific surface [$m^2\ g^{-1}$]
A_{pol}	Polymeric factor [ ]
B_A	Parameter of the Antoine equation [ ]
Bi_m	Biot-number [ ]
b_n	Solutions of a transcendent equation [ ]
C	Concentration in the material phase [$\mu g\ m^{-3}$]
c	Concentration
C_0	Concentration in the material phase at time t = 0 [$\mu g\ m^{-3}$]
C_A	Parameter of the Antoine equation [ ]
c_P	Concentration in the particle phase [$\mu g\ m^{-3}$]
C_S	Surface concentration (chamber or particle) [$\mu g\ m^{-3}$]
D_a	Diffusion coefficient in air [$m^2\ s^{-1}$]
D_m	Diffusion coefficient in the material [$m^2\ s^{-1}$]
$D_{m,\infty}$	Parameter of the Arrhenius equation [$m^2\ s^{-1}$]
E	Evaporation rate [$\mu g\ m^{-2}\ h^{-1}$]
$E(t)$	Time-dependent evaporation rate [$\mu g\ m^{-2}\ h^{-1}$]
E_A	Activation energy [$J\ mol^{-1}$]
Fo_m	Fourier-number [ ]
H	Parameter of a transcendent equation
h_m	Mass-transfer coefficient [$m\ s^{-1}$]
k	dimensionless constant in equation 2.49 [ ]
K	Distribution coefficient [ ]
K_{AW}	Air/water distribution coefficient [ ]
K_D	Adsorption coefficient of the linear isotherme [m]
K_F	Adsorption coefficient of the Freundlich isotherme [m]
k_H	Henry constant [$Pa\ m^3\ mol^{-1}$]
K_L	Adsorption coefficient of the Langmuir isotherme [$m^3\ \mu g^{-1}$]
K_{OA}	Octanol/air distribution coefficient [ ]
K_{OW}	Octanol/water distribution coefficient [ ]
K_P	Mass-specific adsorption coefficient gas/particle phase [$m^3\ \mu g^{-1}$]
$K_{P,S}$	Surface-specific adsorption coefficient (particle) [$m^3\ m^{-2}$]
K_S	Surface-specific adsorption coefficient gas phase/surface [ ]
l	Length of the sample [m]
L	Loading factor [$m^2\ m^{-3}$]
M	Molar mass [$g\ mol^{-1}$]
$m(t)$	Mass-transfer / emission rate [$\mu g\ m^{-2} h^{-1}$]
n	Air exchange rate [h^{-1}]
N	Number of segments [ ]
n_F	Parameter of the Freundlich adsorption isotherme [ ]

p	Vapor pressure [Pa]
P	Atmospheric pressure [Pa]
p_0	Equilibrium vapor pressure [Pa]
P_{95}	95th percentil
q	Loading of sorbent [µg m^{-2};µg g^{-1}]
Q	Air inflow [m^2 s^{-1}]
q_{max}	Maximum concentration in a sorbent [µg g^{-1}]
q_p	Sorbed compound on particle surface [µg compound µg $particle^{-1}$]
q_s	Sorbed compound on chamber/room surface [µg m^{-2}]
R	Universal gas constant (8.314472 Pa m^3 mol^{-1} K^{-1})
Re	Reynolds-number [ ]
Sc	Schmidt-number [ ]
SER_A	Area-specific emission rate [µg m^{-2} h^{-1}]
Sh	Sherwood-number [ ]
T	Temperature [K]
t	Time [h]
TSP	Mass-concentration of particles in air [µg m^{-3}]
u	Air velocity above sample [m s^{-1}]
u_n	Solutions of a transcendent equation [ ]
V	Volume [m^3]
x	Coordinate
y	Coordinate
y	Concentration in the gas phase [µg m^{-3}]
y^*	Saturation concentration in the gas phase [µg m^{-3}]
y_0	Concentration in the boundary layer [µg m^{-3}]
y_∞	Equilibrium gas phase concentration [µg m^{-3}]
y_{in}	Inflow concentration [µg m^{-3}]
z	Coordinate
α	Dimensionless air exchange rate [ ]
β	Dimensionless loading [ ]
δy	Distance between two grids (CFD) [m]
η	Dynamic viscosity [Pa s]
v	Kinematic viscosity [m^2 s^{-1}]
ρ	Density [g cm^{-3}]
τ	Time [h]
[ ]	dimensionless

1. Introduction

1.1 Semi-volatile organic compounds in the indoor environment

The improved insulation of modern work buildings and dwellings with the objective of higher energy efficiency has drawn public interest on the topic of good indoor air quality (IAQ). Due to increased energy costs (e.g. during the oil crisis in 1973 and 1979/80) building materials were improved to reduce energy loss from the indoor environment. This action was accompanied by the reduction of the air exchange with the outdoor environment and led to a worsening of the indoor air hygiene. Humidity, inorganic gases (e.g. CO_2), and organic indoor pollutants accumulate in case of low air exchange rate and can reach significantly higher concentrations compared to outdoor air. To prevent the exposure against these effects various approaches were followed. The loss of energy was reduced by using heat exchangers that warm up incoming air and, therefore, increase the air exchange. A popular way is also the application of materials for adsorption or degradation of organic indoor air pollutants (e.g. lamb's wool against formaldehyde, cyclodextrine derivates against odors, photocatalytic paint against a variety of volatile organic compounds (VOC)). Considering compounds with low vapor pressure neither the increase in air exchange rate nor the usage of adsorption materials is a practicable lowering approach. In this case the reduction of the source strength is the only effective way.

In view of the total exposure to organic and inorganic air pollutants the indoor air pathway is very important. Compared to the outdoor air concentration the corresponding values indoors can be severely higher. Additionally, the mean length of stay indoors for a person in western industrial nations often exceeds 90 % of the day (Brasche and Bischof, 2005). For semi-volatile organic compounds (SVOC) the air concentrations are typically very low even at high loading factors and low air exchange rate due to its small vapor pressure. At high material concentrations (e.g. plasticizers in flooring materials) the loss of SVOC from the room over time is much less than compared to VOC. This leads to a lower but continuous exposure of a person working or living in this environment. Regarding the exposure against SVOC it is important to consider that the air is not the only pathway of incorporation. Matrices with high percentage of fat or organic carbon can be a sink for aromatic compounds from air. Therefore, polymer packaging materials that contain several

additives can be an important source of exposure. SVOC also attach to sinks with large surfaces like dust. Dust is a mobile sink and can be resuspended due to foot motion and can be inhaled or ingested. Finally, the direct exposure against SVOC due to environmental tobacco smoke (ETS) which often contains high amounts of polycylic aromatic hydrocarbons (PAH) might also be of importance.

Despite these sources the indoor air has a central relevancy for exposure pathways because it is the matrix “in-between”. If direct contact between source and sink (e.g. for packaging materials) is not the case the pollutant transfer happens via the gas phase. In the first case the occurrence is called “migration” and for the second case “emission”. If the transfer happens via the gas phase the measurement of this matrix can provide information about the contamination of the other matrices of the room. In the case of migration this is not possible. Regarding the monitoring of SVOC in indoor air several problems occur. Due to the low vapor pressure the expected concentrations are very low and need a long accumulation on a suitable sorbent. Many SVOC (e.g. plasticizers) are ubiquitous in the environment and might contaminate the analysis. To determine the emission rate of the target material it is also necessary to know air exchange rate, temperature, relative humidity, and the sink behavior of the tested environment. In the real indoor situation temperature changes over the day occur and this affects the emission rate of the material. The precise measurement of the indoor concentration is, therefore, impossible to measure in the case of a non-constant emission rate. This complicates a reliable toxicological exposure analysis. By performing an emission chamber test of the target material the problem of changing environmental conditions can be solved but this result cannot be transferred to a real environment because the sink behavior of the room is, typically, unknown.

These findings led to two possible approaches to get an exposure assessment. On the one hand, the measurement of the adsorbed compounds in the sinks might provide information about the contamination of the other matrices. Several studies showed that the connectivity between air concentration and dust concentration is not given in any case (e.g. Butte and Heinzow (2002)). A weak correlation between dust contamination and air concentration was reported by Weschler et al. (2008) for a collective of German homes. However, the contamination of dust is not limited on the air pathway but may also occur via other sources (e.g. cleaning agents) as was

shown by Kolarik et al. (2008a; 2008b). Therefore, a strict relation cannot be assumed in every case.

The determination of the material/air partitioning parameters and the initial concentration in the material are sufficient for the mathematical modeling of the emission rate (Little, et al., 1994; Xu and Little, 2006). However, the transfer of modeling results under idealized conditions into the real indoor environment contains several unknown aspects and the validation of such models is currently unfinished. The main problem of the modeling approach is the necessary simplification of the problem to solve the governing equation. Also, for the indoor environment several important parameters (like the external mass transfer coefficient and the sink parameters) are very difficult to determine and are usually assessed from correlation equations.

Beside these disadvantages, mathematical modeling is a very useful tool to estimate interactions of the target compound with other matrices. Especially small particles that stay suspended in the air for long time are important when assessing fate and behavior of SVOC in the indoor environment. By determining the particle characteristics the influence on the emission from materials can be quantified by usage of the mentioned models. The precision of predications from these physically based models might vary from case to case but they are useful to validate the results from an analysis.

1.2 Modeling fate and behavior of organic compounds

Mathematical modeling of indoor pollutant distribution requires a precise characterization of sources and sinks of the target compound. The diffusion of a compound in polymers like a polyvinylchloride (PVC) floor covering can be measured with moderate effort e.g. using a microbalance. Multilayer or inhomogeneous materials like oriented strand board (OSB) or coated materials are much more complicated. The diffusion in the material has to be determined via regression of measured concentrations with the appropriate model.

The mathematical description of an interphase transfer requires knowledge about the partition coefficients between the phases. The coefficients for the partition of n-octanol into water and air respectively are experimentally determined for many compounds. These parameters allow the rough calculation of material/gas phase

partitioning if this parameter cannot be measured directly. Beside the phase transfer the movement of the compound inside the material by diffusion has to be described to determine the diffusion blocking of the emission. Most models use approaches in which the diffusion can be described by fickian diffusion equations. The solution of this differential equation using several side parameters is based on the solutions described by Crank (1975). Migration models for the description of polymer additives into food from plastic packaging especially focus on the diffusion in the material. In these models no phase change occurs and the sink is very strong. Therefore, the change-over of the compound between the two materials is mostly governed by diffusion. In the case of emission the time-depending step is not the diffusion but the transfer from the material surface into the well-mixed air. This transfer is characterized by the external mass transfer coefficient. This is the main difference between these two modeling types.

The description of diffusion in multilayer materials is used for some migration models. Here, the transfer of a polymer additive from a plastic cup into the contained matrix can be calculated even if several cups are stacked together. Migration models were also used for cases in which direct dermal contact to the material occurs. In 2003 the Federal Institute for Risk Assessment in Germany applied a migration model to determine the amount of incorporated di-n-octylphthalate (DnOP) when earplugs made of soft rubber are used. The model allowed the conclusion that the exposure lays below the tolerable daily intake after a daily 8 h use (Bundesinstitut für Risikobewertung, 2003).

It is expected that the usage of modeling tools will increase in the future because of their lower costs. Actually, the migration of the residual monomer bisphenol A (BPA) from flasks made of polycarbonate is an important topic. This results from the usage of these flasks for small children and babies. In 2007 the Federal Institute for Risk Assessment stated that no health risks for toddlers exist due to the usage of polycarbonate bottles. Actual studies from the United States disagree with these findings (Le, et al., 2008) and are therefore under serious discussion (e.g. Austen (2008)). Migration models for the calculation of possible “worst-case” situations to ensure safe food packaging are expected in this case. Due to the fast and reliable assessment of possible food exposure via migration modeling this tool is used as

registration requirement for food packaging by the European Union (Official Journal of the European Communities, 2002).

To ensure the practicability of mathematical models they have to be calibrated and validated using a high amount of real measurement data. For the available food migration models this is the case (Hinrichs and Piringer, 2002). Regarding the indoor emission models the validation is mostly done by using emission test chamber data. The extension of the model from homogenous polymer materials to inhomogeneous and porous materials is also an unsolved problem. Regarding the sink effect in a real room the general description of dust characteristics is impossible due to the different chemical compositions between several households. Dust consists of inorganic (minerals) and organic (fungus spores, abrasion from skin, etc.) fractions. Additionally, dust shows various particle sizes and contains agglomerates in which smaller particles are attached together in fractal structures. The broad chemical nature and surface area hinders the modeling of that sink. Overall, models are only usable for a statistical analysis for a broad variety of indoor environments and not feasible for the individual case.

1.3 Objectives

This work summarizes the actual available emission modeling approaches and uses the most variable model to describe the findings in several chamber experiments using the target compounds di-butylphthalate (DBP) and di(2-ethylhexyl)phthalate (DEHP). By successive reduction of the experimental complexity from a simulated indoor environment using wall paint as a source to an emission chamber test of liquid plasticizers the applicability and limits of the used model are observed. The data is used to identify the impact of the governing parameters of the emission models on the predicted air concentrations by residual analysis. On the basis of the experimental results a sink-minimized chamber is developed that allows a faster determination of the distribution of phthalates between air and particle phase. In the same chamber the impact of airborne particles on the emission rate of a phthalate-containing surface is measured. In addition to the interaction between phthalates and airborne particles the distribution between DEHP/DBP and settled dust is determined.

The lead substances of this work are DBP and DEHP due to their high difference in vapor pressure and the feasibility of TD/GC/MS for the measurement of the air concentrations. In the list of phthalic acid esters DBP represents a volatile type of plasticizers because it reaches maximum air concentrations of ~ 160 µg m^{-3}. DEHP is a ubiquitous compound in the environment that reaches maximum air concentrations 100 times lower than DBP. Plasticizers with lower or similar vapor pressures than DEHP are currently of vast industrial interest (e.g. DINP, DIDP) but they are not suitable for modeling evaluation because the reliable measurement of air concentrations of these compounds is of much higher effort than for DEHP. However, the production and application of DEHP was of large amounts in the past years and, thus, will remain of interest for indoor science for the next decade.

2. Basic principles

2.1 Application of semi-volatile organic compounds

Compounds with a boiling point between 240°C and 400°C are categorized as semi-volatile organic compounds (SVOC) according to the World Health Organization (WHO, 1989). This high boiling point is associated with a low vapor pressure and a low Henry constant respectively. The reduced removal from the source due to the low volatility is used to ensure a constant long-term property of a material (e.g. plasticizers in polymers). Another typical example is the application of pesticides in agriculture. After application of a crop protection product a long contact time between plant and compound is anticipated to ensure an enduring protection. SVOC easily attach to soil and dust and are mostly transported in this bound form. Even pesticides can be transported into the indoor environment by this way if they are applied in the surroundings of residential buildings (Butte, et al., 2006). The low air exchange rate and the high amount of possible sinks promote the slow removal of SVOC from indoors. Regarding possible sources, large area materials like floor and wall coverings are very important. Especially plasticizers can be found in high concentrations in materials made of PVC or other polymers. In case of electric appliances like television and computers flame retardants are used for security purpose. Both classes of compounds are typically not bound to the polymer chain and may diffuse to the surface and emit into the air. Most plasticizers are esters of organic acids like phthalic acid, adipic acid, sebacic acid, phosphoric acid, and citric acid. In this listing the phthalates are the compounds with the biggest market share due to their low price.

2.1.1 Physicochemical data of phthalate esters

The applicability of phthalate esters in polymers bases on the slow loss of substance over time due to the low vapor pressure and small diffusion coefficients. The vapor pressure of a compound is of high importance if the mobility of the compound is estimated because it determines the maximum gas phase concentration in air. A high precision is necessary when determining the vapor pressure experimentally. Not only the experimental setup has to provide a high accuracy but also the sample has to be cleaned up thoroughly. Some phthalates are ubiquitous in the environment (e.g. DEHP) which complicates the cleanup of a singular phthalate. From this reason the

experimental results of vapor pressure measurements that were published over the past 50 years show a vast spread for the same compound. This spread increases with decreasing vapor pressure. A summary of various physicochemical data of some phthalates are shown in Table 1. For the analysis of the distribution of compounds in a multi-phase system the distribution coefficients between air and water phase k_{AW}, as well as the distribution coefficients between air/water and n-octanol k_{OW}/k_{OA} are used. The octanol phase represents a strong lipophilic matrix. These parameters are usually easy to determine experimentally and characterize the phase-transfer behavior of the compound. Another parameter that contains information about the transfer between gas-phase and condensed phase is the henry constant (k_H). It is derived from the fact that the vapor pressure of a soluted compound is linear depended on the substance amount fraction in the solution.

$$k_H = \frac{p}{c_{aq}} \tag{2.1}$$

Therefore, this parameter characterizes the volatility of the compound. It is defined as the ratio of the partial pressure of the compound and the concentration of the compound in a water solution (2.1).

Table 1: Physicochemical data of several phthalates from different publications

Phthalate	Abrev.	CAS	Formula	M [g mol^{-1}l]	Bp. [℃]	p** [Torr] (25℃)	ρ [g mL^{-1}]	log K_{OW}	log K_{OA}	log K_{AW}	k_H [Pa m^3 mol^{-1}] (25℃)
Di(2-ethylhexyl)-phthalat	DEHP	117-81-7	$C_{24}H_{38}O_4$	390.6	370	see	0.985 (25℃) [1]	7.73 [2]	10.53 [2]	-2.8 [2]	3.95 [2]
					384	Tab. 4		7.6 [4]			0.027 [4]
Di-n-butyl-phthalat	DnBP	84-74-2	$C_{16}H_{22}O_4$	278.4	340	see	1.043 (25℃) [1]	4.27 [2]	8.54 [2]	-4.27 [2]	0.133 [2]
					340	Tab. 4		4.5 [4]			0.18 [4]
Di-iso-butyl-phthalat	DIBP	84-69-5	$C_{16}H_{22}O_4$	278.4	296	$6.65 \cdot 10^{-3}$ [4]	1.037–1.041	4.27 [2]	8.54 [2]	-4.27 [2]	0.133 [2]
					296	$4.720 \cdot 10^{-5}$ [5]	(20℃)	4.11 [4]			0.12 [4]
Di-pentyl-phthalat	DPP	131-18-0	$C_{18}H_{26}O_4$	306	342	$9.6 \cdot 10^{-6}$ [2]	-	3.4 [2]	8.04 [2]	-4.64 [2]	0.0569 [2]
						$1.96 \cdot 10^{-4}$ [4]		5.62 [4]			0.090 [4]
Di-iso-nonyl-phthalat	DINP	28553-12-0	$C_{26}H_{46}O_4$	418.6	-	$5.4 \cdot 10^{-7}$ [4]	-	8.6 [2]	11.03 [2]	-2.43 [2]	9.26 [2]
						$5.1 \cdot 10^{-8}$ [6]		9.37			0.15 [4]
Di-iso-decyl-phthalat	DIDP	26761-40-0	$C_{28}H_{46}O_4$	446.7	250*	$5.28 \cdot 10^{-7}$ [4]	-	9.46 [2]	11.52 [2]	-2.06 [2]	21.6 [2]
						$1.35 \cdot 10^{-8}$ [6]		10.36 [4]			0.11 [4]
Benzyl-butyl-phthalat	BBP	85-68-7	$C_{19}H_{20}O_4$	312.36	370	$8.25 \cdot 10^{-6}$ [4]	1.100 (25℃) [1]	4.7 [2]	8.78 [2]	-4.08 [2]	0.205 [2]
								4.73 [4]			0.12 [4]
Dimethylphthalat	DMP	131-11-3	$C_{10}H_{10}O_4$	194.2	283	$3.08 \cdot 10^{-3}$ [4]	1.190 (25℃) [1]	1.61 [2]	7.01 [2]	-5.4 [2]	0.00978 [2]
					284	$2.250 \cdot 10^{-3}$ [7]		1.6 [4]			0.003 [3]
Diethylphthalat	DEP	84-66-2	$C_{12}H_{[2]}O_4$	222.2	297	$2.10 \cdot 10^{-3}$ [4]	1.120 (25℃) [1]	2.54 [2]	7.55 [2]	-5.01 [2]	0.0244 [2]
					295	$7.425 \cdot 10^{-4}$ [8]		2.42 [4]			0.0012 [3]
Di-n-octylphthalat	DnOP	117-84-0	$C_{24}H_{38}O_4$	390.6	286	$1.00 \cdot 10^{-7}$ [4]	0.950 (25℃) [4]	7.73 [2]	10.53 [2]	-2.8 [2]	3.95 [2]
						$1.00 \cdot 10^{-7}$ [9]		8.1 [4]			0.26 [4]
Dihexylphthalat	DHP	84-75-3	$C_{20}H_{30}O_4$	334.4	210	$1.40 \cdot 10^{-5}$ [4]	1.002 (25℃) [4]	6 [2]	9.53 [2]	-3.53 [2]	0.726 [2]
						$1.40 \cdot 10^{-5}$ [11]		6.82 [4]			2.60 [4]
Diisohepthylphthalat	DIHP	7188-89-6	$C_{22}H_{34}O_4$	363	-	$6.99 \cdot 10^{-7}$ [2]		6.87 [2]	10.04 [2]	-3.17 [2]	1.69 [2]
Diundecylphthalat	DUP	3648-20-2	$C_{30}H_{50}O_4$	447.7	523	$1.22 \cdot 10^{-9}$ [4]	0.955 (20℃) [10]	10.33 [2]	12.02 [2]	-1.69 [2]	50.5 [2]
						$8.40 \cdot 10^{-19}$ [10]		11.49 [4]			5.67 [4]
Ditridecylphthalat	DTDP	119-06-2	$C_{34}H_{58}O_4$	530.8	-	$2.51 \cdot 10^{-11}$ [4]	-	12.06 [2]	13.01 [2]	-0.095 [2]	275.0 [2]
								13.45 [4]			22.59 [4]

*4 Torr ; ** 1 Torr = 101325/760 Pa ≈ 133.322 Pa

[1] (Sigma-Aldrich, 2007); [2] (Cousins and Mackay, 2000); [3] (Sander, 1999); [4] (National Libary of Medicine ChemIDplus Advanced, 1981); [5] (BASF, 2007); [6] (Cousins, et al., 2002); [7] (Rohac, et al., 1999); [8] (Rohac, et al., 2004); [9] (Teil, et al., 2006); [10] (BASF, 2005); [11] (Howard, et al., 1985).

The spread of vapor pressure measurements for DBP and DEHP from several publications is listed in Table 2.

Table 2: Vapor pressure of DBP and DEHP from several publications [Torr]

Reference	DEHP	DBP
(Werner, 1952)	$2.80 \cdot 10^{-7}$	$1.90 \cdot 10^{-5}$
(Quackenbos jr, 1954)	$3.30 \cdot 10^{-7}$	$3.60 \cdot 10^{-5}$
(Frissel, 1955)	-	$3.50 \cdot 10^{-5}$
(National Libary of Medicine ChemIDplus Advanced, 1981)	$1.42 \cdot 10^{-7}$	$2.01 \cdot 10^{-5}$
(OECD, 1981)[1]	$9.83 \cdot 10^{-8}$	-
(Glückel, et al., 1982)	-	$2.08 \cdot 10^{-5}$
(Dobbs and Cull, 1982)	$4.10 \cdot 10^{-6}$	-
(Harnisch, et al., 1983)	-	$4.10 \cdot 10^{-5}$
(Dobbs, et al., 1984)	$7.10 \cdot 10^{-7}$	$1.70 \cdot 10^{-5}$
(Howard, et al., 1985)	$6.40 \cdot 10^{-6}$	$7.30 \cdot 10^{-5}$
(Hinckley, et al., 1990)	$1.43 \cdot 10^{-7}$	$4.20 \cdot 10^{-5}$
(Hüls AG, 1997)[1]	$2.55 \cdot 10^{-7}$	-
(Cousins and Mackay, 2000)	$1.89 \cdot 10^{-7}$	$3.55 \cdot 10^{-5}$
(Clausen, et al., 2002)	$1.43 \cdot 10^{-7}$	-
(Afshari, et al., 2004)	$1.40 \cdot 10^{-6}$	-
(EPIWIN, 2006)[2]	$1.52 \cdot 10^{-7}$	-
(BASF, 2007)	-	$1.120 \cdot 10^{-5}$
(Staples, et al., 1997)	$1.33 \cdot 10^{-7}$	$2.70 \cdot 10^{-5}$

In 1997 Staples et al. published vapor pressures for DEHP and DBP which were used as reference values for a long time. Some years later Cousins and Mackay (2000) published vapor pressures which were calculated by QSPR (quantitative structure property relationship) methods. The results were adopted by the Handbook of Environmental Chemistry. However, these values have a big disadvantage regarding isomeric compounds. According to this model the substance di(2-ethylhexyl)phthalate should feature the same vapor pressure as di-iso-octylphthalate or di-n-octylphthalate though this is not the case. A comparison of experimental techniques to determine the vapor pressure was carried out by Růžička et al. (2004)

[1] Taken from Staples et al. (1997).
[2] EPIWIN is availabe via http://www.syrres.com/ .

using DEP as target compound. The basis of valuation for the different techniques was the match of the measured value with the predicted vapor pressure by the Antoine equation (2.2).

$$\log_{10} p = A_A - \frac{B_A}{C_A + T} \quad (2.2)$$

The compound specific parameters A_A, B_A, and C_A were determined at higher temperatures and were used to calculate the vapor pressure at room temperature. Růžička et al. (2004) were able to show that the experimental determination of the vapor pressure of DEP below temperatures of 60°C can only be achieved by the Knudsen effusion method (Cammenga, 1967; Knudsen, 1909). The congruence between the measured values and the results of Staples et al. (1997) and Cousins and Mackay (2000) is limited due to deviations around 35 %.

It was mentioned before that the purity of the sample is of high importance for a reliable measurement of the vapor pressure. A related problem is the explicit characterization of the sample. This could be observed from the European Union Risk Assessment Report for DINP (European Commission, 2003) that reported three considerably different vapor pressures for DINP. These findings are explained by the fact that DINP is not a singular compound but a mixture of several phthalates which changes with the particular manufacturing method. Three main DINP exist: DINP 1 (CAS 68515-48-0), DINP 2 (CAS 28553-12-0) are produced using n-buten while DINP 3 (CAS 28553-12-0[3]) bases on n- and iso-buten.

The uncertainty of published results is not limited to the vapor pressure but can also be found for the solubility, the octanol-water-partition coefficient (K_{OW}), the octanol-air-partition coefficient (K_{OA}), and the Henry constant (k_H). In the review by Cousins et al. (2002) the authors describe strong deviations e.g. between several measured values of solubility of DOP ranging between 0.4 and 3000 µg L^{-1}. The deviations are explained by the authors by different measuring techniques.

Regarding the whole literature about the physicochemical properties of phthalates the available values are associated with a high uncertainty which extensively complicates the modeling of these compounds. Especially, if the modeled results are used for an exposure analysis small deviations in the governing parameters (like the

[3] The CAS numbers for DINP2 and DINP3 are the same although the manufacturing process is not the same. Therefore, different physicochemical data due to deviations in possible contaminants and changes in compound mixture are expected.

vapor pressure) have significant influence on the conclusions. Together with the expected variation in sink properties indoors (e.g. organic carbon content of dust) this uncertainty limits the usage of models to a rough estimation.

2.1.2 Toxicology of phthalate esters

The esters of the phthalic acid (benzene-1,2-dicarboxylic acid) are widely used as plasticizers because they have a high stability against chemicals, light, and heat. They are colorless and non-odorous compounds, available in high amounts, and feature a low price. A very important compound of this class is di(2-ethylhexyl)phthalate (DEHP) which had a production volume of 460 000 t in 1999 (42 % of the total plasticizers production) (Lorz, et al., 2002). In 1995 the International Agency for Research on Cancer (IARC) classified DEHP as possible carcinogen for humans. Before, some studies had shown that DEHP had a teratogenic effect on animals (Ritter, et al., 1987). By this reason, the European Commission adopted the evaluation of the IARC and classified DEHP as a category 2 compound (possible carcinogenic). In the United States the Department of Health and Human Service (DHHS) and the Environmental Protection Agency (EPA) came to the same conclusions (ATSDR, 2002; EPA, 1993). Therefore, the market share of DEHP decreased from 42 % to 24 % (244 000 t) in 2003. However, during the last decades large amounts of DEHP had been produced and were applied in many products. Due to the wide spread usage and the slow release of the compound from the product into the indoor environment DEHP is currently still important and will presumably remain for several years. Nowadays, other phthalates like diisononylphthalate (DINP) and diisodecylphthalate (DIDP) are market leaders. These substances show similar desired effects but are assessed as no possible health hazard by the European Commission.

Despite its carcinogenic effect the impact of DEHP on the health of unborn or young children is of very high interest. The reproduction toxicity of DEHP is still under research but several studies proved a deranged hormonal development of children that were exposed to DEHP during pregnancy (Latini, et al., 2006; Swan, et al., 2005). The indicator for these studies was the decrease in anogenital distance (AGD) of children exposed to DEHP. The methodology of these studies is not without controversy because the NIEHS and the European CERHR were not able validate the reported effects. However, in 1999 the European Union decided to ban six

common phthalates (DINP, DEHP, DNOP, DIDP, BBP, and DBP) with higher mass-concentrations than 1 % from toys to reduce children's exposure (Guideline 76/768/EWG, Decision 1999/815/EG).

The incorporation pathways are not limited to inhalation but also include ingestion (food, dust) and absorption by skin. For the latter one, modeling studies predict that the contribution of skin permeation on the total exposure is higher than the inhalation pathway (Little, et al., 2008). These predictions are currently not validated. However, results of exposure studies prove that the most important source for plasticizers is not inhalation/permeation but the ingested food (Clark, et al., 2003a). Only toddlers might be an exception because the amount of ingested contaminated dust is higher compared to other age groups. A strong short-term exposure against plasticizers is possible in case of drug usage (Hauser, et al., 2004). Therefore, the oral pathway is still very important in the exposure assessment for phthalates. The fact that the exposure against phthalate contaminated air is not exclusively decisive for the incorporated amount was shown by Adibi et al. (2003). The authors of this study measured the air concentration of DEP, DBP, BBzP, and DEHP in the apartments of 30 women (age 20 to 40) in New York and Krakau and the associated primary metabolites in the urine of the inhabitants. For the first three compounds a link could be detected but the correlation was insufficient for DEHP. This illustrates that women of child-bearing age are marginally affected by DEHP in the gas phase. A similar approach regarding the dust concentration was performed by Becker et al. (2004) who measured the concentrations of DEHP in dust and the primary (MEHP) and secondary (5OH-MEHP, 5oxo-MEHP) metabolites in the urine of kids in the age between 3 and 14. Statistical analysis showed no correlation between dust contamination and metabolite concentration. The analysis was complicated by the fact that the metabolism of DEHP is different for young and older children due to adolescence.

To provide a rapid exposure assessment it would be useful if the concentrations of dust and gas phase were linked for the observed compounds. The transfer of phthalates from the source to the sink is done via the gas phase. Therefore, both concentrations should show correlations. In a study conducted by Weschler et al. (2008) a weak linear correlation between gas phase concentration and dust concentration of several phthalates could be found. To find these correlations the

authors analyzed a large amount of measurement data and fitted the dust and gas phase concentration. The main conclusion of their findings was a validation of the theoretical connection between the concentrations in a large sample collective but the authors state clearly that this cannot be transferred to a singular case. This consequence from the broad spread of the data which allows no significant calculation of an air phase concentration solely basing on a dust measurement. This result is supported by comparable publications (Butte and Heinzow, 2002; Butte, et al., 2008; Butte and Walker, 1994).

The different exposure pathways for the plasticizers DMP, DEP, DiBP, DnBP, BBzP, DEHP, DINP, and DIDP were summarized by Wormuth et al. (2006). The authors compared oral exposure (food and dust) with dermal and inhalative uptake using an exposure model and measurement data from 2003 to 2005. Regarding different ages the results showed high fluctuations. The modeled values proved good correlations for adults but for small children the expected uptake was lower than the measured values. These findings result from the fact that the model did not include the more intensive contact of children with settled dust (e.g. due to crawling on the floor). Also drug usage was not included in the model. The results of the study follow the finding of Clark et al. (2003b) regarding the different sources. His findings are summarized in Table 3 for DBP and DEHP.

Table 3: Percentage of different pathways to the total daily exposure (data from Clark et al. (2003b))

% of total-TDI	Adult (20-70 a)		Teenager (12-19 a)		Child (5-11 a)		Toddler (0.5-4 a)	
	DBP	DEHP	DBP	DEHP	DBP	DEHP	DBP	DEHP
Outdoor Air	0.01	0.01	0.01	0.01	0.01	0.01	0.01	0.01
Indoor Air	3.15	0.44	3.35	0.43	4.13	0.48	3.64	0.38
Water	0.09	0.07	0.13	0.08	0.18	0.10	0.16	0.09
Ingested Soil	0.002	0.0003	0.002	0.0003	0.002	0.0004	0.003	0.0005
Ingested Dust	0.54	4.41	0.57	4.24	0.75	5.04	1.06	6.51
Food	96.2	95.1	96.0	95.2	95.0	94.3	95.1	93.0
TDI [µg d^{-1} kg^{-1}]	5.96	8.46	6.64	10.40	11.21	19.45	14.21	27.13

For every age group the exposure is higher in the case of DEHP although the gas phase concentration is much higher for DBP. This results from the fact that DEHP accumulates in the dust and is incorporated in high amounts even if the ingested mass of dust is low. With decreasing age the impact of DBP in air is of more

importance because the breath frequency is higher for children compared to adults. Anyhow, Table 3 illustrates that toddlers are much stronger exposed against plasticizers than adults.

Within recent years the exposure against plasticizers had been connected to chronic diseases like asthma and dermatitis. In 2004 an extensive correlation study with 10852 children was conducted by Bornehag et al. (2004). 198 children of this collective showed allergic symptoms. The analysis of the household dust of the corresponding homes revealed a statistical correlation between elevated concentrations of BBzP and DEHP in dust and asthma, coryza, and eczema. The latter two diseases were connected to high concentrations of BBzP while asthma was linked to DEHP. The described study was carried out in Sweden. Therefore, the authors suspect that the transfer of results from the presented study to countries with other social economic conditions or differing demographic data is limited. Nevertheless, the increase of respiratory diseases in developing countries and the simultaneous increase in production and application of phthalates over the past 30 years might be connected causatively. The authors were not able to prove this presumption.

A summary of the toxicological effects of phthalates to humans was published by Heudorf et al. (2007) which was updated in 2008 and focused on the health effects of phthalates in children. The authors report highest exposure against phthalates due to medical treatment (medical devices and drug coating). However, even at ambient concentrations reproductive toxicity effects of some phthalates has been reported in humans. Due to the fact that children are more affected by phthalates and the blood concentrations of phthalate metabolites are usually higher than in adults, safety precautions have to be focused on this group. The authors demand a research effort on the mechanism of the toxicity effects which could be observed to clarify the hazard from phthalates on the human health.

2.2 Particulate matter in the indoor environment

In addition to gaseous compounds in indoor air micro- and macroscopic contaminations are important for the assessment of possible health hazards. Deposited dust is a strong sink for SVOC in indoor air and contributes to the total exposure due to the mobility of this sink. However, the removal of this source of exposure can easily be performed. For smaller particles this is not the case. With advancing of the analytical methods for submicron particles the exposure of inhabitants against airborne particles is of increasing interest, nowadays. Here, not only the direct influence of the particle itself but also the compounds bound to the particle matrix are concerned to be a possible threat to human health. The main task regarding this topic is the characterization of the airborne particles and dust.

2.2.1 Instruments and basic particle theory

The analytics of airborne and settled particles is associated with a high instrumental effort. Two parameters are essential for the thorough determination of the particle characteristics: a) the particles size determines the penetration depth in the human lung and the mobility in the indoor environment. b) The chemical composition of the particles predefines the strength of the sink effect of this particle and its direct health hazard. Regarding its sorption capacity the first parameter and the shape of the particle define the free surface where compounds can attach and the second parameter influences the capacity of adsorption. To reduce the complexity of this problem the shape of the particles can be defined as spherical and the sorption of a compound can be considered as the solution of the compound in the particle matrix. In this case the measurement of the particle size can be performed with instruments that measure equivalent diameters of the particle and the sorption can be characterized using available partition coefficients. A very common equivalent diameter is the aerodynamic diameter which relates the particle properties to the sink velocity of a sphere with unit-density with the same diameter as the particle under observation. Alternatively, the mobility diameter using inertia or the mobility in an electric field is measured by some instruments.

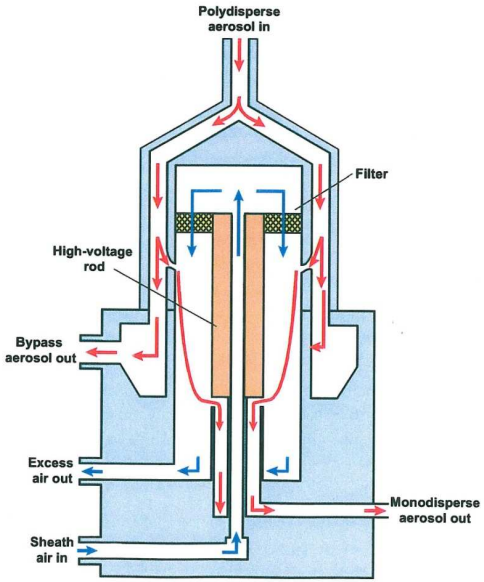

Figure 1: Schematic layout of an electrostatic particle classifier (taken from 3080 Electrostatic classifier datasheet, TSI Inc.)

Regarding analytical instruments to measure the size distribution of a particle collective several devices are commercially available. The oldest instruments use the forced sedimentation of particles in a solution (e.g. within a gradient). The detection is performed using the interaction of the particle with light (e.g. laser) or sound. The sedimentation method is not suitable for airborne particles but can be used to characterize household dust. The air analysis is typically performed using direct laser scattering. For particles > 300-500 nm the aerosol can be measured directly (e.g. via aerodynamic particle counter (APC)) while lower particle diameters need modification of the particles before detection (e.g. condensation particle counters (CPC)). The latter systems are able to detect particles with diameters > 5 nm. In case of direct aerosol measurements the size distribution can be determined. To achieve this using a CPC the aerosol has to be filtered. Usually, this is done via classification of the particles on the basis of their mobility in an electrostatic field. In the following such a scanning mobility particle sizer (SMPS) is described exemplarily.

This measuring device bases on the deflection of charged particles in the electric field depending on their surface charge. The device consists of three sub units: Within the “neutralizer” the particles are charged with a defined charge distribution using a γ-ray emitter (^{85}Kr). Thereafter, the particles are directed into the cylindrical “classifier” that contains a charged electrode in the middle (Figure 1). This electrode is surrounded by a particle-free sheath air with a selectable velocity. The aerosol passes this sheath air in parallel while the charged particles are attracted to the electrode. At a certain height of the electrode a small gap exists were particles with a certain size can be collected. Smaller particles reach the electrode and are discharged while bigger particles are carried out by the sheath air. The collected particles are directed into a detection unit which often consists of a condensation particle counter (CPC) which enlarges the particles by leading the particles through a heated saturated solvent air (n-butanol, water, iso-propanol). By cooling this stream the solvent condenses on the particle which leads to an increase of the diameter. The detection is performed via laser scattering. By changing the voltage of the classifier electrode the device can measure different particle sizes in a row from ~ 1 µm to ~ 5 nm (depending on the CPC). This measuring principle is limited to an aerosol that undergoes no change in size distribution over time.

As mentioned before, the determination of the particle size distribution of the aerosol is not sufficient for a mathematical description of indoor particles. In fact, the particle composition is more important when assessing the transport of compounds bound to the particle matrix. To measure their chemical composition particles can be accumulated on suitable filter materials and analyzed via solvent extraction and GC/MS or HPLC/UV for thermal labile compounds. Alternatively, direct spectroscopy of the deposited matter by energy-dispersive x-ray fluorescence (XRF) allows the fast elemental analysis of the particles. For particle sizes below 1 µm the accumulation on filters is complicated by the penetration of submicron particles (especially between 300 nm and 100 nm) through many filter materials while high efficiency filters (HEPA, ULPA) do not allow the subsequent chemical analysis. This minimum in the precipitation of particles is a result of the transition from the gravitational controlled settling to the diffusion dominated deposition. Other techniques utilize the inertia of the particles to impact them on materials that can be easily analyzed. These cascade impactors, like the “electrical low pressure impactor” (ELPI), allow a size depending chemical analysis of particles with sizes above ~30 nm but are limited to high aerosol

concentrations. This method is not feasible for the indoor environmental analysis because the particle concentrations in indoor air are too low which would lead to high sampling time and a high loss of particle bound compounds due to high air flow.

The adsorption of SVOC on a solid particle phase is an important aspect in the transport mechanism of SVOC in the indoor environment. The strength of the adsorption is given by the ratio of the target compound concentration in the gas phase (y) and the particle phase (c_P) and is characterized by the gas/particle distribution coefficient (K_P). Together with the total suspended particulate matter (TSP), the fraction of particulate bound compounds in the indoor environment can be calculated (2.3).

$$K_P = \frac{c_P / TSP}{y} \tag{2.3}$$

This method was introduced by described in detail by Pankow (1994).

2.2.2 Dust analysis and technical standards

Despite the airborne particles, resuspended dust in indoor air is measurable with lower effort. According to the VDI guideline 4300 sheet 8 (VDI, 2001) dust is divided into “old dust” and “fresh dust”. The age of the dust can be determined for the latter one only. The sampling of “fresh dust” is performed by cleaning a defined area from settled dust and repeating this procedure after a certain time. An actual indoor contamination with SVOC can be detected by analyzing the obtained sample. Regarding the long-term exposure a qualitative analysis of “old dust” may be used as screening-method for hazardous compounds. In contrast to the analysis of gaseous indoor air contaminants the passive sampling of dust samples is more reliable than the active sampling due to the reduced loss of compounds bound to the particle matrix. In general, the active sampling of dust in air is performed using a vacuum cleaner or a pump with a suitable filter. Due to the increased airflow particle-bound compounds might be released from the particles and pass the filter while gaseous SVOC might be accumulated on the combined particle/filter system. Therefore, the quantitative detection of SVOC via this method is associated with a high measurement uncertainty. Another important aspect of the active sampling in the case of vacuum cleaning is the increase of abrasion which could have considerably influence on the measured results. Due to the large amount of available sampling

units for household dust (see Möhlmann (2005)) that fulfill the specifications of the VDI guideline the comparison between several published results is difficult. Especially the analysis of different particle size fractions has a major influence on the overall results (Butte and Walker, 1994; Walker, et al., 1999).

For some organic compounds standards for the measurement of indoor dust are available. As an example the VDI guideline 4301 sheet 5 (VDI, 2007) describes the determination of phosphor-organic plasticizers and flame retardants (TBEP, TBP, TCEP, TCPP, TEHP, TKP and TPP). The dust sample is spiked with an internal standard (^{13}C-γ-HCH or ^{13}C-DDE) and extracted via soxhlet or sonic assisted extraction using dichloromethane. The extract is concentrated and measured using GC/MS. The method bases on the results of Hansen et al. (2001) who showed possible errors sources in the sorption by glassware, non-feasible solvent mixtures, and contamination free extraction equipment. This example illustrates the problems of a reliable SVOC analysis in dust regarding sampling and analytical issues.

The characterization of dust is not only a problem of analytics but also for the modeling of indoor air emissions. Dust mainly consists of minerals (sand, clay, silt), soot, pollen, spores, abrasion from textiles and furniture, hair, and dander from inhabitants and pets. This variety of sources leads to a high fluctuation of the organic carbon content of dust between different houses. Together with different activities and cleaning patterns of the residents the variation in parameters are intense.

For the analytics this problem can be reduced by sieving the dust sample. If the ratio of coarse inorganic matter (e.g. sand) in the sample is reduced the analysis can focus on the particles in the dust with large free surface and high adsorption capacity. A limited number of conventions exist in different countries for the sieving of dust. For example, in Germany the dust fraction < 63 µm is analyzed while in the United States the dust is sieved to particles < 150 µm. This different pre-treatment of the samples complicate the comparison of studies between these countries and affect choosing of reference values for evaluation of analytical and modeling results.

2.2.3 Outdoor and indoor concentrations of phthalates

The cumulated fraction of air and dust has a constant impact on human health even if the gas phase concentration is low. Regarding the background concentration in the outdoor air Teil et al. (2006) measured the concentration of six phthalates (DMP,

DEP, DnBP, BBP, DEHP, DnOP) in Paris. The fluctuation of the concentration was high due to rain events and seasonable temperature changes. Statistical analysis showed that dry deposition (bound to particles) and wet deposition (rain) had a nearly similar impact on the total deposition. The authors concluded that these findings were caused by the low particle concentration of 21 µg m^{-3} (glass fibre filter, pore diameter 0.45 µm) in the outdoor air of Paris. Highest gas phase concentration of a phthalate was measured for DBP (59.3 ng m^{-3}) with a total amount of 109.3 ng m^{-3} for all six compounds. The mean concentration in outdoor air was 55.3 ng m^{-3} and the total deposition was measured to be 1480.6 µg m^{-2} a^{-1}. These concentrations penetrate the indoor environment and provide a background concentration that cannot be lowered by increasing the air exchange rate. Compared to the outdoor concentrations the values indoors are considerably higher if a source is present. Most studies on plasticizers indoors provide measurement data for both air and dust. In the study by Fromme et al. (2004) 59 apartments and 74 kindergartens were examined regarding the concentration of several phthalates in air and dust. According to the authors the data of the apartments are representative for most European cities. The highest concentration in the air of the apartments was found for DMP (13907 ng m^{-3}) because it is a more volatile phthalate. In the case of the kindergartens the highest concentrations were found for DMP (13233 ng m^{-3}) and DBP (13305 ng m^{-3}). The mean gas phase concentrations in the apartments for a single phthalate were found to be < 1200 ng m^{-3}. The values in the kindergartens were higher with a mean < 2400 ng m^{-3}. Due to the strong sorption of phthalates into dust the mean amounts in dust were approximately 50 mg kg^{-1}. The only exception was DEHP which showed considerably higher dust concentrations (775.5 mg kg^{-1}). The comparison of these findings and other studies is very difficult due to different sampling techniques and analytical methods. A list of reference values from different studies is shown in the following chapter.

Generally, the described studies show a high contamination of dust with high-boiling phthalates while the gas phase concentrations are slightly elevated compared to the outdoor values. With decreasing vapor pressure of the compound the air concentration drops while the dust concentration rises. Therefore, the estimated exposure against DEHP is more influenced by the dust concentration than the air concentration

Beside the mentioned natural contents indoor dust contains many anthropogenic substances (Table 4). Elevated concentrations in dust are typically found for plasticizers, pyrethroides, and chlorophenols while other compounds show concentrations below 1 mg kg^{-1}.

Table 4: Common examples for anthropogenic compounds in indoor dust

Compound class	Example(s)	Application/Source
Alkylphenol	Nonylphenol	Detergents, textile treatment, water based paints
Carbamates	Natrium-N-methyldithiocarbamat	Biocide
Chlorophenols	Pentachlorophenol (PCP)	Biocide
Organic phosphorous acid esters	Chlorpyrifos	Plasticizer, flame retardants, insecticides, acaricide
Organic tin compounds	Tributyltinhydride	Stabilisators (polymer), biocides
Polycyclic aromatic hydrocarbons (PAH)	Benzo[a]pyren	Adhesive, wood protection
Perfluoronated sulfonic or carboxylic acid	Perfluorooctanesulfonate (PFOS)	Textile treatment
Phenoxycarboxylic acid	2,4,5-Trichlorophenoxyacetic acid	Herbicide
Phthalic acid esters	DBP, DEHP, DINP	Plasticizers
Polybrominated diphenyl ethers	PentaBDE	Flame retardants
Polyclorinated biphenyles	Decachlorobiphenyl	Plasticzers, dielectric fluid
Pyrethroids	Permethrine	Biocides

Three important pathways for the contamination of indoor dust with anthropogenic compounds exist. By abrasion from treated wood or polymers small particles with high contamination can be transported into the dust directly. Also, the direct sorption of emitted substances from the gas phase into the dust increases the dust content. The third pathway is the direct transfer of a substance due to the contact between source and dust (e.g. dust on PVC flooring). Between these three ways seamless transitions exist. A large collective of results regarding dust measurements indoors is available. A list of several published values for air and dust concentration of several phthalates is summarized in Table 5.

The values show that most air concentration of phthalates are below 1 µg m^{-3} and have to be quantified with high effort. Regarding the concentrations in dust the values

of DEHP deviate considerably from the more volatile. Less volatile phthalates, like DINP and DIDP, show also elevated concentrations in dust and cannot be detected in indoor air (Kersten and Reich, 2003). The spread of the results follow from the combination of the limited mobility of SVOC, different sampling/analytical techniques, differences in resident's behavior, and deviating sorption strength of dust due to different composition. The sampling and analytical techniques are briefly summarized below Table 5. In most cases dust of unknown age (old dust) was analyzed which severely hinders the comparison of the different measurements. Additionally, the treatment of the samples is not the same in each study because most German studies use sieved fractions (< 63 µm) for analysis. In principle, the measured concentration in these samples should be higher because non-sorbing parts (e.g. sand) has been removed prior to the analysis. As a result, a general comparability is not given for the values summarized in Table 5.

The examples of this chapter illustrate that the modeling approach is not feasible for a specific household but can only be used for a general estimation. Results from modeling studies that include household dust show a high uncertainty and have to be assessed critically regarding a possible exposure analysis.

Table 5: Reference values for concentrations of different phthalates in air and dust

	Concentration in air [µg m^{-3}]						Concentration in dust [mg kg^{-1}]					
	n	Min	Max	Median	P_{95}	Ref.	n	Min	Max	Median	P_{95}	Ref.
DEHP	26	0.018	1.046	0.111	-	[1]	2	2380	4100	-	-	[1]
	59	-	0.615	0.156	0.39	[4]	12	230	4000	500	3150	[2]
	40	0.062	2.204	0.306	1.6507	[2]	65	1	2700	-	1600	[3]
	102	<0.059	1	0.077	-	[5]	30	-	1763	703	1542	[4]
	107	0.02	0.24	0.055	-	[1]	55	2	4580	471	-	[1]
							101	16.7	7700	340	-	[5]
							177	790	1170	-	960	[10]
							199	0.2	7530	-	1190	[6]
							252	-	-	-	1840	[7]
							286	-	-	-	2600	[8]
							346	0	40459	770	4069	[9]
DnBP	26	<0.003	9.445	0.551	-	[1]	12	20	510	65	377	[2]
	40	0.023	33.268	0.923	11.20	[2]	26	0.005	678	56	-	[1]
	59		5.586	1.083	2.45	[4]	30	-	141	47	130	[4]
	120	0.052	1.1	0.22	-	[5]	65	1	600	-	180	[3]
							119	<24	352	20	-	[5]
							177	6590	9360	-	7860	[10]
							199	0.2	502	-	160	[6]
							286	-	-	-	240	[8]
							346	0	568	150	568	[9]
BBP	26	<0.003	0.465	0.013	-	[1]	8	<1	1700	19	-	[1]
	59	-	0.575	0.018	0.075	[4]	30	-	815.7	29.7	219	[4]
	120	<0.031	0.48	<0.031	-	[5]	65	1	700	-	230	[3]
							119	3.87	1310	45.4	-	[5]
							177	280	380	-	320	[10]
							199	0.2	745	-	207	[6]
							286	-	-	-	320	[8]
							346	0	45549	135	599	[9]

	Concentration in air [µg m^{-3}]						Concentration in dust [mg kg^{-1}]					
	n	Min	Max	Median	P_{95}	Ref.	n	Min	Max	Median	P_{95}	Ref.
DEP	26	0.025	3.234	0.171	-	[1]	7	0.9	7	3	-	[1]
	59	-	5.481	0.643	1.86	[4]	30	-	632.2	6.1	159.6	[4]
	120	0.13	4.3	0.59	-	[5]	65	1	570	-	350	[3]
							119	<4	111	4.98	-	[5]
							177	290	420	-	350	[10]
							199	0.1	1233	-	89.7	[6]
							346	0	2425	0	115	[9]
DMP	26	< 0.001	0.129	0.010	-	[1]	7	<0.2	5	0.5	-	[1]
	59	-	13.907	0.436	4.648	[4]	30	-	157.9	1.5	46.4	[4]
							65	1	64	-	20	[3]
							177	210	320	-	260	[10]
							199	0.1	75.8	-	3.7	[6]
DMPP	59	-	5.887	0.459	1.466	[4]	30	-	161.3	37.5	144.4	[4]
							65	1	17	-	8	[3]
DiBP	120	0.011	0.99	0.061	-	[5]	65	1	470	-	78	[3]
							119	<1	39.1	1.91	-	[5]
							199	0.2	192	-	130	[6]
							286	-	-	-	130	[8]
							346	0	3810	45	311	[9]

[1] (Clark, et al., 2003b); age and fraction of dust are not given
[2] (Beratung und Analyse Verein für Umweltchemie, 1992); old dust, with broom, on aluminum foil, no sieving
[3] (Kersten and Reich, 2003); old dust, vacuum cleaner bags of inhabitants, < 63 µm fraction is analyzed
[4] (Fromme, et al., 2004); old dust, vacuum cleaner bags of inhabitants, no sieving
[5] (Rudel, et al., 2003); old dust, Teflon covered vacuum cleaner, < 150 µm fraction is analyzed
[6] (Becker, et al., 2002); old dust, vacuum cleaner bags of inhabitants, < 63 µm fraction is analyzed
[7] (Becker, et al., 2004); old dust, vacuum cleaner bags of inhabitants, < 63 µm fraction is analyzed
[8] (Butte, et al., 2001); old dust (~ 4 weeks), vacuum cleaner bags of inhabitants, < 63 µm fraction is analyzed
[9] (Bornehag, et al., 2005); old dust, vacuum cleaner with membrane filter (cellulose), no sieving
[10] (Kolarik, et al., 2008a); old dust, vacuum cleaner with ALK dust collector and filter, no sieving

2.3 Analytics of semi-volatile organic compounds

Identification and quantification of semi-volatile organic compounds in several matrices need a high instrumental effort. With the exception of direct source analysis and matrices that cumulate SVOC the concentrations are usually very low and need a thorough preparation of sampling and analytical devices. Due to the low amount of compound in a collected sample small contaminations have considerable influence on the results. The problems of a reliable SVOC analysis will be illustrated in the following.

Common analytical methods for SVOC in air are non-continuous. The compounds are collected during sampling on a suitable adsorbent (solid or liquid) and desorbed for analysis. To achieve a representative sampling the knowledge about the most important environmental parameters like temperature, relative humidity, air velocity, and air exchange rate is necessary. A standardized emission test is consequently performed in an emission test chamber made of low-adsorbent materials in which all mentioned parameters can be controlled. To obtain the comparability between the results of different testing laboratories the procedure and conditions were standardized in the ISO 16000. The requirements for emission test chambers are defined in ISO 16000-9 (2006). An emission test chamber volume equal or below 1 m^3 is adequate for most materials. However, bigger chambers (12 – 80 m^3) are reported in the literature for the emission test from whole groups of parts (e.g. kitchen). Much smaller chambers (ranging down to 50 mL) are much cheaper and space-saving but the transferability of the results to bigger chambers or even the indoor environment is strictly limited due to the unusual environmental conditions (Schripp, et al., 2007). The application of emission cell systems (e.g. field and laboratory emission cell (FLEC)) is a common alternative against emission test chamber measurements. The emission cell can be attached to flat surfaces so the testing material itself is part of the cavity from which sampling is performed. Usually, the loading factor and air exchange rate in an emission cell are higher than during an emission chamber test.

Regarding measurements of the real indoor environment fluctuations in the environmental conditions have to be tolerated (e.g. temperature, air exchange rate). From Table 5 it can be observed that phthalate concentrations in indoor air are noticeably below 1 µg/m^3. The sampling volume necessary for a reliable analysis of

SVOC is therefore very high (e.g. 2.7 - 2.8 m³ according to VDI guideline 4301-5 (VDI, 2007)). During this long sampling time a constant emission profile has to be established.

The sampling of SVOC can be performed using active and passive methods. Active sampling uses a calibrated pump to direct a precise volume of air over the sorbent material. This method allows a quantitative determination of the SVOC concentration. The expected low air concentrations require a long-term sampling. The passive sampling can be performed on a variety of materials that provide a vast surface area and can be prepared without prior contamination. The disadvantage of this method is the longer sampling time compared to active methods and the lack of quantitative information. Due to the high boiling point of SVOC they preferentially condense on surfaces cooler than the room air (e.g. windows). This effect is utilized for a passive sampling method called “fogging” measurement especially in the automotive industry (DIN 75201, 1992). Two polished stainless-steel plates that are cooled to 15°C are exposed to the contaminated air for 14 days and measured via extraction and GC/MS. The obtained value can be used as a material specific constant but cannot be used for the assessment of the indoor air concentration.

Usual adsorbents for the collection of SVOC feature a low adsorption strength compared to the adsorbents necessary for VOC analysis. This results from the high sampling volume which is needed to accumulate enough matter to reach the limit of detection. If a strong adsorbent is used VOC with higher concentrations in air are also accumulated on the surface which leads to an overload of the adsorbent. In the case of a weak adsorbent breakthrough of the target compound is possible if it is not retained sufficiently at the used airflow. For the SVOC analysis Tenax TA is a strong adsorbent while medium adsorbents are XAD, PU-foam, and quartz wool. Regarding compounds with a very low vapor pressure (like PAHs) a stripe of cotton wool is sufficient for the collection. The selection of the suitable adsorbent for the target SVOC is vital to obtain reliable results and a sufficient recovery rate. A very common method for the sampling of SVOC like PCDD/F, PCP, biocides, etc. is the usage of a combined sorption material (according to VDI 4301-5 (VDI, 2007)). The first layer is a fiber filter that retains the particle fraction in air while the gaseous compounds are collected in a downstream PU-foam. The separate analysis of both fractions gives information about the contamination of particles and air.

After trapping the analytes on the adsorbent they can be desorbed via liquid extraction or thermally desorbed. In the case of liquid extraction the insertion of the extract into the gas chromatograph is done using a split/splitless injector which flash evaporates the solution. To reduce the contamination of the sample during clean-up thermal desorption of the adsorbent and adjacent gas chromatography is useful. The thermal desorption injector desorbs the compounds at high temperatures (~ 300℃) and accumulates them on a cold trap (-30℃ to 0℃) which is packed with a weak adsorbent. The following rapid heat-up of this trap allows a uniform injection into the column. While thermal desorption reduces a possible contamination of the analytical procedure due to the elevated temperature and the permanent sealing of the sample this is not the case for solvent extraction. The usage of several glass flasks and exposure against the laboratory air can increase the measured value of SVOC (Otake, et al., 2001). The glassware can be contaminated by touch of the user because plasticizers are present on the human skin. The effort for the clean-up of glass ware is demonstrated by Fromme et al. (2004). Here, the flasks are cleaned using organic solvents and heated afterwards between 200℃ and 400℃. For every clean-up step the measurements of a blank sample is necessary. This complicates the detection of SVOC by solvent extraction noticeably and increases sources of error.

The analysis of a solid material regarding its content of SVOC is less complex than the analysis of air. In most cases the matrix is extracted via soxhleth or sonic assisted extraction using a suitable solvent and can be analyzed directly via GC/MS or HPLC/UV. To increase the detection limit derivatization can be performed after the extraction of the compound. This is a common technique in the case of herbicidal analysis where the compounds are attached to electrophilic residues (like pentafluorobenzyl) and can be detected more sensitively via GC/ECD (e.g. Thio et al. (1988)). For phthalates a further derivation is not necessary. Modern commercially available selective electrodes basing on tin (IV) porphyrins allow the direct determination of phthalates in solution without separation and derivatization (Santos, et al., 2005). However, the separation and quantification using a GC/MS system gives additional information about the mixture of compounds.

Finally, the quantification of the SVOC using an external standard is complicated by the fact that no gaseous standards are available. The preparation of a stable and

known SVOC air concentration in a certain volume is impossible due to loss from the surrounding walls and the intense disturbance of the equilibrium when sampling from this space. From this reason, a standard is only available in the liquid phase (e.g. DEHP in methanol). By spiking a definite amount of this solution on a sorbent tube the external standardization can be achieved. Some publications prove the high correlation between liquid standardization compared to the usage of a gas standard (Martin, et al., 2007; Massold, 2002).

A modern approach on the measurement of air pollutants is direct mass spectrometry using a “proton transfer reaction mass spectrometer” (PTR-MS) that features a detection limit below 1 ppb for most compounds. The application of this technique for the determination of SVOC is difficult due to unknown fragmentation pattern in the mass spectrum. A specific mass for singular phthalates or even this class of compounds could not be found in prior experiments (see Appendix A) and is not available from the literature. The feasibility of this technique is given in principle because the phthalates feature a higher proton affinity than water. However, further instrumental development is necessary to get a reliable continuous SVOC analysis in air.

2.4 Modeling of indoor air pollutions

The application of mathematical models for the description of the mass-transfer between different matrices that consider the strength of sinks and sources is widely used in chemical engineering. Besides, it is nowadays a very common technique in food science to assess the transfer of plastic additives of the packaging into the food. The mathematical bases of these models are mostly the same. They all base upon the solutions of Fick's second law of diffusion published by Crank (1975). To validate such a model certificated reference materials with known properties are necessary. By measuring the mass-transfer from these materials and compare the results to the values predicted by the model the applicability of the model can be checked. In the case of food science this was performed by a project of the European Union (Stoffers, et al., 2005; Stoffers, et al., 2004). Regarding indoor air models this systematic evaluation is still missing.

When developing and implementing indoor air models knowledge about the boundaries of the described system are vital for the evaluation of the results. The main boundaries are the spatial specific (indoor models, atmospheric models) and compound specific (adsorption behavior, volatility) conditions. To face the complexity of the indoor environment disregard of several parameters is required. This simplification may not lead to an extensive deviation between predicted and measured value. Additionally, the ignoring of parameters takes the risk of constraining the general applicability of the model by overlooking inconsiderable but fundamental aspects. If the intention of the model focus on the estimation of exposure against a certain chemical simplification risks the over- or underestimation of the real intake.

Basis for every model application is the reduced but representative description of the system under observation. Especially the precise characterization of the emission source is necessary. To calculate the source strength knowledge about the initial concentration of the compound in the material (C_0), the diffusion properties of the compound in the matrix (D), and the partition coefficient between the two matrices (K) have to be available. These parameters in addition to the environmental conditions (e.g. air velocity on the surface) determine the mass-transfer from the source into the destination matrix. In case of the indoor environment sink effects and exchange with

the outdoor air have a vast influence. Consequently, diffusion and sorption are deciding for the compound partition in the indoor environment. The most important parameters for the mathematical modeling will be described in the following.

2.4.1 Diffusion

Diffusion describes the phenomenon of movement of mass in a system from one position to another due to the thermal motion of the particle. It explains the fact that a system with a gradient in concentration aspires to reach uniform distribution. From a statistical point of view particles from a region of high concentration are more likely to trespass into a region with lower concentration than contrariwise. This leads to a net-mass transfer along the concentration gradient. The mathematical characterization was done by Fick who used the theories of heath transfer for description of the mass transfer. The first Fickian law describes the proportionality between particle movement and concentration gradient while the second Fickian law (2.4) allows a calculation of the change in concentration due to diffusion depending on time and space.

$$\frac{\partial C(x,y,z,t)}{\partial t} = D_m \left(\frac{\partial^2 C(x,y,z,t)}{\partial x^2} + \frac{\partial^2 C(x,y,z,t)}{\partial y^2} + \frac{\partial^2 C(x,y,z,t)}{\partial z^2} \right) \tag{2.4}$$

In this case the independence between diffusion coefficient in the material (D_m) and time, space, and concentration is assumed. Basis of this assumption is the steadiness of the system over a long period of time despite of the diffusion. This is the case for very low concentrations like endowed solid state bodys (Mehrer, 2005) or very high concentrations of a high-boiling additive in a polymer (Xu and Zhang, 2003). Even though the diffusion coefficient is not changing with time it strongly depends on the temperature of the system. The connection between temperature and diffusion coefficient is described by the Arrhenius equation (2.5).

$$D_m = D_{m,\infty} e^{\frac{E_A}{RT}} \tag{2.5}$$

Here, $D_{m,\infty}$ is a constant that has to be determined experimentally. Equation (2.5) illustrates that small changes in the environmental conditions have a vast influence on the diffusion properties of the material. Therefore, the temperature has to be precisely monitored when validating the modeled data with practical experiments. If the diffusion properties have a considerable influence on the emission rate changes

in the temperature due to time of day and season have to be included for modeling a real indoor environment.

The solution of Fickian's second law for a certain purpose requires several assumptions that can be derived from the observed system. However, an analytical solution is not possible for most cases. Therefore, numerical methods have to be used to get results for the corresponding problem. All following models assume the isotropic distribution of the compound in the matrix. This means that the molecules in the matrix have no preferred orientation or direction. This limits the usage of these models against multi-layered inhomogeneous materials like laminate or paper. The following general specifications are necessary to find a solution of the second Fickian law:

1. Information about the geometry of the described system in which the diffusion takes place.

2. Description of the initial conditions of the system at the beginning of observation.

3. Specification of the compound behavior at the boundaries of the system.

In the framework of this work the source of emission is a flat material (e.g. floor covering) with the height l. In this material the additive under observation is homogenously distributed. This allows disregarding the diffusion parallel to the surface and reduces the second Fickian law to the one-dimensional case (2.6).

$$\frac{\partial C(x,t)}{\partial t} = D_m \frac{\partial^2 C(x,t)}{\partial x^2} \tag{2.6}$$

Additionally, the homogenous distribution mathematical specifies the start conditions (2.7).

$$C(x,t) = C_0 \; ; \; 0 \leq x \leq l \tag{2.7}$$

The behavior of the compound at the material boundaries are different for every single model and will be described later in detail. However, despite of the simplification by these two assumptions the solution of the equation is still very complex. Therefore, the solutions by Crank (1975) are typically the basis for most solutions and are adapted for the specific problem.

2.4.2 Sorption

Sorption is the generic term for the attachment and release of compounds to/from an adsorbent. The sorption of a compound is usually accompanied by a phase transfer. Regarding the attachment of a compound on a sorbent two possibilities exist: the compound is *absorbed* by the matrix and thus irreversible bound to the sorbent or *adsorbed*. In case of the latter one the compound is bound to the adsorbent by weak interactions (physisorption). The resulting equilibrium state is affected by concentration, temperature, and surface properties.

The concentration development of a compound in indoor air is determined by the formation of several adsorption/desorption equilibria. The addition of a compound to a surface can be mathematically described by adsorption isotherms. For modeling purpose three different isotherms are commonly used.

1. Linear adsorption isotherm

$$q = K_D y \tag{2.8}$$

2. Freundlich isotherm

$$q = K_F y^{n_F} \tag{2.9}$$

3. Langmuir isotherm

$$q = \frac{K_L q_{max} y}{1 + K_L y} \tag{2.10}$$

The comparison of these equations is illustrated in Figure 2. The linear and the Freundlich isotherms show an identical development for low concentrations. In this region the linear isotherm can be used. At higher concentrations, the increased loading of the surface constrains further adsorption energetically. This is described by the Freundlich isotherm. The exponent n_F is fixed which leads to an infinite increase of the function value and, thus, this equation does not allow the description of a saturated surface. For a system near the surface saturation the Langmuir isotherm should be used because it is the only of the mentioned isotherms that is not infinitely increasing.

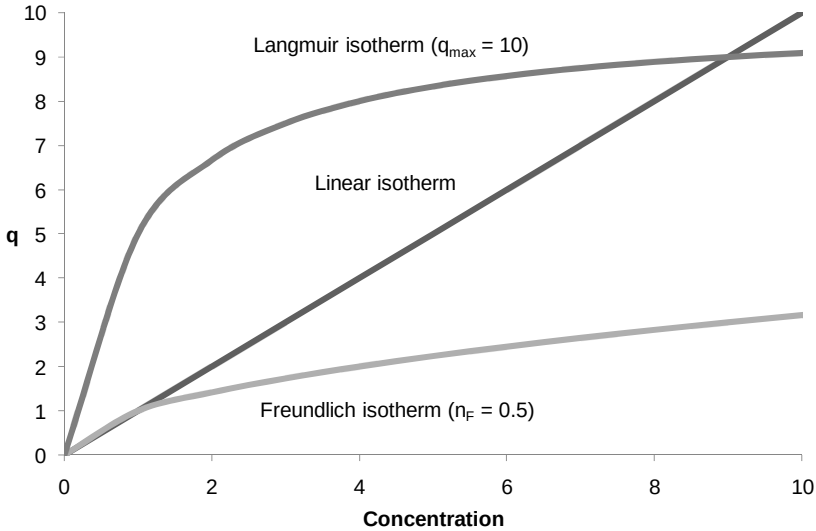

Figure 2: Different development of sorption isotherms for $K_D = K_L = K_F = 1$.

Further models that describe the multi-layered adsorption of compounds on a surface like the commonly used Brunauer, Emmett, Teller (BET)-model is not necessary for SVOC because super-saturation of these compounds is not likely in the indoor environment (Tichenor, et al., 1991). Due to the low concentrations, the linear adsorption isotherm is usually used.

Regarding the mathematical models two types are discriminated: a) the equilibrium adsorption model (EA) that assumes that the concentration of the compound in air is directly linked to the concentration in the condensed phase and b) the boundary layer diffusion controlled adsorption model (BLDC) that assumes an additional phase between adsorbents and complete mixed gas phase (Axley, 1991). For the latter model the equilibrium is formed between the adsorbent and the surface-near gas phase. The passover of the compound into the well-mixed air is characterized by the external mass-transfer coefficient (h_m). This model is commonly used for the indoor air pollution modeling. Axley (1991) showed the feasibility of the linear and the Langmuir adsorption isotherm for both models if the concentrations in air are low. He also proved that the BLDC-model merges into the EA-model with increasing h_m.

If an equilibrium between gas phase concentration and surface concentration exists a partition coefficient (K_S) according to (2.11) can be determined.

$$K_S = \frac{C_S}{y_\infty} \tag{2.11}$$

The conditions of adsorption and absorption for a specific compound cannot be reliably predicted theoretically. Endo et al. (2008) analyzed the sorption behavior of aliphatic and cyclic hydrocarbons between C_5 and C_8. They found a preferred absorption of cyclic compounds against aliphatic compounds with the same carbon content. The adsorption was not different. With increasing sterical hinderence of the compound the adsorption of aliphatic hydrocarbons was favored. Not only the specifications of the compound decide about the sorption but also the properties of the sorbent. To determine the transport mechanism of these compounds the sorption of different air pollutants on aerosols (urbane aerosols, diesel exhaust) and soil organic matter (SOM) were closely studied by Roth et al. (Roth, et al., 2005a; b) and Niederer et al. (2006). They found a correlation between the adsorption strength of the particles and their elemental carbon (EC) content. The adsorption of organic matter bound to these particles interferes with this correlation. According to the authors the general conclusion of the sorption properties of mixed aerosols was not possible from the observed data. This illustrates that the theoretical prediction of sorption properties of an aerosol or inhomogeneous matrices (e.g. dust) is not possible without experimental data.

2.4.3 Determination of parameters for the modeling of pollutant distribution

The mass-transfer models that describe the release of compounds from a source into a defined space use special parameters to predict the development of concentration over time. Most of these parameters can be determined from data about compound and environment. These parameters are described in detail in the following.

Diffusion coefficient D

The diffusion coefficient contains information about the mobility of the compound in the matrix. Consequently, D can be derived from compound- and material-specific parameters. These correlations were experimentally determined by the food packaging technology industry. A summary of different diffusion models was published by Mercea (2000). To determine D for a specific polymer knowledge about

cavities in the polymer and the molecular volume of the compound is necessary. From these information the activation energy for the transfer of the compound from one cavity into the next can be calculated. Weak interactions between compound and polymer matrix are ignored in the calculation because these models are limited to small molecules (e.g. nitrogen, hydrogen). From this reason, an empirical model using correlation equations of experimental data should be preferred to these thermodynamic models. Regarding the diffusion in polymers many correlation equations are available for several compounds (e.g. Piringer (2000a)). In these models D is determined from the temperature, molecular mass, and the empirical polymer factor A_{pol}. The polymer factor contains information about the compound and the polymer and can be derived from migration of n-alkanes. A listing of this factor for several combinations of polymer and additive was published by Begley et al. (2005). Two examples for correlation equations are given in the following.

For the application of a migration model O'Brien and Cooper (2001) used equation (2.12) to estimate the diffusion coefficient in the packing material.

$$D_m = e^{(A_{pol} - 0.01M - \frac{10450}{T})} \tag{2.12}$$

A enhanced correlation equation was used by Brandsch et al. (2002).

$$D_m = e^{(A_{pol} - 0.1351M^{2/3} + 0.003M - \frac{10454}{T})} \tag{2.13}$$

Equation (2.13) is suitable for most polymers according to Piringer (2000a). It was derived from the measurement of several n-alkanes in amorphous polymethylene and is a feasible approximation for most hydrocarbons or other compounds with low polarity. Plasticizers and flame retardants usually contain heteroatoms which leads to a higher polarity compared to hydrocarbons. Calculation of the diffusion coefficient using equation (2.12) or (2.13) is consequently associated with a high error. Equations that consider the weak interactions of a polar compound with the polymer matrix are not available from the literature yet. For the emission models the diffusion coefficient can be estimated from fitting of experimental results to the model.

The experimental determination of the diffusion properties of a polymer material can be performed based on the increase in mass of the material. The sample is placed in a small chamber with air flowing through. The air contains a specific amount of an

organic compound (e.g. toluene) which is taken up by the material. The mass increase is monitored continuously by a balance (usually a micro-balance) till saturation of the material is reached. Afterwards the chamber is supplied by pure air and the decrease in mass of the sample is monitored. From the detected mass-changes the diffusion coefficient of the compound in the polymer material is calculated. In most cases, volatile organic compounds are used for this experiment because a defined air concentration of an SVOC is difficult to establish. Therefore, microbalance-data about the diffusion of plasticizers in a specific polymer is not available in the literature.

Partition coefficient K

The partition coefficient contains information about the transfer of the compound from one matrix into the other. This transfer is not necessarily connected to a phase transfer (e.g. in the migration modeling). For the emission modeling the parameter describes the transfer of the compound between the material and the air. In this case the material can be source or sink (e.g. chamber wall, particles) for the compound. The partition coefficient between emission source and gas phase can be calculated by the concentration in the material phase C and the gas phase y under equilibrium conditions (2.14).

$$K = \frac{C}{y} \tag{2.14}$$

The concentration in the material phase can be determined experimentally by extraction of the material. Due to the mass-transfer from the material C decreases over time. At low concentrations this leads to a dependence of K on time. For SVOC modeling this is usually not the case due to the very high initial concentrations in the material and the low loss of additive mass over time. Therefore, it is assumed that the actual concentration of the compound in the material is very similar to the initial concentration ($C \approx C_0$).

The determination of y under equilibrium conditions is much more complicated because the measurement of a low air concentration under static conditions is not possible in most cases. Under dynamic conditions the measurement of the well-mixed air concentration is not meaningful because the partition takes place between the material and the boundary layer gas phase ($y = y_0$). This concentration cannot be

measured without disturbing the boundary layer system. The calculation of K using the ideal gas law is more useful but needs a good estimation/measurement of the vapor pressure of the compound.

$$K = \frac{C_0 R T}{p M} \tag{2.15}$$

Consequently, the partition coefficient determines the maximum reachable concentration in the gas phase if the material is present.

External mass-transfer coefficient h_m

The study of Xu and Little (2006) showed an improved correlation between experimental results and predicted values for SVOC if the BLDC-model was used. In this case the emission is not only governed by D_m and K but also by the mass-transfer from the surface boundary layer and the well-mixed gas phase (h_m). With decreasing h_m the emission rate from the material decreases independently of D and K. This direct influence on the emission rate is more important than sorption effects or mass-exchange with the outdoor environment.

The mass-transfer coefficient depends on the environmental conditions and geometry of the sample. The most important parameter for h_m is the air velocity on the surface of the sample. Further parameters are diffusion properties of the compound in air, and the air viscosity. Also the flow field of the air (laminar, turbulent) which is characterized by the Reynolds number has to be known. For emission chamber tests only estimated mass-transfer coefficients are available from the literature because the air usually does not flow against the sample laminar and is well-mixed. Other emission test instruments like the field and laboratory emission cell (FLEC) are easier to describe. Zhang and Niu (2003) used computational fluid dynamics (CFD) calculations to estimate the mass-transfer from the surface into the air flow of the FLEC. A transfer of this approach for the emission test chamber or the real indoor environment is, however, impossible.

A common used estimation for the mass-transfer coefficient was derived from Axley (1991). Principally, the method uses the analogy between heat transfer and mass transfer but directed flow above the surface without mixing of the air is required. To calculate h_m Axley used the correlation equations by White (1988) for laminar flow (Re < 500 000).

$$Sh = 0.664 Sc^{1/3} Re^{1/2} \tag{2.16}$$

The Reynolds number is determined by the velocity of the air above the sample u, the length of the material d and the kinematic or dynamic viscosity of air.

$$Re = \frac{ud}{\nu} = \frac{ud\rho}{\eta} \tag{2.17}$$

The Schmidt number consists of the ratio of the kinematic viscosity and the diffusion of the compound in air.

$$Sc = \frac{\nu}{D_a} \tag{2.18}$$

The Sherwood number contains the mass-transfer coefficient.

$$Sh = \frac{lh_m}{D_a} \tag{2.19}$$

To determine h_m from equation (2.19) the diffusion coefficient of the compound in air has to be known. This parameter depends on several other parameters (e.g. air humidity). Huang and Haghighat (2002) proposed to use the Fuller-Schettler-Giddings (FSG)-method (Fuller, et al., 1966) if D_a cannot be derived from the literature. This correlation method uses known parameters of air to calculate the diffusion coefficient.

$$D_a[cm^2/s] = \frac{T^{1.75}\sqrt{M_r}10^{-3}}{P(V_{air}^{1/3} + V_{compound}^{1/3})^2} \tag{2.20}$$

In equation (2.20) P [atm] is the atmospheric pressure, M_r [g/mol] the mean molar weight according to (2.21), and V [cm³/mol] the volume of air and the gaseous compound.

$$M_r = \frac{M_{air} + M_{compound}}{M_{air} M_{compound}} \tag{2.21}$$

The parameters are available from the CRC handbook (Lide, 2007) or can be calculated using a suitable software (e.g. ChemSketch, ACDlabs). Alternatively, the molar volume can be calculated directly from the atomic volumes (according to Fuller et al. (1966)) or the reduced LeBas volume (according to Lyman et al. (1982)).

Correlation equation (2.20) can be used to calculate the diffusion of nonpolar compounds in air at room temperature. If the equation is used for polar compounds the estimated error is 10 % in minimum (Lugg, 1968). The different results of several modeling approaches for the two compounds DEHP and DBP are displayed in Table 6.

Table 6: Results of different calculations of the mass-transfer coefficient (l=1 m; u=0.3 m/s; M_{air}=20.97g/mol; ρ_{air}=1.161 kg/m³; η_{air}=18.6·10^{-6} Pa s; P=1 atm)

	Molar volume [cm³/mol]		h_m [m/h]	
	DEHP	DBP	DEHP	DBP
ChemSketch	397	264.2	2.08	2.39
(Lyman, et al., 1982)	470	315	1.97	2.26
(Fuller, et al., 1966)	493.2	329.8	1.94	2.23

The presented equations allow the calculation of the mass-transfer coefficient from known environmental parameters. It is important to consider that the basis of the calculation are several correlation equations and that the results can be associated with a high uncertainty.

Main difficulty of the application of the equations is the assumption of a laminar flow above the sample. This is usually not the case in emission test chamber measurements. In principle, the link between Reynolds- and Sherwood number has to be determined for a chamber and every sample geometry (Sparks, et al., 1996). Also, measurements at different air velocities would have to be performed. Sparks et al. (1996) published correlation curves between diffusion coefficient in air and h_m. The equations are valid in the range between D_a = 0.02 to 0.03 m²/h and are, therefore, much too high as an estimation method for SVOC properties.

Initial concentration in the material C_0

To assess the partition coefficient the concentration in the material has to be known. If the concentration is only slightly changing over time the initial concentration in the material C_0 can be used. In some studies C_0 is determined via regression of experimental data to the used model. Regarding the aspect of model validation this approach is not useful. The extractive determination of C_0 gives a more precise value and reduces the amount of adjustments of the model. If pure liquids are used as a

source of emission the initial concentration is given by the density of the fluid at the actual temperature.

Concentration in the boundary layer y_0

For the modeling of SVOC the BLDC-model has to be used. Here, the emission rate is mainly influenced by the external mass-transfer coefficient and the boundary layer concentration. Like the partition coefficient for the EA-model y_0 determines the maximum reachable concentration in the well-mixed air. The boundary layer concentration is determined from the partition between the material and the adjacent air under equilibrium conditions. As a consequence, y_0 is not depending on the environmental conditions (e.g. air velocity) but is used as a static value.

Summary

Most parameters used for the modeling are calculated from correlation equations and are associated with an unknown uncertainty. A detailed sensitivity analysis for the modeling parameters was published by Xu et al. (2009b). The principle influences of the used parameters on the results are displayed in Table 7.

Table 7: Impact of modeling parameters on the results

Parameter	Impact
D_m	Level of equilibrium concentration
h_m	Level of equilibrium concentration (if diffusion dominates), Time to reach equilibrium (if diffusion can be neglected)
K, y_0, C_0	Level of equilibrium concentration
Q, n	Level of equilibrium concentration, h_m (indirect by changing u)
K_S, n_F	Time to reach equilibrium
K_P ,TSP	Level of equilibrium concentration, Time to reach equilibrium

2.4.4 Mass-transfer models

Every mathematical description of the mass-transfer from a source into the target matrix (e.g. air) contains the diffusion of the compound to the boundary of the material and the transfer between the two matrices (*mass-transfer-term*). In the case of indoor air pollution the modeling of adsorption, desorption, and mass-exchange with the outdoor environment have to be additionally considered (*mass-balance-*

term). The mass-balance-term can be changed modularly according to the specifications of the system while the mass-transfer-term determines the release of compounds into the system. The governing parameters are illustrated in Figure 3.

An additive of the outlined floor covering can diffuse to the surface and evaporates according to the partition coefficient K into the surface boundary layer. Depending on the environmental conditions the compound is transferred into the well mixed gas phase. This is characterized by the external mass-transfer coefficient. The gas phase concentration undergoes changes due to the inflow into the chamber (Q) and the sorption to the chamber surfaces. Depending on the system the concentration in the outdoor air y_{in} and adsorption to additional sinks (e.g. particles) can be added to the mass-balance-term.

The easiest mass-balance equation is given by (2.22) because it only considers the emission from the source and the decrease in concentration due to the air exchange.

$$\frac{dy(t)}{dt} = L \cdot SER_A(t) - n \cdot y(t) \qquad (2.22)$$

The addition of terms to reflect sorption equilibrium and mass-intrusion from the outdoor environment will be shown later. First, the mathematical solution for the used differential equations will be discussed in the following.

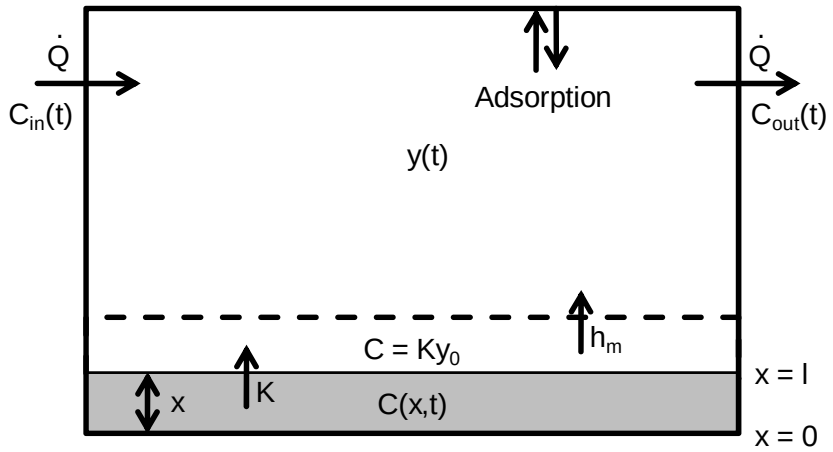

Figure 3: Illustration of the mass-transfer from a floor covering into the well-mixed air and existence of adsorption/desorption equilibria (Xu and Little, 2006; Xu and Zhang, 2003)

Dimensionless characteristics

To solve the differential equations and to find correlations between the physical parameters dimensionless numbers are useful. It additionally enhances the clarity of the equations and assures the consistence of units. A first approach was published by Xu and Zhang (2003) and extended by Qian et al. (2007). They used the following combination of parameters.

1. Fourier-number (dimensionless time)

$$Fo_m = \frac{D_m t}{l^2} \tag{2.23}$$

2. Biot-number (dimensionless mass-transfer)

$$Bi_m = \frac{h_m l}{D_m} \tag{2.24}$$

3. Dimensionless air exchange

$$\alpha = \frac{n l^2}{D_m} \tag{2.25}$$

4. Dimensionless loading factor

$$\beta = \frac{A l}{V} \tag{2.26}$$

The application of these numbers to establish correlation equations for the rapid determination of the emission rate from a certain material will be shown later.

Transcendental equations

For the solution of the differential equations of diffusion often a Fourier-transformation is used. In these equations some parameters are connected by a transcendental equation like

$$H = b_n \tan(b_n l) \tag{2.27}$$

or if dimensionless numbers are used the equation is modified to

$$\frac{Bi_m}{K} = u_n \tan(u_n) \tag{2.28}$$

Due to the symmetry of the tangent-function this equation has an infinite amount of solutions. For the modeling purpose only the positive solutions are used. By using the Newton iteration method the numerical solutions for u_n are available. This can be performed using commercial software like MatLab or Mathematica. Unfortunately, these programs do not check the plausibility of the results. If the wrong starting conditions are used the functions deliver the discontinuities of the tangent instead of the desired values. In most cases the symmetry of the equations can be utilized because the desired solutions are shifted with π or π/l from the first solution. For a higher transparency the dimensionless numbers should be used.

2.4.5 Mass-transfer-term for the gas phase

The calculation of the emission rate using a mass-transfer-term uses several assumptions for the solution of Fick's second law. For every observed model three assumptions are identical.

1. The distribution of the compound in the material is homogenous.

2. The material is attached on a surface without reception of the target compound.

3. Diffusion is independent on the concentration.

The second assumption can be formulated mathematically via equation (2.29).

$$\frac{dC(x,t)}{dt} = 0 \; ; \; t>0 \; ; \; x=0 \tag{2.29}$$

An EA-model for the mass-transfer of VOC from a homogenous sample into the gas phase was published by Little et al. (1994). The validation was performed on the basis of emission chamber tests of carpets. After regression the model was feasible to predict the concentration development under the given conditions. Further studies used BLDC-models to improve the correlation between experimental results and predicted values. For example Huang and Haghighat (2002) used an additional mass-transfer-coefficient to describe the release of compounds from the material.

$$m(t) = -D_m \frac{dC(x,t)}{dt} = h_m(y_0(t) - y(t)) \tag{2.30}$$

In equation (2.30) the concentration in the boundary layer depends on time. The supply of the boundary layer with the target compound happens via diffusion in the material. Huang and Haghighat (2002) described two different solutions for the diffusion equation: a numerical and an analytical solution. The analytical model is exceptional because it allows the explicit calculation of the concentration for a specific time on the basis of only four parameters. In this approach only D_m, K, h_m, and C_0 are needed.

The numerical description of the material phase concentration is given by

$$C(x,t) = \frac{1}{H}\left(\frac{D_m}{\delta y} C(x-\delta y,t) + \frac{\Delta y}{\Delta t} C(x,t-\Delta t) + \frac{h_m}{n\Delta t + lh_m\Delta t + 1} y(t-\Delta t)\right) \tag{2.31}$$

with

$$H = \frac{D_m}{\delta y} + \frac{\Delta y}{\Delta t} + \frac{h_m}{K} - \frac{lh_m^2\Delta t}{K(n\Delta t + lh_m\Delta t + 1)} \tag{2.32}$$

and δy as distance between two grids and Δy as distance between two control volumes. These parameters show the similarity to CFD-calculations and need an extensive calculation for a specific time and space. By calculating the surface concentration of the compound the transfer into the gas phase is available. The concentration at time t-Δt has to be known to use equation (2.33).

$$y(t) = \frac{lh_m \Delta t}{K(n\Delta t + lh_m \Delta t + 1)} C(x,t) + \frac{1}{n\Delta t + lh_m \Delta t + 1} y(t - \Delta t) \tag{2.33}$$

The authors describe high correlations between this numerical model and experimental data of TVOC, hexanal, and α-pinene from OSB panels in a 50 L emission test chamber. The parameter K and D are available from a CFD study by Yang et al. (2001) who used the same experimental data.

This models needs long computing time and is still an approximation of the solution. From this reason, Huang and Haghighat (2002) developed an analytical solution by separating the material surface concentration and the well-mixed air concentration. The latter one is usually much smaller than the first which leads to assumption (2.34).

$$h_m(y_0 - y(t)) \approx h_m \frac{C(l,t)}{K} \tag{2.34}$$

The mass-transfer-term is not longer depending on the actual air concentration if equation (2.34) is used and can be calculated explicitly. Using the distribution function of the compound in the material

$$C(x,t) = 2C_0 \sum_{n=1}^{\infty} \frac{\sin(b_n l)}{b_n l + \sin(b_n l)\cos(b_n l)} e^{-b_n^2 D_m t} \cos(b_n x) \tag{2.35}$$

in which b_n are the positive roots of the transcendental equation

$$H = \frac{h_m}{KD_m} = b_n \tan(b_n l) \tag{2.36}$$

the concentration in air is given by

$$y(t) = 2C_0 l D_m \sum_{n=1}^{\infty} \frac{b_n \sin^2(b_n l)}{(n - b_n^2 D_m)(b_n l + \sin(b_n l)\cos(b_n l)} (e^{-b_n^2 D_m t} - e^{-nt}) \tag{2.37}$$

This application of this model is limited to special cases. The concentration in the inlet air cannot be changed (y_{in} = 0 µg/m³). Also sink effects cannot be described. However, the effort of calculation is low for the analytical model compared to the numerical model. The main disadvantage of this approach is the existence of a transcendental equation (2.36) even in this analytical model. Regarding its application a numerical solution is still necessary.

The ignoring of the interaction between emission rate and actual gas phase concentration might be an excessive assumption. A mass-transfer-model that includes this connection is given by Xu and Zhang (2003). Here, the mass-transfer-term is

$$m(t) = D_m \sum_{n=1}^{\infty} \sin^2(b_n l) \frac{2(b_n^2 + H^2)}{l(b_n^2 + H^2) + H} \left((C_0 - Ky(0)) e^{-Db_n^2 t} + K \int_0^t e^{-Db_n^2 (t-\tau)} dy(\tau) \right) \quad (2.38)$$

using the same transcendental equation (2.36) as the previous model. To solve this integral the gas phase concentration at time t has to be known. This leads to a feedback between the mass-transfer-term and the mass-balance-term. The doubled iteration (b_n and y(t)) elevates the calculation effort but provides a good correlation between experimental and theoretical results. The enhancement of this model regarding different sorption effects (surfaces and particles) was published by Xu and Little (2006). The used mass-balance-equation is given by

$$V \frac{dy(t)}{dt} = A_{sample} m(t) + Qy_{in}(t) - Qy(t) - A_{chamber} \frac{dq_S(t)}{dt} - V \frac{dq_P(t)}{dt} - Qq_P(t) \quad (2.39)$$

where $q_s(t)$ is the sorption on surface basing on the Freundlich isotherm and $q_P(t)$ is the sorption to particles according to a linear isotherm.

$$q_P(t) = K_P y(t) TSP \quad (2.40)$$

In principle, the sorption isotherm may be also referenced to the particle surface. Usually the particle specific surface a_{TSP} = 2 m²/g, which was proposed by Liang et al. (1997), is used for calculation. In this case, the particle partition coefficient has to be divided by a_{TSP} to derive a surface-area-normalized coefficient. If this new equation is used the mass-balance equation (2.39) has to be modified to (2.41).

$$V\frac{dy(t)}{dt} = A_{sample}m(t) + Qy_{in}(t) - Qy(t) - A_{chamber}\frac{dq_S(t)}{dt} - \frac{V}{a_{TSP}TSP}\frac{dq_P(t)}{dt} - Qq_P(t) \quad (2.41)$$

As a result, a_{TSP} is reduced from the equation and has no influence. Both sorption functions depend on the actual gas phase concentration which can only be calculated if the mass-transfer-term can be solved analytically. This is not the case for equation (2.38). By insertion of equation (2.38) in equation (2.39) an iterative solution is available. Xu and Little (2006) compared the predicted concentrations with measurements of DEHP from PVC floor coverings in a FLEC and CLIMPAQ and found good correlations. However, the model is not validated for system where particles are present. The model predicts an increase in the emission rate if the particle concentration in air rises. This presumption bases on sorption values in the literature and was not validated experimentally.

In 2004 another analytical model was proposed by Deng and Kim (2004) which circumvent some disadvantages of the model by Huang and Haghighat (2002) and gives an explicit formulation of the equations. However, the sorption is still not considered. Using the dimensionless parameters the concentration in the gas phase is given by

$$y(t) = 2C_0\beta\sum_{n=1}^{\infty}\frac{b_n\sin(b_n)}{a_n}e^{-D_m l^{-2}b_n^2 t} \quad (2.42)$$

with

$$a_n = (K\beta + (\alpha - b_n^2)KBi_m^{-1} + 2)b_n^2\cos(b_n) + (K\beta + (\alpha - 3b_n^2)KBi_m^{-1} + \alpha - b_n^2)b_n\sin(b_n) \quad (2.43)$$

and b_n as the positive roots

$$b_n\tan(b_n) = \frac{\alpha - b_n^2}{K\beta + (\alpha - b_n^2)KBi_m^{-1}} \quad (2.44)$$

and the mass-transfer-term

$$m(t) = 2AC_0 l\sum_{n=1}^{\infty}\frac{(\alpha - b_n^2)\sin(b_n)}{a_n b_n}(1 - e^{-D_m l^{-2}b_n^2 t}) \quad (2.45)$$

Due to the fact that only four parameters are used in this model the calculation effort is rather low. The validation of the model was done using the same data set like

Huang and Haghighat (2002). The correlation was adequate excepting the values of α-pinene. The application for SVOC was not validated. The present approach reduces the effort to calculate the emission rate but is still not feasible as an easy approach.

From this reason, Qian et al. (2007) used the dimensionless parameters to assemble empirical correlation equations from experimental data to quickly estimate the mass-transfer-term. The correlation has limited duration limits like the following equation for $Fo_m \leq 0.01$.

$$m(t) = 1.34\alpha^{-8.4\cdot10^{-8}}(\beta K)^{-1.3\cdot10^{-3}}\left(\frac{Bi_m}{K}\right)^{0.26} e^{-\frac{0.0059}{Fo_m+0.0038}} \quad (2.46)$$

This method provides fast results with good correlations to the experimental data but is very inflexible. The transferability for compounds with different volatility has to be assessed experimentally and cannot be used if dissimilar sample materials are used.

2.4.6 Mass-transfer-term for the condensed phase

As mentioned before, the migration of a compound due to the direct contact of two matrices with a concentration gradient can be described using models similar to the presented ones. Especially in food packaging technology were the additives in the plastic wrapping can migrate into the food matrix these models are widely used. Migration models are of high interest because they have been validated by large amounts of experimental data. Due to their precision they are allowed to be used for registration purposes by the European Union.

Like in the gas phase modeling D and K are the governing parameters of the migration. K decides about the maximum amount in the target matrix and D about the velocity of the mass-transfer. All migration approaches are summarized in the book by Piringer and Baner (2000). They showed necessary correlation equations to estimate the governing parameters (Piringer, 2000a) and discuss possible solutions of the differential diffusion equation (Piringer, 2000b). The migration modeling has a focus on plasticizers in the polymers because they are widespread. Piringer (200b) also discusses the evaporation of plasticizers when they diffuse to the polymer surface. He indicates two possible cases of diffusion.

1. If the diffusion is smaller than the rate of evaporation then the transfer into the gas phase is diffusion hindered.

2. If the diffusion is higher than the rate of evaporation the surface can contain zones with pure liquid plasticizers (“sweating” of the material).

The model to describe the evaporation of a compound into the gas phase from a diffusion hindered material has been described by Piringer (2000b) using equation (2.47)

$$\frac{m(t)}{m(\infty)} = 1 - \sum_{n=1}^{\infty} \frac{2H^2 e^{-b_n^2 D_m t l^{-2}}}{b_n^2 (b_n^2 + H^2 + H)} \tag{2.47}$$

with

$$H = \frac{lk}{D_m} = b_n \tan(b_n) \tag{2.48}$$

This model has strong similarities to the previous described indoor emission models. The main difference is the dimensionless constant k that contains the strength of evaporation. This parameter has to be determined experimentally. The flexible adaption of the model to other problems is limited due to the usage of this new parameter.

The application of migration models for the food industry was published by several work groups who used correlative methods to determine the diffusion coefficient in the material (Begley, et al., 2005; Brandsch, et al., 2002; O'Brien and Cooper, 2001; Piringer and Baner, 2000). A modern model for migration modeling (according to Begley et al. (2005)) that contains the findings from previous works is given by equation (2.49).

$$\frac{m(t)}{A} = C_0 \rho_{Pol} l \left(\frac{H}{1+H}\right)\left(1 - \sum_{n=1}^{\infty} \frac{2H(1+H)}{1+H+H^2 b_n^2} e^{-D_m l^{-2} b_n^2 t}\right) \tag{2.49}$$

with

$$H = \frac{V_F}{K_{F,Pol} V_{Pol}} = \frac{y_\infty \rho_F V_F}{C_\infty \rho_{Pol} V_{Pol}} = -\frac{\tan(b_n)}{b_n} \tag{2.50}$$

In equation (2.50) Pol stands for the polymer phase and F for the fluid phase that is the target matrix for the compound. Using the properties of air this model can also be used to predict the emission characteristics of the material.

All mathematical descriptions of the mass-transfer via migration have the same disadvantage regarding its applicability for the emission modeling. The models do not include a feedback between the actual concentration in the target matrix and the emission rate. For the food modeling this term is not necessary because the target matrix is static (no mass-loss from the system). In the case of air analysis the matrix undergoes changes due to sorption and mass-exchange with the outdoor environment. This limits the usage of migration models considerably because the direct feedback like in equation (2.38) is indispensable to describe a fast-changing dynamic system.

However, for future applications a combination of migration and emission models will be necessary because the described emission models are not able to describe multi-layered building materials. The movement of a compound to the surface in such a material can be described using the migration models while the emission models use the information about the environmental conditions to predict the concentration development under the given conditions. The applicability of such a combined model is currently under research to assess the emission from structural insulated panels (SIPs) (Kumar and Little, 2003; Little, et al., 2002). It is likely that such a combined model can also be used to describe other multilayered materials like floor covering (e.g. laminate) and furniture.

2.4.7 Totally empirical models

The previous described models use physicochemical data of the compounds and information about the environmental conditions of the system to predict the emission behavior and concentration development. However, some parameters (e.g. sink parameters) have to be determined via regression of the model to experimental data. This reduces the approach from an “ab initio” calculation to a semi-empirical calculation. By ignoring the system-related parameters a total empirical model can also be used. In this case all parameters are obtained via regression.

Especially to assess the sink effects of emission test chambers this approach can be used. The first model was proposed by Dunn (1987) that was able to distinguish

between sources with constant or decreasing emission rate. The applicability was shown by Dunn and Tichenor (1988). The parameters of this model are fitted to the experimental data via multi-variant analysis and allow the comparison of measurements in the same system and similar materials. Total empirical models are useful if the system has a reduced complexity (like emission test chambers) compared to the indoor environment and thus allows extrapolations on analog experiments. A transfer of such a model to describe the indoor environment is associated with a higher error than the previously described emission models due to their higher flexibility.

2.4.8 Specifics of the SVOC modeling

For the description of SVOC indoors the complexity of the shown emission models can be reduced without changing their conclusions. For most sources of SVOC the initial concentration in the material is high. PVC floor covering contained high amounts of DEHP up to 17 % (Clausen, et al., 2004) and even 30 % (Cadogan and Howick, 1996). Xu and Little (2006) showed that such a system behaves similar to a liquid phase of DEHP. In such a case the diffusion in the material can be ignored due to the “sweating” of the material. Also the initial concentration in the material becomes less important. The compound evaporates at the surface into the boundary layer establishing a concentration near the saturation concentration. Then, the emission is only controlled by the external mass-transfer-coefficient and the gradient between well-mixed gas phase concentration and boundary layer concentration (Weschler and Nazaroff, 2008). The emission rate is reduced to (2.51).

$$SER_A(t) = h_m(y_0 - y(t)) \tag{2.51}$$

If a mass-balance equation is used that considers both, sorption interactions and additional mass-exchange due to present particles (like equation (2.39)), this simplified approach can be used to model the partition of SVOC indoors.

2.4.9 Summary

With the exception of the total empirical models all presented models base on the solutions of the second Fickian law. The individual differences result from different assumptions and simplifications that limit the usage in some cases. Even though some models are called “analytical models” each needs a numerical solution of the

equation in some ways. Regarding its flexibility the model proposed by Xu and Little (2006) is superior due to the broad formulation of the mass-balance equation.

If the material under observation shows no diffusion hindrance of the compound release the complex mass-transfer-term developed by Xu and Zhang (2003) can be reduced to two governing parameters: the concentration in the boundary layer (y_0) and the external mass-transfer-coefficient (h_m). The first parameter can be derived from the vapor pressure of the compound or experimentally and the latter one by correlation equations using the environmental parameters. The considered parameters of the presented models are summarized in Table 8.

Table 8: Summary of model properties

Model	Validated for		Solution	Considers			
	VOC	SVOC		BL	K_S	K_P	y_{in}
(Little, et al., 1994)	x	-	analytical*	-	-	-	-
(Huang and Haghighat, 2002)	x	-	numerical/ analytical	x	-	-	x
(Xu and Zhang, 2003)	x	-	numerical	x	-	-	-
(Xu and Little, 2006)	-	x	numerical	x	x	x	x
(Deng and Kim, 2004)	x	-	analytical*	x	-	-	-
(Begley, et al., 2005)	-	(x)	analytical*	-	-	-	-

* contains numerical solution of the transcendental equation ; (x) without phase transfer

The main problem of the modeling approach is the derivation of some parameters by regression to the model. Other parameters, like the mass-transfer-coefficient, are derived from correlation equations and are consequently also a result of regression. This reduces the desired “ab initio” calculation to a semi-empirical approach.

3. Material and methods

The performed experiments needed the determination of phthalates in air and solid matrices (e.g. dust). To assure controlled environmental conditions for the experiments they were performed in various test chambers. A summary of the applied analytical devices will be provided in the following.

3.1 Materials

3.1.1 Chemicals

The plasticizers DBP and DEHP were used in two different purities depending on their experimental usage.

Di-2(ethylhexyl)phthalate (PESTANAL®, analytical standard) from Sigma-Aldrich.

Di-2(ethylhexyl)phthalate (purity 98 %) from ABCR GmbH & Co. KG.

Di-n-butylphthalate (PESTANAL®, analytical standard) from Sigma-Aldrich.

Di-n-butylphthalate (purity 99 %) from ABCR GmbH & Co. KG.

The high-purity compounds were used as analytical standards for the GC/MS analysis while the lower-quality compounds are used for the experiment described under 3.3.3. Standard solutions of the plasticizers were prepared in

Methanol (picrograde®, purity ≥ 99%) from LGC Promochem.

For extraction purpose the following solvents were used:

Acetone (picrograde®, purity ≥ 99%) from LGC Promochem.

Toluene (picrograde®, purity ≥ 99%) from LGC Promochem.

For the experiment 3.3.6

Carbon nanopowder < 50nm (BET), 99+% (amorphous) from Sigma-Aldrich

was used.

3.1.2 Paints

For the purpose of this study two types of plasticizer-endowed wall paints are used: emulsion paints and a latex paint. The paints were manufactured and endowed by Caparol. The different types and composition of the used paints are given in Table 9.

Table 9: List of endowed paints

Paint	Type	Content*
A	Emulsion paint	1 % DBP
B	Emulsion paint	1 % DEHP
C	Latex paint	1 % DBP
D	Latex paint	1 % DEHP
E	Emulsion paint	0.5 % DBP / 0.5 % DEHP

* given by manufacturer

For each experiment the content of the paint is checked by liquid extraction (acetone) of a paint sample and analysis via CIS-GC/MS. Before applying the paints they are mixed for 10 min using a mechanical stirrer.

3.1.3 PVC materials

PVC samples with known composition were manufactured by Byk Additives & Instruments for this study. In total, two endowed PVC polymers are used: Polymer A contains 96 % PVC Solvin 264 PC and 4 % DEHP while polymer B contains 83 % PVC Solvin 264 PC and 17 % DEHP. Both polymers are stabilized with 1 % Baerostab OM 710 S. Each sample has a thickness of 1 mm.

3.1.4 Dust samples

Three dust samples were used during the experiments. All samples were taken from households without known contamination situation. The dust samples were sieved to the < 63 µm fraction using a vibration-sieving machine “Analysette” (Fritsch GmbH, Idar-Oberstein). The characterization of all used sorbent-samples is summarized in Table 11. Two dust samples (dust C and D) were used without further treatment while the third sample (dust E) was soxhleth-extracted for 16 h using acetone/n-hexane (1:1). All samples were stored in cleaned glass-bottles without contact to plasticizer-containing materials.

3.2 Test and analytical equipment

3.2.1 Emission test chambers

Several experiments of the present study were performed in emission test chambers that fulfill the specifications of ISO 16000-9 (2006). The tolerance of temperature is ± 2℃ and the tolerance of relative humidity is ± 5 %. The air velocity ranges between 0.1 m s^{-1} and 0.3 m s^{-1} near the surface of the sample. Emission test chambers of different size and surface material were used.

1 m³ glass emission test chamber

The 1 m³ glass emission test chamber has dimensions of 0.8 m x 1 m x 1.26 m and contains a combined fan and heating unit. The (S)VOC/particle-free air enters the chamber from the top and is distributed in the chamber by the fan. The inflow is controlled by a mass-flow controller and the air humidity can be set by choosing the ratio of a dry and humid air stream. The chamber is cooled by the surrounding room air and is loaded from the top. Between the experiments the chamber is baked out at 65℃ for 24 h.

0.5 m³ stainless-steel emission test chamber

The 0.5 m³ stainless-steel emission test chamber has dimensions of 0.75 m x 1.03 m x 0.65 m. The chamber is loaded from the front and contains a stainless-steel fan on the opposite side of the door. The chamber itself is located in an enclosed box that is used to control the temperature. The temperature inside of the inner chamber is monitored by a temperature sensor that manages heating elements on the outer surface of the inner chamber. The mass-flow-controlled clean air enters the chamber near the fan. The air is humidified by a water bath that is tempered to the specific dew point (e.g. 12.02 ℃ for 50 % r.h. at 23 ℃ cha mber temperature).

3.2.2 Large climate chamber

The large climate chamber at WKI is separated by an exchangeable structural element into “warm chambers” (0 ℃ to 35 ℃) and “c ool chambers” (-40 ℃ to 60 ℃). The “warm chamber” side has a length of 8 m and is 3.6 m broad. The maximum height in the chambers is 2.5 m. The “warm chambers” can be segmented by

inserting insulated stainless-steel walls according to Figure 4. These sub-chambers are 1.8 m broad and feature a volume of ~ 18 m³.

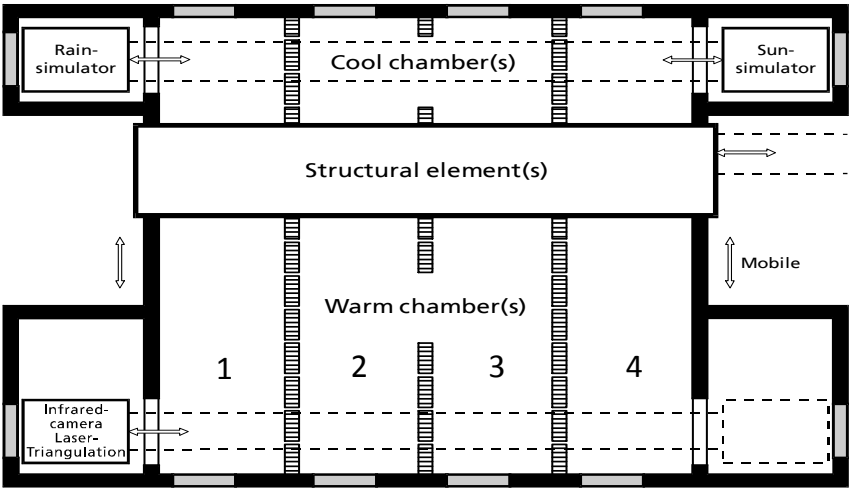

Figure 4: Schematic layout of the large climate chamber at WKI (taken from Greubel et al. (2001)).

The temperature is controlled by a heat-exchanger on top of each sub-chamber. The air humidity is adjusted in the range between 20% and 95 % by inserting water vapor into the chamber. The air exchange rate of the chamber cannot be set. The "natural" air exchange in each sub-chamber was measured to be ~ 0.1 h^{-1}.

3.2.3 Tube chambers

Two types of sink-minimized tube chambers were constructed for the determination of aerosol/phthalate interactions. Main differences are the used construction materials. One type is made from polyvinylchloride (PVC) while the second type is mainly polymethyl-methacrylat (PMMA). The chambers are purged with (S)VOC/particle-free nitrogen and the flow is set by a mass-flow controller. The chambers are located in a climatic room at 23℃ and 50 % relative humidity.

PVC chambers

The PVC tube chambers have a length of 1.3 m and an inner diameter of 10 cm. At the inlet and outlet of the tube mixing chambers are attached that contain a PVC grid.

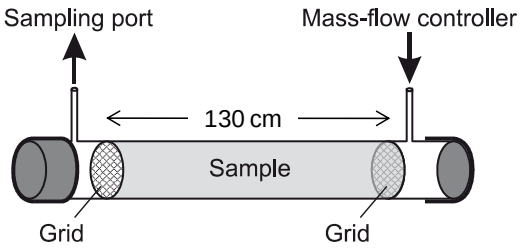

Figure 5: Scheme of the used PVC tube chambers

These pre- and post-chambers provide a laminar inflow and sampling of a well-mixed chamber air. A schematic description of this chamber type is shown in Figure 5. The volume of the tube is 10.2 L and the inlet- and outlet-chambers have an additional volume of 0.8 L.

PMMA tubes

The PMMA tube chambers have a length of 0.65 m and an inner diameter of 10 cm. The air enters the tube through a small hole on one side of the chamber and flows through a stainless-steel grid. After passing the sample, the air flows through another stainless-steel grid and leaves the chamber through a hole in the middle of the cover. The total volume of the chamber is ~ 5.1 L.

3.2.4 Analytics

Air sampling is performed using stainless-steel tubes (ø 6,35 mm, l 9 cm) filled with 350 mg Tenax TA 60/80. Before sampling, the tubes are conditioned with nitrogen at 300 °C in a TC-20 Tube Conditioner (Markes Int.). Sampling of a defined air volume is done using a FLEC air pump (Chematec). The tube is sealed airtight after sampling, thermally desorbed, and measured by coupled gas chromatography and mass-spectrometry. The quantification is done on the basis of phthalate-standards that were applied on tenax tubes as methanol solution.

The extraction of solid samples (e.g. dust and paints) is performed by weighing a defined amount of sample in a 10 mL measuring flask. 5 mL of a suitable solvent is added and the mixture is placed in a sonic bath for 3 x 5 min. In the time gaps the solvent is cooled down for 5 min. The extract is filtered by a 0.2 µm PTFE filter and measured via CIS-GC/MS.

A summary of the used analytical systems is given in Table 10.

Table 10: List of used analytical systems for the analysis of phthalates

	GC1 (TD/GC/MS)	GC2 (TD/GC/MS)	GC3 (CIS-GC/MS)
Gas chromatograph	7890A GC System, Agilent Technologies	HP 5890, Hewlett-Packard	HP 6890 GC
Detector	5975C inert XL Mass selective detector, Agilent Technologies	FID	HP 5973 MSD
Thermal desorber	UltrA TD (Autosampler)/Unity, Markes Int.	TurboMatrix ATD, Perkin-Elmer	
Column	DB-5MS, Capillary 25mm*60m*0.25µm	ZB-5, Capillary 25mm*20m*0.25µm	DB-5MS, Capillary 25mm*30m*0.25µm
GC-method	50℃ (2 min) with 15℃/min to 170℃ (0 min) with 5℃/min to 220℃ (0 min) with 4℃/min to 280℃ (10 min) ; SIM (m/z 149, 234)	50℃ (2 min) with 10℃/min to 325℃ (15 min)	100℃ (2 min) with 10℃/min to 325℃ (15.5 min) SIM (m/z 149, 234)
Injector/TD-method	Transfer/Valve: 200℃	Transfer/Valve: 280℃	Cold In jection System, Gerstel: 60℃
Primary TD	T (tube)=300℃; T (trap)=-10℃; t (purge)=1min; t (desorb)=30min	T (tube)=300℃; T (trap)=-30℃; t (purge)=1min; t (desorb)=15min	-
Secondary TD	T (trap)=300℃; t (trap)=8min	T (trap)=310℃ mit 40℃/s; t (trap)=12min	-

3.3 Experimental setup

3.3.1 Measurement of DBP/DEHP emission from paints

The experiments are performed over 14 days in two 1 m^3 glass emission test chambers at 23℃ and 50 % relative humidity. The air exchange is set to 1 h^{-1}. Each chamber is equipped with a fogging apparatus which consists of a cooled aluminum corpus (15℃) that holds two clean stainless-steel plates (15 cm x 15 cm). After 14 days the fogging plates are removed and extracted in acetone for 2 x 15 min in a sonic bath. Prior to the experiment a blank measurement of each chamber was performed. Thereafter, endowed wall paints (paint A and paint B, see Table 9) are applied each on 3 glass plates with dimensions of 1 m x 0.33 m. The paints dried for one week in the laboratory and are loaded in the chamber afterwards. Sampling on Tenax TA takes place with a sampling volume of 20 L after 1, 2, 3, 7, 10, and 14 days. The Tenax tubes are analyzed via TD/GC/MS (GC1) and the fogging extract is analyzed via CIS-GC/MS (GC3).

The experiment is repeated analogously with the endowed latex paints C and D.

3.3.2 Measurement of DBP/DEHP emission from a wall paint and uptake into dust

For the following experiment two 0.5 m^3 stainless-steel chambers (A and B) are used. The temperature of the chambers is set to 23℃. The incoming air is dry (~ 10 % relative humidity) and enters the chamber with 1 L/min (n = 0.12 h^{-1}). Chamber B is known to feature a lower air velocity than chamber A.

For both chambers three glass plates with a total length of 109 cm (36 cm/36 cm/37 cm) are coated with an endowed wall paint (paint A) using a 150 µm spreading knife of 23 cm width. The resulting loading factor is 0.5 m^2/m^3. The paint dried for 24 h in the laboratory. Prior loading of the chambers an area of 15 cm x 40 cm is cleaned on the inner surface of the door using acetone. The glass plates are placed inside of the 0.5 m^3 chamber together with a stainless-steel plate covered with 3 g extracted house dust (dust E, see Table 11). Sampling on Tenax TA is performed after 36, 38, 44, 47, 50, 51, 52, 55, 56, 58, and 59 days after loading of the chamber. The sampling volume is 6 L. After 45 days the dust is removed from the chamber and extracted in a sonic bath using acetone. At the same day, the cleaned door surface is

wiped with a pre-extracted tissue. This tissue is extracted via soxhlet extraction for 48 h using acetone. The extracts are measured via CIS-GC/MS.

The experiment is repeated using the endowed wall paint B. Air samples are taken after 36, 44, 45, and 48 days on Tenax TA using a sampling volume of 10 L.

3.3.3 Measurement of pure liquid DBP/DEHP emission and uptake in various adsorbents

The same 0.5 m^3 stainless-steel emission test chambers (A and B) as used in previous experiment are loaded with two small petri dishes (ø 35 mm) filled with pure liquid DBP and DEHP. Prior loading of the chambers an area of 15 cm x 40 cm is cleaned on the inner surface of the door using acetone. The temperature of the chamber is set to 23℃ and the air humidity is ~ 10 % r.h.. The air exchange rate is 0.12 h^{-1}. Five different adsorbents are placed in the chamber. The total organic carbon of the adsorbents is analyzed via dry combustion according to ISO 10694, 1995. The results are summarized in Table 11.

Table 11: Characteristics of the five adsorbents of the pure liquid distribution experiment

Sample	Description	Total organic carbon [%]	Amount in chamber A [g]	Amount in chamber B [g]
A	Silica sand	~0	6.6	6.6
B	Soil	30	2.4	2.4
C	House dust 1	16	0.8	0.8
D	House dust 2	36	0.5	0.5
E	House dust 3*	18	0.6	0.6

* extracted dust sample

Air sampling is performed on Tenax TA between day 11 and 45 after insertion of the samples. A sampling volume of 9 L is used. The tubes are measured via TD/GC/MS. After 45 days the adsorbents are removed from the chamber and extracted in a sonic bath using acetone. Wipe samples are taken from the cleaned surface at the chamber door and the tissues are extracted via soxhleth extraction for 48 h. The extracts are measured via CIS-GC/MS.

3.3.4 Measurement of the DBP/DEHP emission from wall paints in a large climate chamber

The determination of the distribution of DBP and DEHP in a simulated indoor environment is performed in the large climate chamber of WKI. The structural element between the “warm chambers” and “cold chambers” is a double layered brick wall (30 cm) that contains four square single-layered segments (19 cm). The “warm chamber” side is segmented according to Figure 4 (Chamber 1-4). The “cold chamber” side is set to a temperature of ~5℃. Due to the irregular thickness of the wall thermal bridges are established within each chamber. On the front end of each sub-chamber (attached to the brick wall, below the thermal bridge) a heater is installed. The heater is set to moderate temperature (half of maximum strength). With the exception of the door side, the stainless-steel walls are equipped with gypsum plaster boards. The gypsum boards and the structural element are covered with ingrain wallpaper. Endowed wall paint containing 0.5 % DBP and 0.5 % DEHP (paint E) is applied on the surfaces according to the following list:

- Chamber 1: gypsum board and structural element are painted with endowed paint.
- Chamber 2: only the gypsum boards are painted with endowed paint.
- Chamber 3: only the structural element is painted with endowed paint.
- Chamber 4: none of the walls is painted with endowed paint.

The remaining walls are painted with non-endowed wall paint. The same fogging apparatus as used in 3.3.1 is installed in chamber 1 and 4. Sampling on Tenax TA is performed via holes in the ceiling above the heater in each sub-chamber at day 1-30 after applying the paint. The sampling volume is chosen to 20 L. The tubes are analyzed using a TD/GC/MS. The fogging apparatus is removed after 14 days. The plates are extracted in a sonic bath using acetone. The extracts are measured via CIS-GC/MS.

This experiment was performed in the framework of the UBA research project “Black Magic Dust (BMD)” (UFOPLAN Ref. No. 205 61 231, 2007).

3.3.5 Measurement of DBP/DEHP emission from wall paint in a tube chamber (PVC)

Two ingrain wall papers with each an area of 0.4 m² are painted with endowed wall paints. The first sample is prepared with paint A (1 % DBP) and the second sample is prepared with paint B (1 % DEHP). The backside of the wall paper is wrapped with aluminum foil. The two samples are placed in two PVC tube chambers so that the sample covers the inner surface of the tube. The flow through each chamber is set to 160 mL/min. Air samples are taken on Tenax TA within 50 days after insertion of the sample using a sampling volume of 9 L. The Tenax tubes are analyzed via TD/GC/MS.

3.3.6 Determination of the gas phase/particle interaction of DEHP in a tube chamber (PMMA)

Ingrain wall paper is cut to 0.2 m² and painted with paint B (1 % DEHP). The backside of the wall paper is covered with aluminum foil and the sample is placed in a PMMA tube chamber. The chamber is supplied with air from an aerosol generator (Model 3076 constant output atomizer, TSI Inc.) followed by a diffusion dryer (Model 3062, TSI Inc.) and a neutralizer (Model 3077A, TSI Inc.). The source solution of the atomizer contains 2 mg carbon nanopowder <50 nm (Aldrich) in 1 L distilled water. The solution is dispersed in a sonic bath and constantly stirred afterwards using a magnetic stirrer. The aerosol generator is operated at 2.5 bar (nitrogen). After installation of the generator, the particle size distribution of the aerosol is measured by a fast mobility particle sizer (Model 3091, TSI Inc.). The assembly of the experiment is illustrated in Figure 6. The flow through the system (~ 150 mL/min) is determined by the nitrogen pressure at the aerosol generator.

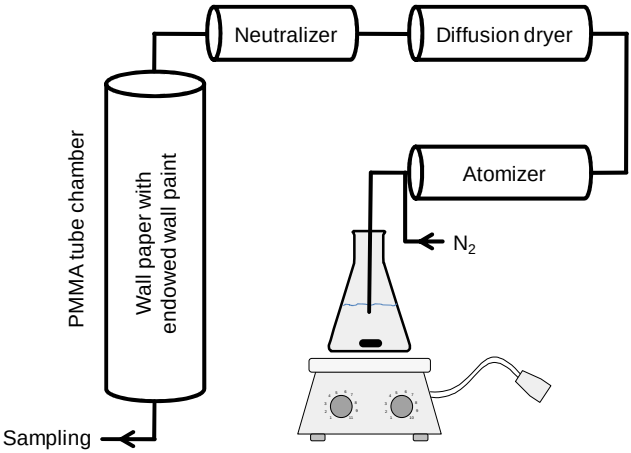

Figure 6: Scheme of the experimental determination of phthalate/particle interactions

Two types of adsorbents are used for air sampling. Beside Tenax TA tubes, stainless-steel tubes containing quartz wool are prepared. For the weak quartz adsorbent, sampling is performed with two tubes in a row to measure breakthrough. The sampling volume is chosen to 432 L for both adsorbents. The sampling tubes are analyzed via TD/GC/MS.

The tubes were prepared solely for this experiment and have been cleaned thoroughly. After cleaning them in a tube conditioner (see above) for 2 hours at 300℃ the blank of the tube is measured via TD/GC/M S. No tube showed a blank of DEHP.

To confirm the results, the whole experiment is performed twice.

3.3.7 Measurement of the DEHP uptake into dust from an endowed polymer

Two glass flasks with an interior volume of 2.8 L are equipped with a two-stage framework. Below, a magnetic stirrer, that carries fan blades, is operated. Within chamber 1 the air velocity is measured to be 0.25 m/s while in chamber 2 the air velocity is 0.1 m/s. Clean nitrogen enters the flask from the top at a flow of 50 mL/min ($n \approx 1.1\ h^{-1}$). The flasks are placed in a climatic room at 23℃ and 50 % relative humidity.

The PVC polymers A and B were used for this experiment.

The polymers are placed on the first stage and 130 mg dust (dust E, see Table 11) is directly applied on the polymer surface. On the second stage a petri dish that contains also 130 mg dust E is placed. The scheme of the experiment is shown in Figure 7. The system is operated for 14 days. Afterwards, both dust samples are extracted using acetone and a sonic bath. The extract is measured via CIS-GC/MS.

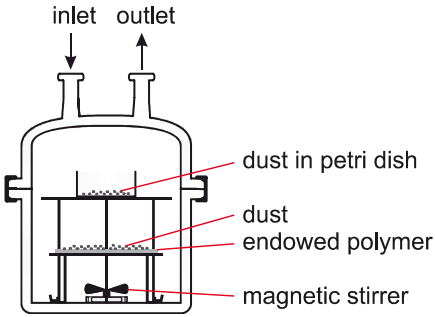

Figure 7: Scheme of 3 L glass flask experiment

4. Results and Discussion

4.1 Emission of plasticizers

The emission of additives from polymer materials is influenced by several parameters. As mentioned above, knowledge about these material-specific and environmental specific parameters in combination with feasible emission models allow the prediction of the gas phase concentration of the compound under the given conditions. Several experiments were performed using dibutylphthalate and bis(2-ethylhexyl)phthalate as target compounds. The experimental results were compared with predictions of an emission model. Due to the considerations in chapter 2.4 the emission model by Xu and Little (2006) was chosen. The mass-transfer-coefficient was calculated on the basis of equation (2.38) and the mass-balance equation (2.39) was used. The equations were solved numerically using MATLAB 7.7 (MathWorks Inc.). The algorithm solves the transcendental equation (2.36) by the Gaussian iteration method. The same method is used to find the solution of the mass-balance equation of the observed system. The iteration stops when the difference between actual and prior value is below 0.001 %.

Some modeling parameters are known due to the setup of the experiment. Other parameters can be derived from a multivariate data analysis that delivers the best fit to the experimental data. However, the concentration in the boundary layer is exceptional. This parameter is an important link between the mass-transfer-coefficient and the diffusion coefficient. The only limitation of y_0 is given by the fact that this concentration has to be lower or equal to the saturation concentration of the compound in air. For the two compounds a vast range of measured vapor pressures exist that hinders the determination of the real saturation concentration. Additionally, the experimental determination of y_0 is impossible without disturbing the characteristics of the boundary layer. As a consequence, this parameter has to be fixed to a certain value that concerns experimental and theoretical aspects. Then, the calculation of other parameters like the diffusion coefficient, mass-transfer-coefficient, and sorption coefficient is corresponding to this given value. However, the performed experiments, that often use strong sources and low ventilation, deliver another limitation of the parameter. The concentration in the boundary layer has to be equal or higher than the highest detected air concentration during the experiments. The

highest concentrations were found during the tube experiments that showed DEHP concentrations in the range of 1 µg m^{-3} and for DBP ~160 µg m^{-3}. For DEHP the value stated by Xu and Little (2006) (y_0 = 1.10 µg m^{-3}) is feasible. Regarding DBP the boundary layer concentration was set to 160 µg m^{-3} due to the found concentrations and the saturation concentration basing on the vapor pressure from the Antoine equation (168 µg m^{-3}). The latter value was found to be the most reasonable vapor pressure for DBP by Weschler et al. (2008). The following determination of parameters by residual analysis bases on the given boundary layer concentrations.

4.1.1 Measurement of endowed paints in 1 m³ glass chambers

The content of the used wall paints was determined via solvent extraction. The results are displayed in Table 12. The paint was inserted into the 1 m³ glass chamber on glass plates. Air and fogging measurements were performed in the following 14 days. Results of the fogging measurement are summarized in Table 13 and the air concentrations are listed in Table 14.

Table 12: Results of the content analysis of the endowed wall paints A-D.

Sample	Target content [g kg^{-1}]	Actual content [g kg^{-1}]
Paint A (Dispersion, DBP)	10	14.0
Paint B (Dispersion, DEHP)	10	12.5
Paint C (Latex, DBP)	10	9.2
Paint D (Latex, DEHP)	10	9.2

The fogging measurements showed the presence of the other plasticizer (DBP/DEHP) than the endowed one. Contaminations of DEHP were expected because this compound is ubiquitous in the environment and residues can remain in an emission chamber which has been baked out. This assumption is supported by the blank measurements that showed DEHP concentrations in the range of ~ 6 % of the samples results. A correlation between the fogging results and the observed air concentrations could not be detected. A DBP contamination is only present in case of the wall paint and might result from the technical standard that was used to endow the paint.

Table 13: Results of fogging measurements of wall paints A-D in a 1m³ glass chamber.

Chamber	Sample	m(DEHP) [µg]	m(DBP) [µg]
	Blank (Fogging-apparatus)	0.5	0.3
Chamber A	Blank	3.1	0.3
	Paint A (Dispersion, DBP)	13.6	39.2
	Paint B (Dispersion, DEHP)	56.3	8.3
Chamber B	Blank	2.0	0.2
	Paint C (Latex, DBP)	17.5	9.4
	Paint D (Latex, DEHP)	36.1	< 0.1

The concentrations of DEHP in the chamber air are near or below the limit of detection. This is expected because the chamber walls and the fogging-apparatus are supposed to be strong sinks for DEHP that lower the air concentration considerably. A trend in the concentration development cannot be derived from the results. In the case of DBP the results are different due to the higher vapor pressure of the substance. The measured concentrations are more than a factor 100 higher than the measured DEHP concentrations. An increase of the DBP air concentration can be observed for both paints that has a peak value in the case of the wall paint after 7 days. This rapid increase of the concentrations in the case of the wall paint compared to the latex paint can be explained by two opposing effects. First, the endowed amount of DBP was higher in the case of the wall paint. Second, the latex paint forms a dense polymer surface that affects the emission rate due to the diffusion through the polymer.

Table 14: Results of air concentration measurements of DBP and DEHP from wall paints A-D in a 1 m³ glass chamber.

	[DBP] [µg m^{-3}]		[DEHP] [µg m^{-3}]	
Day	Paint A	Paint C	Paint B	Paint D
1	32.7	0.3	0.7	< 0.2
2	68.5	4.5	< 0.2	< 0.2
3	93.3	43.5	< 0.2	< 0.2
7	108.5	47.9	< 0.2	0.2
10	103.4	54.0	< 0.2	< 0.2
14	88.2	54.6	0.6	< 0.2

The reliability of the detected DEHP concentrations is lowered by the small sampling volume. It cannot be excluded that the observed concentrations above the limit of detection are artifacts of contamination. It seems that DBP redesorbs from the

fogging plate while they are a final sink for DEHP because the air concentrations of DBP are higher but the fogging results are lower than the comparable results for DEHP. However, the observed values for the fogging measurements of DEHP show a good consistency with published results. When performing similar experiments with wall coverings Uhde et al. (2001) found maximal fogging values of 60.37 µg after 14 days. The air concentrations of DBP in these experiments were much lower than the present experiments (~ 5 µg m^{-3}) and, therefore, the fogging results are much different. It is important to note that the comparison of fogging measurements is limited to identical conditions. In this case the chambers and the fogging apparatus were the same while the only deviation is the 5 % smaller air humidity (T = 296 K; 45 % r.h.; L = 1 m^2 m^{-3}; n = 1 h^{-1}). The influence of the air humidity on the sorption behavior of plasticizer is expected to be low in this case and, therefore, the direct comparison of present values with the cited values is allowed.

The setup of the glass chamber experiments allows the calculation of the mass-transfer coefficient on the basis of the correlation equations by Axley (1991). The air flows directed over the flat sample surface with a velocity of 3 m s^{-1}. Due to the small resulting boundary layer the mass-transfer into the air is elevated. As a result, the air concentrations should be slightly affected by the thickness of the boundary layer but more by the diffusion of the compound in the material. Additionally, the sorption of the chamber influences the increase in concentration. These two parameters (K_s and D_m) were used to perform a residue analysis for the results of the model by Xu and Little (2006). K_s and D_m were increased in small steps and the resulting residue matrix was recorded. The matrix minimum gives the set of parameters with a good fit to the experimental data. The sorption coefficient in both experiments should be nearly the same because it is a chamber-specific parameter while the diffusion coefficient is expected to be lower in the case of latex paint. This results from the denser matrix and the raised molecular interactions. The model by Xu and Little (2006) was used to predict the development of the gas phase concentration of DBP on the basis of the experimental parameters. The height of the paint layer (160 µm) was calculated using a density of 1.5 g cm^{-3} and the amount of paint that was applied on the 1 m^2 glass surface. The initial concentration was measured previously by solvent extraction of the wet paint.

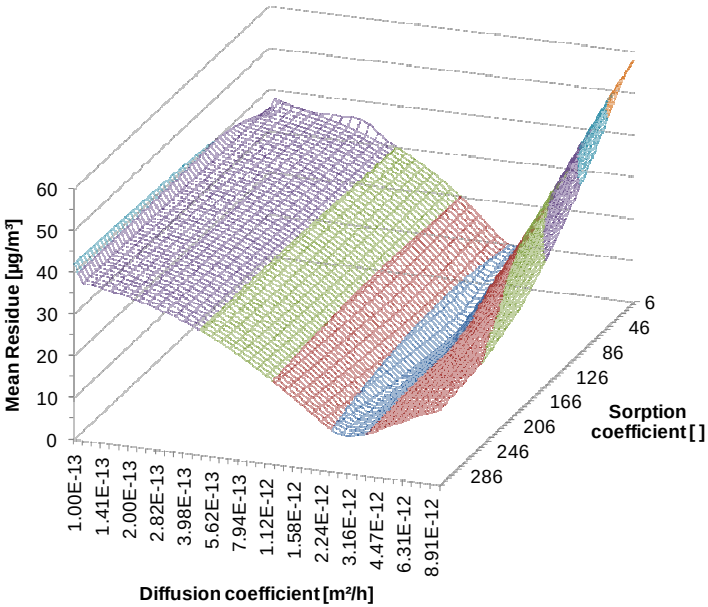

Figure 8: Results of the residual analysis for paint C in a 1 m³ glass chamber.

The results of the residual analysis of the latex paint are shown in Figure 8. Within a small combination of diffusion coefficient and sorption coefficient the mean deviation between experimental value and modeled value is below 7 µg m^{-3}. The diagram illustrates that the deviations are small for a narrow range of diffusion coefficients but a broad range of sorption coefficients. The derived set of parameters (see Table 15) provides a good correlation of the modeled values to the experimental values (see Figure 9). The diagram shows a large deviation between predicted and measured concentration for the first day. Within the first 24 h of the experiment the slope of the concentration/time-curve is high. As a consequence of the long sampling time and the non-constant emission profile the standard deviation of this measuring point is elevated against the later measured values. Otherwise, the applied model assumes a continuous development of the emission rate over time. Therefore, a deviation of the first data point has to be tolerated.

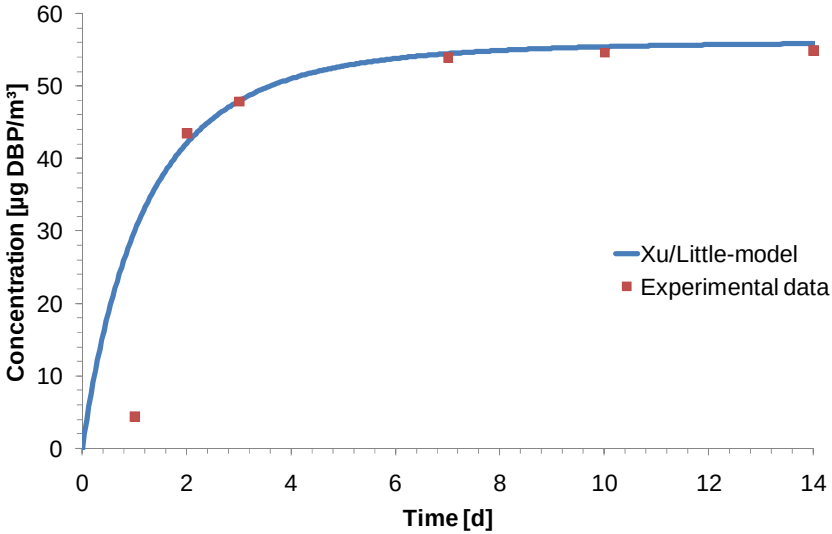

Figure 9: Correlation between experimental results of paint C in a 1 m³ glass chamber (Table 14) and the emission model for the combination of D_m and K_s obtained by the residual analysis (mean Residue = 4.8 µg m^{-3}).

In the case of the wall paint the mathematical analysis also delivers a set of parameters that allows a residue-minimized fit. In contrast to the latex paint the minimum is very confined. The values giving the lowest mean concentration residue between modeled results and experimental values at the present resolution are listed in Table 15.

Table 15: Modeling parameters of the glass chamber experiments of paint A and C. (Fitted values are written in bold.)

	Wall paint (paint A)	Latex paint (paint C)
V [m³]	1	1
Q [m³ h^{-1}]	1	1
$A_{Chamber}$ [m²]	5.1	5.1
A_{Sample} [m²]	1	1
C_0 [µg m^{-3}]	2.10^{10}	2.10^{10}
l [µm]	166	166
h_m [m h^{-1}]	7.56	7.56
y_0 [µg m^{-3}]	160	160
D_m [m² h^{-1}]	**$1.12.10^{-11}$**	**$2.51.10^{-12}$**
K [ ]	$1.31.10^{8}$	$1.31.10^{8}$
K_s [ ]	**90**	**111**
n_F [ ]	1	1

The correlation between modeled concentration development and experimental results is shown in Figure 11.

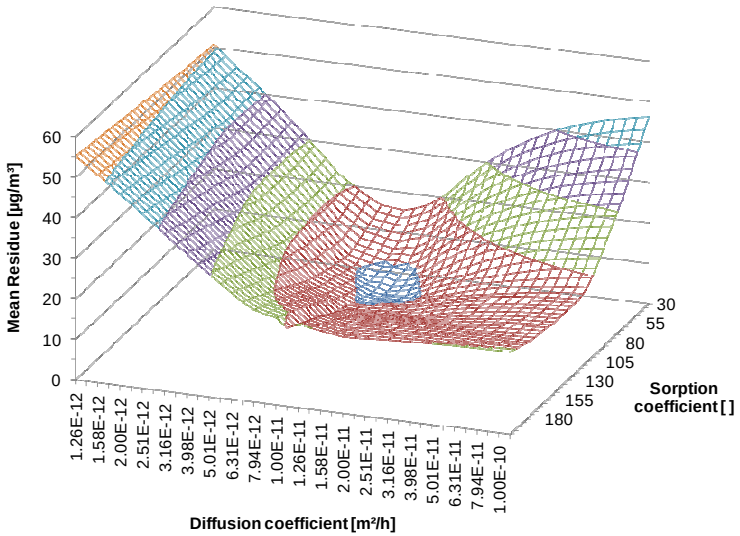

Figure 10: Results of the residual analysis for paint A in a 1 m³ glass chamber.

As expected the optimum sorption coefficient are only slightly different between the two experiments because this parameter is only connected to the compound and

surface specifics. The diffusion coefficient is lower in case of the latex paint which also correlates with the density of the dried material. The concentration development, predicted by the emission model, principially follows the trend of the experimental results. Anyhow, the results in Figure 11 show the weakness in the mathematical modeling. Within the first week the concentration rises and starts to decrease afterwards. The equilibrium concentration that is predicted by the model is consequently higher than the real equilibrium concentration. Like in the case of the 24 h measurement in Figure 9 the emission rate within the first week deviates considerably from the theory. This leads to a wrong derivation of the model parameters.

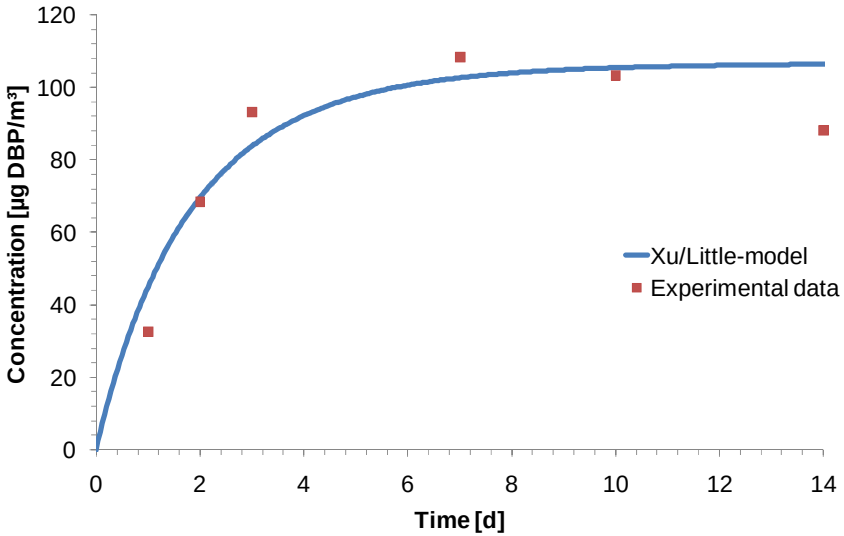

Figure 11: Correlation between experimental results of paint A in a 1 m³ glass chamber (Table 14) and the emission model for the combination of D_m and K_s obtained by the residual analysis (mean Residue = 7.9 µg m^{-3}).

In total, the residual analysis can be used to determine the diffusion coefficient of the material. This is only possible for this case because the mass-transfer coefficient is not governing the emission due to the small boundary layer. The sorption of DBP to the glass chamber is weak and allows a rapid development of an equilibrium concentration though the compound has a low vapor pressure. Within the further

experiments the wall paint was used. The determination of the diffusion coefficient was performed with a good correlation (Figure 10) but from the experimental results it is assumed that this value is associated with a high uncertainty.

The two different shapes of the matrices of the residual analysis illustrate a modeling problem. Even though the experimental data set allows a good estimation of the concentration development a clear minimum of the residual analysis (e.g. in Figure 8) could not be observed. Instead, a large variety of sorption coefficients can be found that feature a low mean deviation for a certain diffusion coefficient. In case of the analysis of the wall paint data a clear minimum can be found but is not the best fit for the experimental data.

To assess the adsorption behavior of the chamber a Freundlich isotherm was used in the model. This allows considering the sorption hindrance due to previously sorbed compound. In case of the glass chamber experimental data a linear isotherm ($n_F = 1$) was used because the influence of the first measuring point on the best fit for n_F was found to be great. In principle, n_F changes the shape of the curve at the beginning of the emission test. This is illustrated in Figure 12 for different n_F.

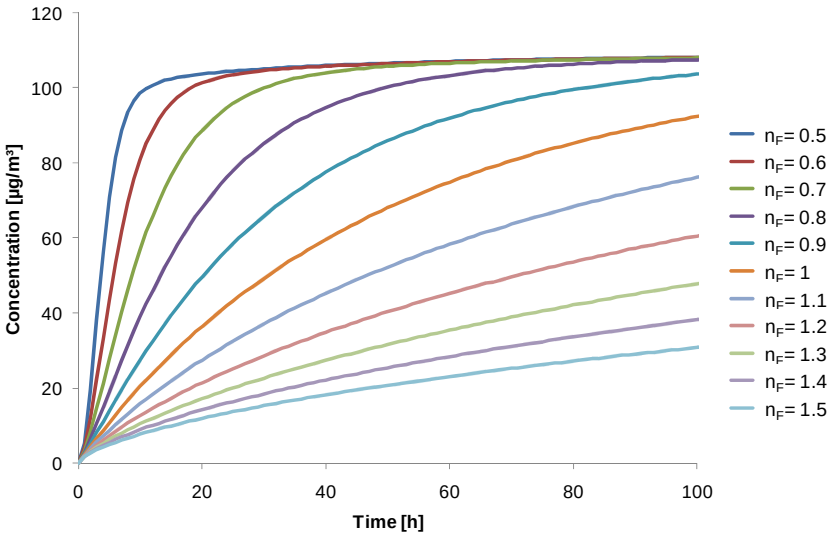

Figure 12: Predicted air concentrations (according to equation 2.39) at different n_F for $K_F = 100$. The other parameters are taken from the glass chamber experiment (Table 15).

Values of n_F above 1 are not reasonable for the used compounds but are reported in the literature (Xu and Little, 2006) due to fitting of experimental results. If n_F is higher than 1 the adsorption of compounds on the chamber wall promotes the further adsorption of the compounds on the surface. This effect might be observed if the surface gets covered with an organic liquid with a higher uptake-capacity for the given compound than the wall material. This effect could not be observed from the wipe samples in the present case.

If n_F is below 1 a sigmoid curve results. Such sigmodial curve is a better fit for the data shown in Figure 9 because the residue between the modeled value and the first measuring point decreases. If the uncertainty of the first data point is large, the fitting of n_F can lead to a wrong result. Additionally, changes in n_F have a vital impact on the value of K_s. In case of the second measurement in the glass chamber (Figure 11) the sigmoidal shape of the concentration curve is not observed. Due to the similarity of the chamber a similar sorption behavior is expected. The reason for these findings is a problem described in chapter 2.3. During the first days the emission profile is not constant while the sampling times are large. This leads to a high uncertainty in the results of the first days. Consequently, the detection of the sigmoidal shape of the concentration curve cannot be performed due to the low resolution of the results and the measuring uncertainty.

However, if the fitting of n_F is performed additional to the fitting of K_s a large deviation between the modeling parameters of the two measurements results. As a consequence, n_F was set constant to the value of the linear isotherm (n_F = 1) for every measurement to allow a better comparison between the sorption behavior of the different chambers.

4.1.2 Measurement in 0.5 m³ stainless-steel chambers

Emission of endowed paints

Like in the prior experiment changes in the phthalate content of the wall paint was checked via solvent extraction and GC/MS. For DBP the content was 0.98 % while for DEHP the content was lower with 0.79 %. The development of the air concentration of DBP in the two chambers is measured between the 36th and 59th day after insertion of the sample (see Table 16). The results demonstrate a considerable different emission behavior between the two chambers. In chamber 2

the measured concentration was 7 times lower than in chamber 1. After remove of the dust from the chambers at day 48 the air concentration increases in chamber 1. This increase is not very distinctive in chamber 2.

Table 16: DBP air concentrations of paint A in a 0.5 m³ chamber

Days after loading [d]	Chamber A [µg m^{-3}]	Chamber B [µg m^{-3}]
36	115	21
38	106	14
44	93	14
47	93	7
50	84	16
51	89	12
52	106	14
55	107	15
56	109	16
58	111	14
59	103	15

The repetition of the experiment using the DEHP endowed wall paint shows some deviating results (see Table 17). Regarding the wipe samples the measured values are slightly higher than for DBP while the air concentrations are much lower. A significant deviation between chamber 1 and 2 could not be observed from the DEHP measurements.

Table 17: DEHP air concentrations of paint B in a 0.5 m³ chamber

Days after loading [d]	Chamber A [µg m^{-3}]	Chamber B [µg m^{-3}]
36	1.2	0.3
44	0.6	0.4
45	0.9	< LOQ
48	1.5	0.5

The same paint which was used in the previous experiments was also used for the stainless-steel chamber experiments. It was also applied on glass plates and, thus, the diffusion in the material phase should be same as derived above. However, in this case the determination of the mass-transfer-coefficient is interfered by the setup of the glass plates in the chamber. The correlation equations by Axley (1991) are not feasible because the air flow over the plates is not directed and laminar. Therefore, this parameter has to be determined via regression. Basing on the previously

determined diffusion coefficient for this paint, h_m and K_s are changed in small steps and the residues to the experimental data are calculated. The experiment focused on the determination of the equilibrium air concentration and the concentrations within the first week were not measured. The development of the air concentration within the first days after insertion of the sample is mainly influenced by the sorption coefficient. This parameter has, basically, no influence on the equilibrium concentration. As a consequence, the range of sorption coefficient that allows a high correlation between experimental data and modeled concentration is broad (see Figure 13 and Figure 14). In contrast, the mass-transfer coefficient mainly influences the equilibrium concentration and shows a small range of values with low residues.

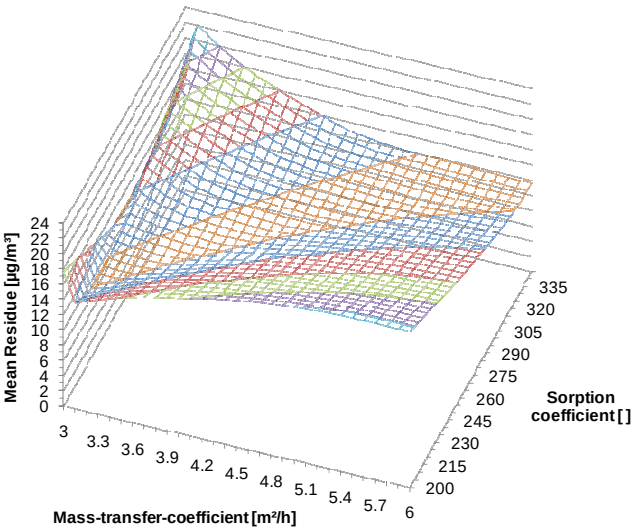

Figure 13: Results of the residual analysis for paint A in a 0.5 m³ chamber (Chamber A).

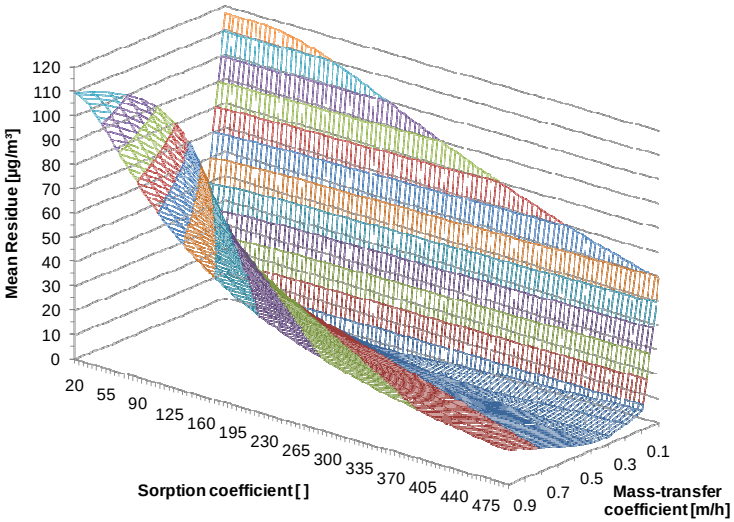

Figure 14: Results of the residual analysis for paint A in a 0.5 m³ chamber (Chamber B).

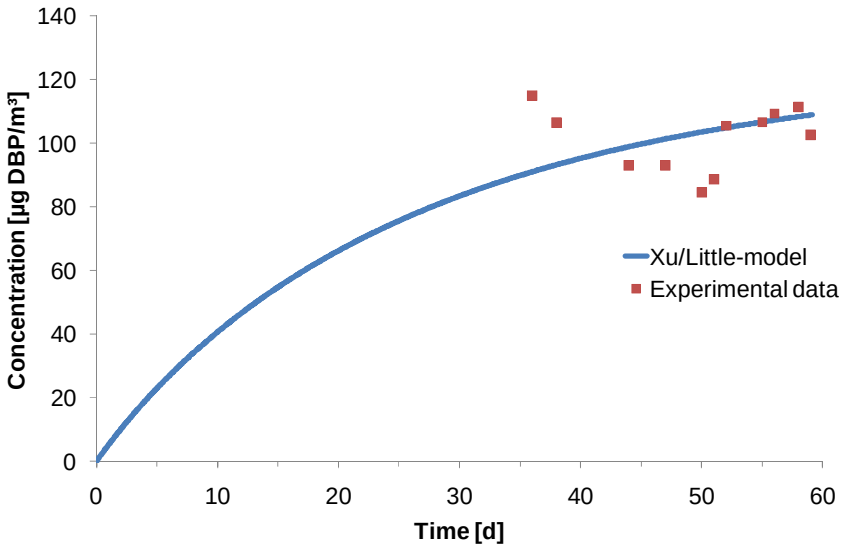

Figure 15: Experimental data of paint A (Table 16) and modeled concentrations for the combination of K_s and h_m with the lowest residues (Chamber A).

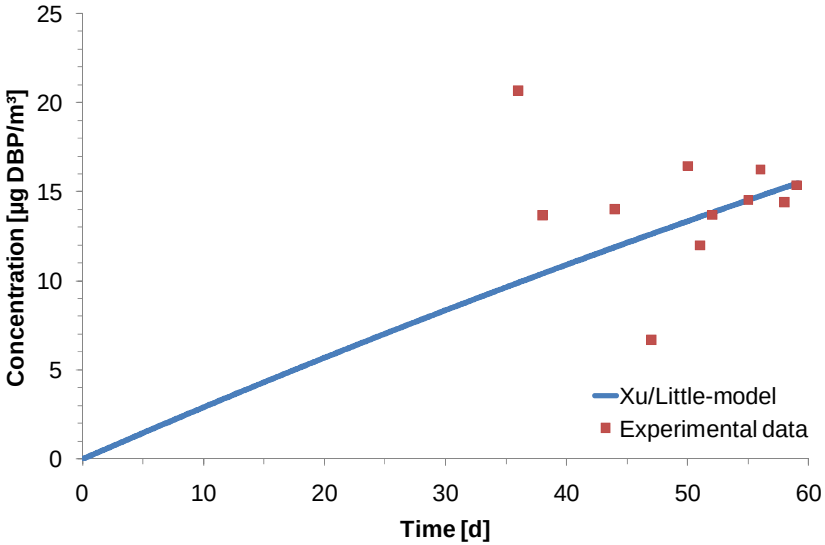

Figure 16: Experimental data of paint A (Table 16) and modeled concentrations for the combination of K_s and h_m with the lowest residues (Chamber B).

The parameters of the modeling are summarized in Table 18. The fitting of the model to the experimental data principally fails due to the missing information about the concentration development within the first days after insertion of the sample. Especially in case of the experiment in chamber B an extrapolation of the concentration development on the basis of the available data is of high uncertainty.

From the modeled results the main difference between the two chambers can be derived. The mass-transfer coefficient is ~30 times lower in chamber 2 than in chamber 1. This is an expected fact because the air velocity on the surface on the sample is different. In case of chamber B the mixing fan in the chamber works with reduced performance and establishes a low velocity air pattern. This directly reduces the mass-transfer coefficient compared to chamber A because the boundary layer is thicker than in the well-mixed chamber. As a consequence, the build-up of DBP in the chamber air is delayed and the expected equilibrium concentration is lower.

Table 18: Modeling parameters of the 0.5 m³ chamber experiments of paint A. (Fitted values are written in bold.)

	Chamber A	Chamber B
V [m³]	0.5	0.5
Q [m³ h^{-1}]	0.06	0.06
$A_{Chamber}$ [m²]	3.8	3.8
A_{Sample} [m²]	0.25	0.25
C_0 [µg m^{-3}]	$2.10 \cdot 10^{10}$	$2.10 \cdot 10^{10}$
l [µm]	150	150
h_m [m h^{-1}]	**5.9**	**0.2**
y_0 [µg m^{-3}]	160	160
D_m [m² h^{-1}]	$1.221 \cdot 10^{-11}$	$1.221.10^{-11}$
K [ ]	$9.1675 \cdot 10^{6}$	$9.1675 \cdot 10^{6}$
K_s [ ]	**340**	**230**
n_F [ ]	1	1

Regarding the time to reach equilibrium conditions the loading factor is half the value of the 1 m³ emission test chambers. Additionally, the ratio of sample area to free chamber area is much larger in case of the 1 m³ chamber than the 0.5 m³ chamber. These two facts lead to a lower emission and higher sorption of the compound and, thus, increase the time considerably in which the system reaches an equilibrium concentration.

Emissions from pure liquid DBP/DEHP

To get more information about the quality of the parameters that were derived from the residual analysis another experiment with another emission source is necessary. If the diffusion of the compound in the emission source can be neglected a better determination of the sorption behavior of the chamber is available. For this reason, the experiment is replicated with pure liquid DBP and DEHP. The liquids were placed in the same chambers in open petri dishes. Samples were taken from day 11 to day 45 after insertion of the samples. The air concentrations of DBP were lower than the previous experiment. The development of the air concentration of DBP is displayed in Figure 17.

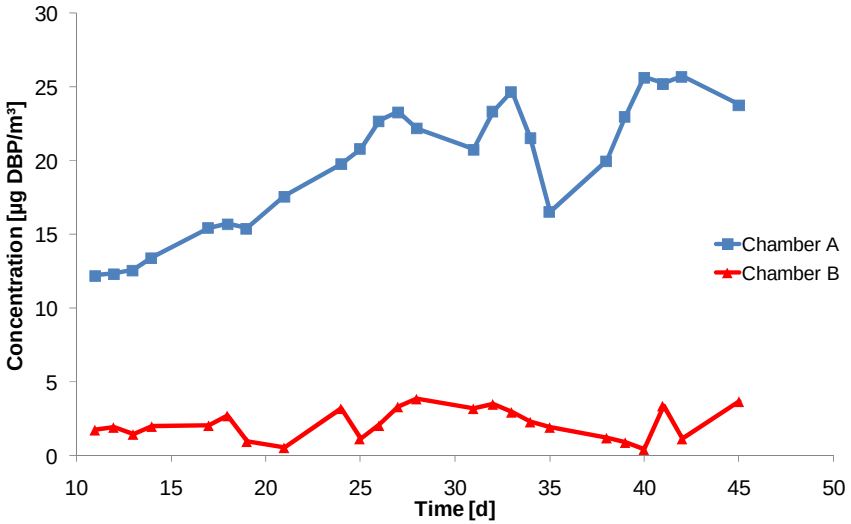

Figure 17: Development of the DBP air concentration in the two stainless-steel chambers over 45 days from pure liquid DBP.

The mass transfer by air exchange was as low as in the experiment using endowed wall paints but the emission source is less strong. The diffusion hindrance of the material is smaller but also is the emitting area. Additionally, the sorbent loading of the chamber is five times higher than in the previous experiment. This leads to an increase in the time to reach equilibrium conditions in the chamber. In both chambers the air concentration undergoes fluctuations which complicate the identification of the equilibrium concentration. However, the concentrations show the same deviation between chamber A and B like in the previous experiment.

Again, this deviation cannot be observed from the DEHP measurements. The results, that show high fluctuations, are displayed in Figure 18. From the DEHP concentrations neither a difference between the chambers nor an equilibrium concentration can be derived. The used method seems to have a high uncertainty for DEHP but that is not a result of artifacts because the analysis was performed with a blank tube between the loaded ones. The chromatograms of these tubes showed DEHP below the limit of detection.

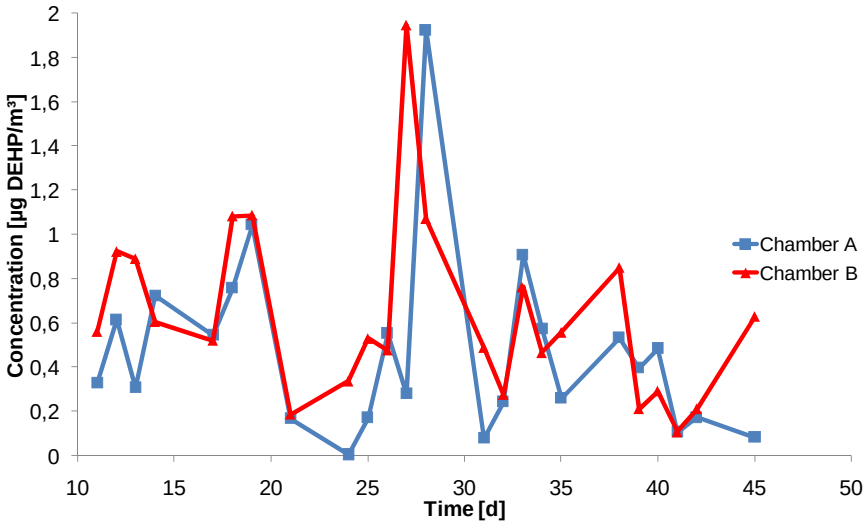

Figure 18: Development of the DEHP air concentration in the two stainless-steel chambers over 45 days from pure liquid DEHP.

From the data it is assumed that the emission source has a non-constant emission profile. Even though the chambers are tempered with a certainty of +/- 1℃ the vaporization of the phthalate might be changing with variations in the environmental conditions. Another effect that influences the air concentration is the desorption of DEHP from the chamber wall due to the temperature control. The chamber is cooled by the surrounding air and the heating units are directly attached to the chamber surface. If the chamber has to be heated due to a decrease in the surrounding air temperature this might lead to a locally higher surface temperature and a promotion of desorption from this area. This single control cycle cannot be measured by the long-term sampling of the used method and therefore the sum of multiple cycles is measured. This might explain the rapid changes in concentration and the very high concentration of ~ 2 µg m^{-3} that cannot be reached in a real environment but was measured in both chambers.

Like in the previous experiment the DEHP data set is inapplicable for a residual analysis. The DBP data of chamber A allows a good fitting of the modeling parameters. The diffusion coefficient of the model by Xu and Little (2006) was set to maximum and the mass-transfer coefficient and sorption coefficient were changed in

small steps. The residue matrix shows a similar shape like Figure 8 and Figure 14 in which the minimum is found for a narrow range of sorption coefficients but a broad range of mass-transfer coefficients. The mean deviation is 1.40 µg m^{-3} (chamber A) and 0.84 µg m^{-3} (chamber B) respectively. The corresponding modeling parameters are summarized in Table 19.

Table 19: Modeling parameters of pure liquid DBP in a 0.5 m³ emission test chamber. (Fitted values are written in bold.)

	Chamber A	Chamber B
V [m^3]	0.5	0.5
Q [$m^3\ h^{-1}$]	0.06	0.06
$A_{Chamber}$ [m^2]	3.8	3.8
A_{Sample} [m^2]	0.001	0.001
C_0 [µg m^{-3}]	10^{12}	10^{12}
l [µm]	2000	2000
h_m [m h^{-1}]	**14.7**	**0.9**
y_0 [µg m^{-3}]	160	160
D_m [$m^2\ h^{-1}$]	1	1
K [ ]	$6.12 \cdot 10^9$	$6.12 \cdot 10^9$
K_s [ ]	**11**	**4**
n_F [ ]	1	1

4.1.3 Measurement in a simulated indoor environment

The measurement of emissions in a test chamber occurs with artificially reduced complexity compared to a real indoor environment experiment. The application of emission models on such a well describable system is possible due to the available model parameters. In a real indoor environment several unknown influences can affect the concentration of a compound. Especially, the sink effects of a furnished room have to be estimated or calculated by regression from measured data.

In the following experiment a room with mechanical ventilation was simulated in a large climate chamber. The walls were painted with endowed wall paint containing DBP and DEHP. The environmental parameters as well as characteristics of the emitting surfaces are summarized in Table 20. The air velocities in the room and adjacent to the surfaces were measured for the calculation of the mass-transfer coefficient.

Table 20: Initial parameters of the large climate chamber experiment

	Chamber 1	Chamber 2	Chamber 3	Chamber 4
Painted area (endowed) [m²]	20.9	16.7	4.2	0
Painted area (not endowed) [m²]	0	4.2	16.7	20.9
Stainless-steel surface* [m²]	32.5	32.5	32.5	32.5
Air exchange [h^{-1}]	0.13	0.12	0.11	0.13
Air flow [$m^3 d^{-1}$]	50.6	46.9	45.0	52.0
Mass of endowed paint [kg]	3.706	2.322	0.889	0
c(DBP, wet paint) [µg m^{-3}]**	$2 \cdot 10^{10}$	$2 \cdot 10^{10}$	$2 \cdot 10^{10}$	$2 \cdot 10^{10}$
c(DEHP, wet paint) [µg m^{-3}]**	$1.8 \cdot 10^{10}$	$1.8 \cdot 10^{10}$	$1.8 \cdot 10^{10}$	$1.8 \cdot 10^{10}$
Estimated thickness of paint layer [µm]	100	100	100	0

* without heat-exchange unit; ** concentration in the liquid phase

In principle, the experimental parameters allow a mathematical modeling in which only the sorption coefficient and the diffusion coefficient have to be determined via regression. Unfortunately, the air-exposed surface cannot be measured with high precision. The air circulates in the chamber through a heat-exchanger with artificially high stainless-steel surface. Therefore, the area of the adsorbing surfaces has to be estimated as well. This inhibits the determination of the sorption coefficient. Additionally, the stainless-steel surface of the heat-exchanger features a lower temperature than the chamber walls. This leads to two different sorption coefficients for the stainless-steel surface. In fact, this experiment features the same modeling problem as the real indoor environment: neither the free sorbing surface (e.g. dust, furniture) nor the different sorption coefficient are available and, thus, have to be determined via regression as a cumulative value. The results of the measurement of DBP in the chamber air are displayed in Figure 19. The concentrations of DEHP are much lower and seldom exceed 0.2 µg m^{-3} (see Table 21). The exceeding values are not following a trend and occur as sudden peaks.

Table 21: Air concentrations of DEHP during the first 26 days after set up of the large chamber experiment.

Day [d]	Chamber 1 [µg m^{-3}]	Chamber 2 [µg m^{-3}]	Chamber 3 [µg m^{-3}]	Chamber 4 [µg m^{-3}]
1	< LOQ	< LOQ	< LOQ	0.3
2	< LOQ	0.7	< LOQ	0.5
3	< LOQ	0.5	< LOQ	1.9
4	< LOQ	0.3	< LOQ	0.4
5	< LOQ	0.5	< LOQ	1.2
6	< LOQ	< LOQ	< LOQ	0.4
7	< LOQ	0.4	< LOQ	0.4
8	< LOQ	0.7	< LOQ	0.5
9	0.4	0.9	< LOQ	0.4
10	< LOQ	0.5	< LOQ	0.5
11	< LOQ	< LOQ	< LOQ	< LOQ
12	< LOQ	< LOQ	< LOQ	< LOQ
13	< LOQ	0.3	< LOQ	0.4
14	0.3	0.3	< LOQ	0.5
15	< LOQ	0.6	< LOQ	0.6
16	< LOQ	0.5	< LOQ	0.3
17	< LOQ	0.4	< LOQ	0.3
18	< LOQ	0.6	< LOQ	2.3
19	< LOQ	< LOQ	< LOQ	0.4
20	< LOQ	< LOQ	< LOQ	< LOQ
21	< LOQ	0.5	< LOQ	0.4
22	< LOQ	0.3	< LOQ	< LOQ
23	< LOQ	0.4	< LOQ	0.5
24	< LOQ	0.5	< LOQ	0.8
25	< LOQ	0.4	< LOQ	0.5
26	< LOQ	0.6	< LOQ	0.4

From the results it is assumed that the measured concentrations of DEHP result from contamination and are not considered in the following. These findings match with the previous considerations that the heat-exchanger with its large cooled surface will be a strong sink for the SVOC.

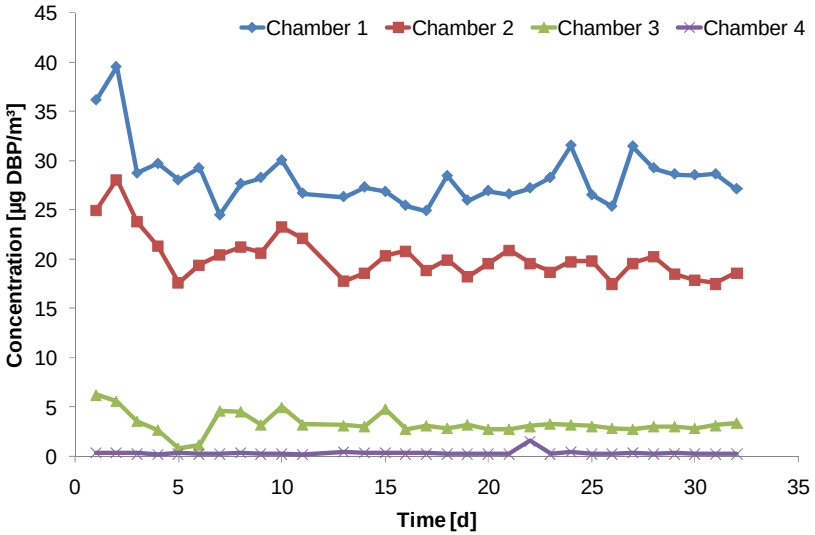

Figure 19: Development of the gas phase concentration of DBP within the first 32 days after insertion of the endowed paint in the large climate chamber.

The concentration development of DBP within the first days after start of the experiment is unexpected due to the large available sinks (see Table 20). The stainless-steel surface is not the only sink that has to be considered but also the not-endowed surfaces and the emitting surfaces as well. However, the DBP concentration reaches a stable value after one week in all chambers. From a modeling point of view several explanations are possible:

- The mass-transfer coefficient is higher than expected.
- The diffusion coefficient is higher than expected.
- The sorption of the chamber is very low for DBP.
- The emission by evaporation during the drying period was strong enough to saturate the sinks with DBP.

Even if the sorption coefficient is very low the DBP concentration should show a small increase but instead the concentration rapidly (~ 1 d) reaches stable values in each chamber. This confirms that the emission rate during the drying period was elevated and high amounts of DBP were emitted evaporation-controlled. With

decreasing water content the emission rate of DBP changes from evaporation controlled to diffusion controlled. Two factors determine the rapid development of a stable concentration in the chamber: First, the paint was applied on the surface in the chamber. During application the emission rate is very high and saturates the available sinks. Second, the emitting areas are large and feature an artificially elevated concentration of plasticizers. Therefore, the emission rate is elevated against a real indoor environment.

The concentrations in the four chambers show a trend according to the area of the endowed paint and the relations between the three endowed chambers roughly match with the ratio of the emitting areas. Basing on the chamber containing the largest endowed area the following chambers should feature a 20 % lower concentration (expected: ~24 µg m^{-3}, real: ~20 µg m^{-3}) and a 80 % lower concentration (expected: ~6 µg m^{-3}, real: ~3 µg m^{-3}) respectively. These slight deviations might result from the uncertainty in measurement. Due to the air humidity control via steam, small variations in the emission rate during sampling have to be tolerated. The overall developments of the concentrations over time are not considerably different between the chambers and are, therefore, not a result of different adsorption in the chambers. Instead, system specific parameters like mass-transfer coefficient, diffusion coefficient, or concentration in the boundary layer seem to differ between the chambers.

4.1.4 Measurement of DBP and DEHP in sink-minimized tube chambers

The previous experiments showed the delay in concentration increase of DEHP and DBP if the ratio of free sorbing surface (e.g. chamber walls) to the emitting surface is large. A tube chamber which is lined with the sample principally circumvents this problem by decreasing the ratio of chamber surface to the emitting surface far below 1. The earlier described PVC tube chamber is equipped with ingrain wall paper which is painted with endowed wall paint A (1 % DBP) and B (1 % DEHP) respectively. To conceive such a chamber mathematically using an emission model the tube is fragmented into N cylindrical chambers. The mass-balance equation is solved for every single unit while the outflow from one unit is used as inflow concentration for the following. The resulting mass-balance equation for a single sub unit is

$$V\frac{dy_N(t)}{dt} = Ah_m(y_0 - y_N(t)) + Qy_{in,(N-1)}(t) - Qy_N(t) - \frac{dq_N(t)}{dt} \qquad (4.1)$$

while the sorption is described by a Freundlich isotherm. An important assumption of this model is the absent backflow of mass in the tube (laminar flow without eddy diffusion). In case of DEHP the diffusion coefficient in air is $4 \cdot 10^{-6}$ m² s^{-1} (calculated on the basis of equation (2.20)).

The air flows through the tube at 160 mL/min, resulting in an air velocity of $3.39 \cdot 10^{-4}$ m s^{-1}. On the basis of the inner diameter (0.1 m) and the kinematic air viscosity at 23℃ and 760 Torr ($15.595 \cdot 10^{-6}$ m² s^{-1}, (Lide, 2007)) the Reynolds number is 0.5. For laminar flow in a tube the critical Reynolds number is ~ 2300 (Baerns, et al., 2006). As a consequence, the air in the tube follows a plug flow and, thus, the air concentration increases with ongoing tube length. The establishing air concentration should affect the emission rate due to the decrease of the gradient between boundary layer and well-mixed air. Therefore, a drop in emission rate over the tube length is predicted (Figure 20).

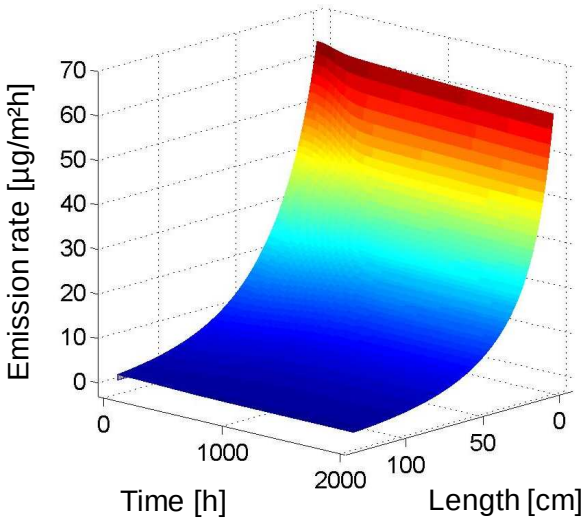

Figure 20: Predicted emission rate in the tube over time and tube length (DBP).

If the sink effect is low, the resulting air concentration should be near the saturation concentration of the compound. The experiment that contained DBP endowed wall paint shows a slow increase of DBP concentration in air within 30 days after insertion of the sample. After 30 days the slope of the concentration curve drops and the

system reaches a concentration of ~ 100 µg m^{-3} which holds for another 20 days (see Figure 21). In principle, the system should reach an equilibrium concentration identical to the saturation concentration of DBP in air (~ 160 µg m^{-3}). The observed increase (maximum concentration of 108 µg m^{-3} on day 43) is smaller than expected and is a sign of an additional sink for this compound. The mixing chamber at the end of the tube as well as the stainless-steel sampling port are possible sinks for DBP and might decrease the air concentration.

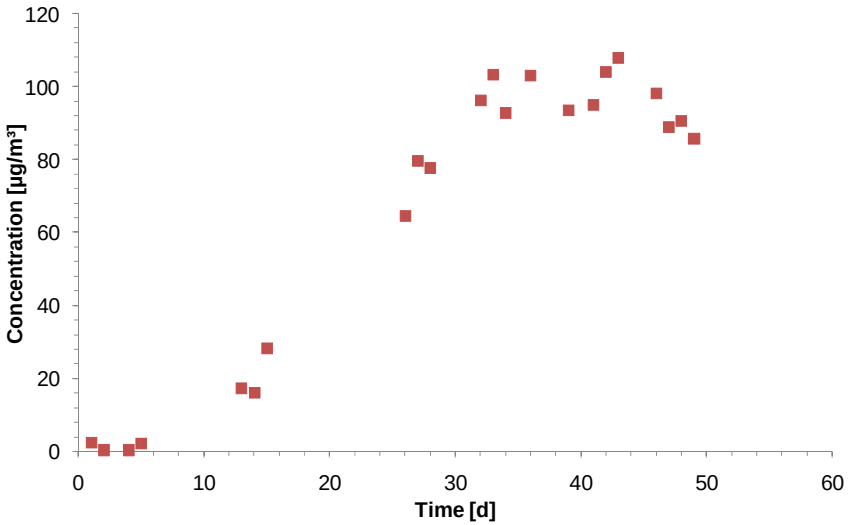

Figure 21: Air concentration of DBP at the outlet of the PVC tube chamber containing endowed wall paint A (1 % DBP).

Even though the tube chamber design theoretically reduces the influence of sinks for phthalates the present chamber still contains surfaces which have a strong sorption capacity for the compound. This effect was partially expected due to the affinity of PVC against phthalates but the necessary time to reach equilibrium is higher than for the performed glass chamber experiments. In case of paint B in the PVC tube chamber the detected concentrations are associated with high fluctuations even though the sampling volume was increased against the chamber experiments (see Figure 22). Again, this effect is caused by the non-constant emission profile over the long sampling time and the affinity of the chamber material to the phthalate in the gas phase. A modeling of the presented data is not possible due to the unknown sorbing surface area and sorption coefficient.

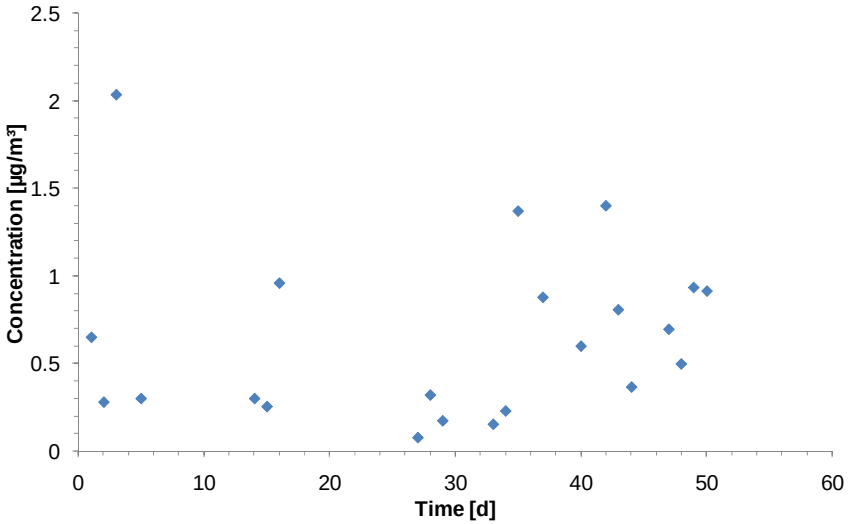

Figure 22: Air concentration of DEHP at the outlet of the PVC tube chamber containing endowed wall paint B (1 % DEHP).

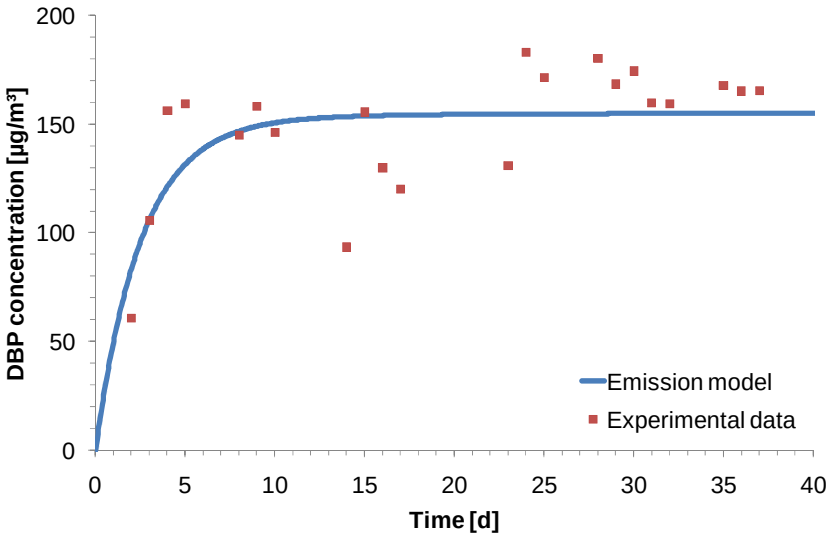

Figure 23: Air concentration of DBP measured at the outlet of the PVC tube chamber and the results of the emission model within the last sub-unit of the chamber.

As a consequence, the surface of the mixing chamber was covered with aluminum foil and the sampling port was shortened. However, the repetition of the experiment focused on the emission of DBP. The DBP concentrations in air during 40 days after insertion of the sample are shown in Figure 23.

The modification of the chamber caused a rapid increase in DBP concentration which reaches equilibrium concentration after 5 days. The detected concentrations are consistent with the equilibrium value which is predicted by the model. Due to the geometry of the chamber and the air flow the concentration at the outlet reaches nearly the saturation concentration of DBP in air. The above described model was used to perform a residual analysis for the sorption coefficient. The result and the modeling parameters are summarized in Table 22. The PVC tube is segmented into sub-units of 1 cm height and the model is solved for every unit.

Table 22: Modeling parameters of the segmented PVC tube chamber measurements of the wall paint A. (Fitted values are written in bold.)

	PVC tube (sub-unit)
Number of sub-units	130
V [m³]	$7.85*10^{-5}$
Q [m³ h^{-1}]	0.01
$A_{Chamber}$ [m²]	0.0031
A_{Sample} [m²]	0.0031
C_0 [µg m^{-3}]	$2*10^{10}$
L_P [µm]	200
h_m [m h^{-1}]	0.8176
y_0 [µg m^{-3}]	160
D_m [m² h^{-1}]	$1.2*10^{-11}$
K_s [ ]	**52**
n_F [ ]	1

The approach of reducing the possible sinks for SVOC by increasing the sample surface and reducing the free chamber surface allows the rapid installation of a time-stable high concentration of DBP. Even for DEHP the concentrations are elevated but the uncertainty of the measurement is still high. For less-flexible or thick material the tube-chamber design might be not applicable. In this case, a “sandwich”-technique, like developed by Xu et al. (2008), allows testing of materials in a well-described environment. In this chamber two flat polymers (e.g. PVC flooring) form the ceiling and bottom of the chamber. They are separated by a stainless-steel component

(approx. height 1 cm) in which a circular space is cut. The resulting chamber has a very large emitting surface compared to the small stainless-steel surface of the inner ring. However, a tube chamber is a feasible system for further research if the flow in the chamber follows a plug-flow and the air is mixed before sampling.

4.2 Interaction of phthalates with deposited particles

The uptake of plasticizers into settled particles can be monitored by the chemical analysis of dust. Publications that deal with this effect usually report high concentrations of less volatile plasticizers in the dust matrix (see Table 5). These findings are often attributed to the adsorption of plasticizers from the gas phase by deposited dust. The pathway of DBP and DEHP from the emission source into the dust under controlled environmental conditions will be discussed in the following.

The experiments in 0.5 m³ stainless-steel emission test chambers allowed the determination of the accumulation of DBP and DEHP in dust via sorption from the air. The first experiments, that use endowed wall paint as emission source, contained a small amount of house dust E (pre-extracted, sieved to < 63 µm fraction, see Table 11) as described in chapter 3.3.2. Additionally, the sorption of DBP and DEHP on the stainless-steel surface has been measured using wipe samples. The analytical results of the extract of the wipe samples from both chambers have a similar order of magnitude (see Table 23). The difference between the results of chamber A and B is not significant due to the uncertainty of this sampling method. The DBP concentrations in the two dust samples are also similar but are nearly 10 times higher than the literature values (Table 5). It has to be considered that the dust samples were loaded for 45 days at artificially high air concentrations. These findings are consequently not comparable to published results. However, the higher sorption of DBP on the surface in chamber B is not an adequate explanation for the different equilibrium concentrations observed from air measurements.

Table 23: Results of the experiment in 0.5 m³ emission test chambers using DBP endowed wall paint as emission source

DBP	Days after loading [d]	Chamber A	Chamber B
Wipe samples [µg m^{-2}]	45	43	73
Dust [mg kg^{-1}]	45	2477	2546

The parameters of the chamber experiments were adapted from measurements of the real indoor environment. The air exchange rate of 0.12 h^{-1} is assumed to be appropriate estimation of indoor air exchange rates. Salthammer et al. (1995) reported a mean air exchange rate of 0.36 h^{-1} (range 0.1 h^{-1}- 1.7 h^{-1}) basing on the investigation of 150 dwellings in Germany. The direct comparison of these values is

not possible due to intraday changes of the air exchange indoors while the air exchange rate in the chamber stays constant over time.

In case of the dust sample in the chamber, the contamination is expected to be artificially higher. Usually, dust is removed from a real indoor environment by cleaning or ventilation. The dust of the present experiment is in contact with polluted air for 45 days. Therefore, the mass-transfer of plasticizer into the dust is artificially elevated against real indoor conditions. However, a generalization from these results is not valid because of the different sorption capacity of indoor dusts.

The repetition of the experiment using a wall paint endowed with DEHP shows results deviating to the DBP sample (see Table 17). Regarding the wipe samples the measured values are slightly higher than for DBP while the air concentrations are much lower. A significant deviation between chamber A and B could not be observed from the DEHP measurements.

Table 24: Results of the experiment in 0.5 m³ emission test chambers using DEHP endowed wall paint as emission source

DEHP	Days after loading [d]	Chamber A	Chamber B
Wipe samples [µg m^{-2}]	48	89	77
Dust [mg kg^{-1}]	48	47	41

A large deviation between results from the literature and the present experimental data can be also observed in case of the dust concentrations of DEHP. Like in the prior experiment, the dust samples show nearly similar results for each chamber but the measured concentrations are approximately 30 times lower than expected from the literature (e.g. P_{95} DEHP = 1542 mg kg^{-1}, given by Fromme et al. (2004), see Table 5). Due to the high source strength and the low air exchange rate, high dust concentrations (like in the case of DBP) were expected but the sorption of dust in case of DEHP was far lower. The most important deviation to previous measurements is the absent direct contact between the dust and the emission source. In the case of Clausen et al. (2004), who measured much higher DEHP concentrations in dust, the sink had direct contact to the PVC flooring. A direct substance transfer into the dust or the abrasion of surface particles might increase the concentration compared to the uptake over the gas phase. The present

experiment shows a much smaller uptake rate of DEHP into dust than expected from real room measurements or other chamber experiments.

However, in some cases exceptional phthalate-contaminations of dust can be found in real room studies. Kolarik et al. (2008b) published data about phthalate concentrations in house dust of Bulgarian homes. The dust had unknown age. While the detected concentrations of DEHP in the dust samples are in the same range as shown in other studies (790 - 1170 mg DEHP kg^{-1} dust) the DBP concentrations are considerably elevated. The authors report concentrations between 6590-9360 mg DBP kg^{-1} dust for the 177 analyzed homes. These values are much higher than the detected concentrations of the previously described experiment. The authors were not able to determine the reason for these high concentrations. Unfortunately, the air concentrations were not monitored. In a subsequent publication (Kolarik, et al., 2008a) basing on the same data the authors tried to correlate their previous findings with the cleaning behavior and possible phthalate sources. They found polishing agents as a strong source of phthalates in case of Bulgarian homes and reduced concentrations in case of high frequency of dusting of furniture. They were not able to identify PVC as an important source for phthalates in indoor dust but attributed this fact to masking effects of the very strong sources (e.g. polishing agents). As a result, these findings support the obtained experimental data because in case of the emission test chamber experiment a constant moderate source is present while the published data seems to be related to short-term events of high source strength.

To confirm the obtained results the experiment was repeated with a variety of adsorbents. The adsorbents were chosen due to different organic carbon content. The emission sources were pure liquid DBP and DEHP. Regarding the results of the wipe samples an increase in surface loading could be detected. The DBP wipe sample from chamber A feature a similar amount like the previous measurements but the other results are noticeably higher. Due to the low air concentration (see Figure 18) and the weak emission source it is assumed that the wipe sample of DEHP has to be contaminated and is not representing real surface load.

Table 25: Results of wipe samples from 0.5 m³ stainless-steel chambers

	DBP [µg m^{-2}]	DEHP [µg m^{-2}]
Chamber A	66	614
Chamber B	362	215

The uptake of DBP into the five sorbents is lower than expected from the previous experiment but this is explained by the weaker emission source and the larger amount of free sorbing surface. The DEHP concentration in dust is much lower than the reference values. The measured concentrations in dust after 45 days as well as the blank concentrations in the same dust before loading the chamber are shown in Table 26.

Table 26: Dust concentrations after 45 days in the emission test chamber A / B and before loading (blank)

Adsorbent	DBP [mg kg^{-1}]			DEHP [mg kg^{-1}]		
	Blank	Chamber A	Chamber B	Blank	Chamber A	Chamber B
Silica Sand	51	81	66	35	36	37
Soil	110	866	555	31	36	36
House dust 1	60	1027	879	246	257	243
House dust 2	63	933	461	598	582	588
House dust 3*	38	1129	844	30	28	32

* pre-extracted with acetone/n-hexane (1:1)

The changes of the DBP concentrations in the five samples are shown in Figure 24. In the chamber with higher air concentration of DBP the dust contamination is also higher. The matrix without organic carbon content, sand, shows practically no uptake of DBP.

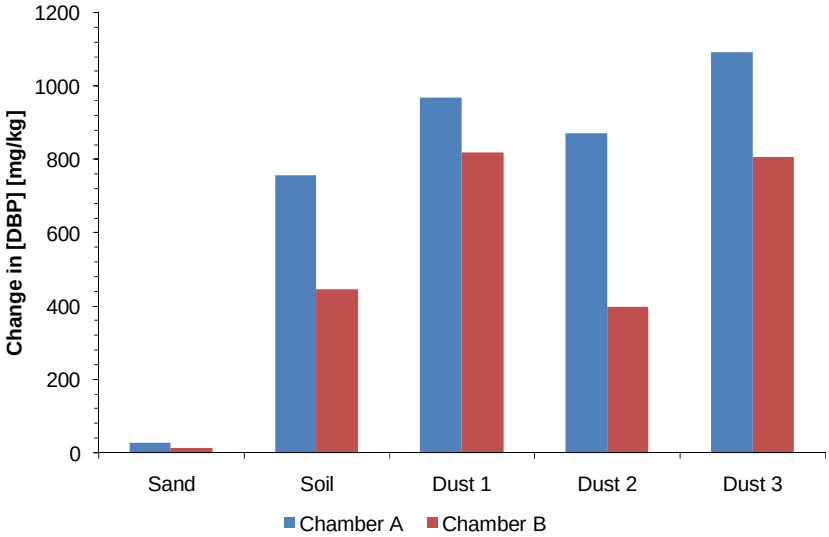

Figure 24: Changes in the concentration of DBP in the five matrices of the distribution experiment.

The detected dust concentrations of DBP in Table 26 are in the range or slightly above the maximum reference values (Table 5) in case of chamber B while they are far above the reference values in case of chamber A. The only exception are the values given by Kolarik et al. (2008a) which are elevated due to a different contamination mechanism (cleaning agents). The detected concentrations in Table 26 are expected due to the low mass-transfer from the chamber and the long exposure time. Regarding the different characteristics of the five matrices the DBP concentrations tends to increase with increasing TOC. A linear fitting of the data is shown in Figure 25. The correlation was found to be weak.

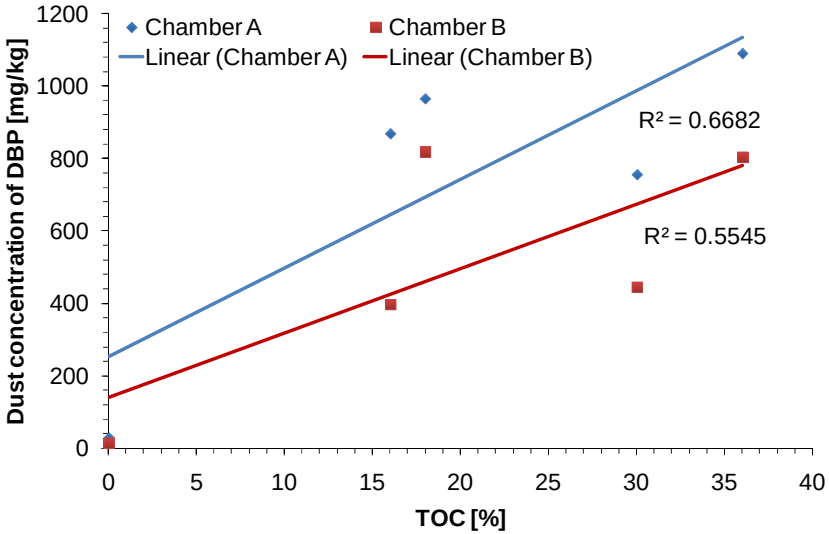

Figure 25: Linear correlation between total organic carbon content of the sorbent matrix and the measured concentration of DBP.

In contrast to the measured DBP concentrations the amount of DEHP bound to dust is much lower. The measured concentrations in both chambers are below the P_{95} values for DEHP given in Table 5. The changes of the DEHP concentrations in dust from beginning to the end of the chamber experiments are displayed in Figure 26. In four samples the change in concentration is negative. It is assumed that DEHP is not released from the sorbent into the chamber air. In fact these deviations result from the inhomogeneity of the dust samples that complicate the comparison between previous and resulting concentrations. Additionally, the total amount in dust is low and does not correlate with reference values of the literature. A correlation between TOC and uptake cannot be observed in this case.

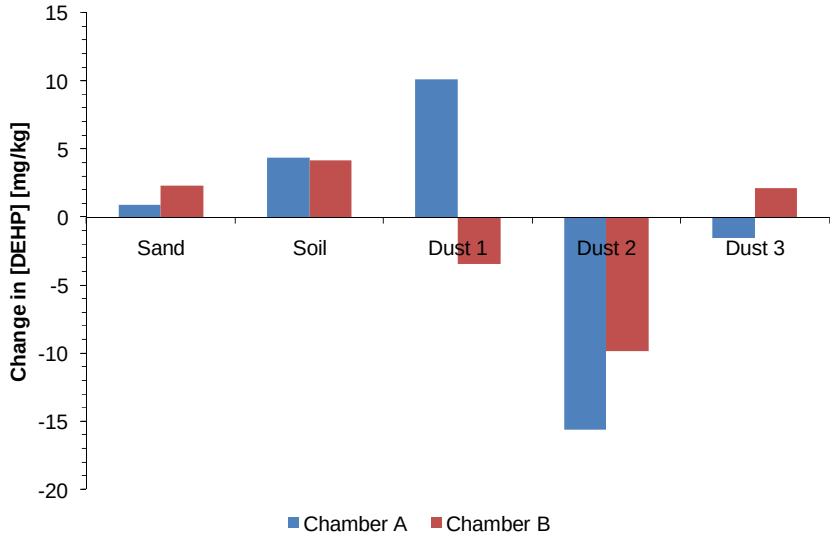

Figure 26: Changes in the concentration of DEHP in the five matrices of the distribution experiment.

The presented results are inconsistent with published values because DEHP is known to greatly accumulate in dust while the detected concentrations are considerably low. In contrast, the DBP concentrations in dust refer to a contamination situation. The latter findings are explained by the fact that the performed experiment represents “worst case” conditions regarding the environmental conditions. The low air exchange and the missing exchange of dust over time do not correspond to the real indoor environment. However, the mass-transfer from the DEHP source into the dust is not performed via the gas phase under the given conditions.

The lower concentration of DEHP in the present dust samples may be explained by the stronger sorption of the stainless-steel surface compared to the dust. This cannot be excluded if small temperature deviations between the cooler chamber surface and the sorbents exist. In this case the SVOC would preferential adsorb on the surrounding walls. However, the sorption capacity of a dust sample with high organic carbon content is assumed to be higher than the sorption capacity of a stainless-steel surface.

However, the saturation of the chamber walls has to be completed till the transfer into the dust can happen at full sorption strength.

Consequently, the present experiment showed the low mass-transfer of DEHP from a source into the dust via air. The higher published values in Table 5 for the real indoor environment have to be linked to mass-transfer of plasticizers in the mobile particle phase or by abrasion of plasticizer-containing surfaces.

As mentioned above, the presented experiments are related to the measurements of PVC flooring by Clausen et al. (2004). However, the length of the Clausen-experiment was much longer (472 days) and the environmental conditions in the CLIMPAQ were rather different (T = 22°C; 50% r.h.; n = 9.8 - 11 h^{-1}). Dust was directly applied on the surface of the PVC flooring and air and dust concentrations were monitored. After 31 days the authors measured a DEHP concentration in dust of ~10,000 mg kg^{-1} and an air concentration of 0.48 µg m^{-3}. These concentrations changed only slightly for the following 37 days (68th day). The experiments by Clausen et al., 2004 showed that the contamination of dust is high if the dust is in direct contact with the source.

In principle dust might be able to uptake the additives that diffuse to the material surface by capillary forces. Another explanation is the direct contact of the dust with the boundary layer on the material surface. The air concentrations in the boundary layer are much higher than in the well-mixed air. The compounds in that layer are slowly transported through the layer (by h_m) or might be adsorbed directly at the dust surface (see Figure 27). This strong difference in the surrounding air concentration of the dust particle would explain the different contamination.

The boundary layer thickness can reach a height of 1 mm. In this case a thin dust layer is completely surrounded by the high contaminated air. If the contact time is long the uptake of the sink can be extensive.

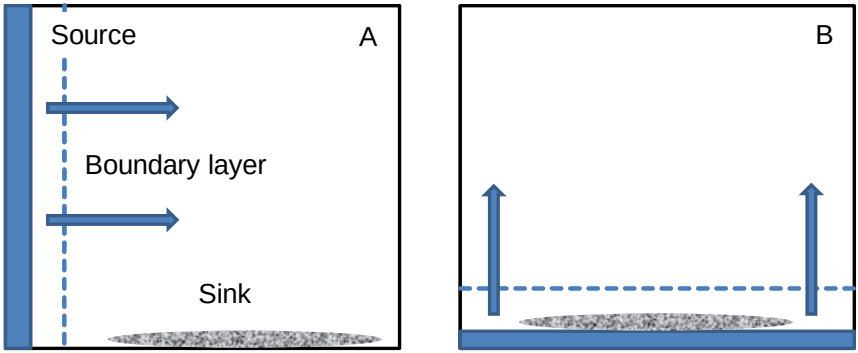

Figure 27: Comparison between two contamination scenarios. Case A) Mass-transfer through the boundary layer and case B) Sink in contact with the boundary layer.

Regarding the samples from real indoor environments a contamination of the dust sample with small particles from abrasion of the material cannot be excluded. If one gram of a phthalate-free dust sample would be contaminated by 1000 particles (100 µm, 1.5 g cm^{-3}) from PVC-flooring containing 17 % DEHP the measured DEHP concentration would be 133 mg kg^{-1}. The same concentration would be derived from only one particle with a diameter of 1 mm. If the expected abrasion e.g. of a chair on a PVC flooring is considered, the dust concentration under real conditions might be increased strongly. If the sampling procedure contains the usage of a vacuum cleaner the abrasion is artificially increased leading to vast errors in the analytical results.

The present experiment, that artificially separates source and sink, allows only the transfer via the gas phase and shows results for the dust concentration that are inconsistent with the literature. Consequently, it is assumed that the direct contact between plasticizer-containing material and dust is a necessary fact to increase the mass-transfer. The respective experiment was performed in two 3 L glass chambers using endowed polymer materials. Dust was placed in the chamber with and without direct contact with the material. The results are shown in Table 27. The initial concentration of the used dust was 202 mg DEHP kg^{-1} dust.

Table 27: Results of dust analysis with and without direct contact with endowed polymer materials (14 days)

Sample	c(dust) direct contact (first stage) [mg kg^{-1}]	c(dust) no contact (second stage) [mg kg^{-1}]
PVC (4 % DEHP)	408	229
PVC (17 % DEHP)	2080	213

The detected concentrations show in agreement with previous results no significant uptake of DEHP from air into dust. In the case of direct contact between polymer surface and dust the mass-transfer is severely higher. As expected from the theory, the initial concentration of the additive in the polymer has a great influence on the inter-matrix transfer in case of the same partition coefficient K. For the polymer under the same environmental conditions this assumption should be given. In this case, the initial concentration in the polymer is linked to the boundary layer concentration. If the dust is in contact with these different concentrations, the uptake into the matrix should be different. As a result, the measured concentration of DEHP in dust is much higher if the mass fraction of the additive in the polymer is elevated.

Air samples were not taken during this experiment because the covering of the polymer with dust artificially reduces the emission rate from the surface and the large glass surface was expected to be a good sink for DEHP. Therefore, the emission profile of DEHP within the first 14 days was expected to be non-constant and, thus, allows no reliable determination of the concentration of DEHP in air. Due to the complexity of the system a modeling of the air concentration development within the system was not performed.

As a conclusion, the transfer of the low volatile compound DEHP from its source into dust is not a result of transport via the gas phase independent of the organic content of the target matrix. The more volatile compound DBP reaches considerable air concentrations which lead to the sorption of the compound on the dust surface. However, if the dust is directly in contact with the emission source, the transfer of DEHP is given due to the contact between sink and boundary layer of the emitting material. In this case, the uptake of DEHP into the dust occurs depending on the initial concentration in the polymer.

4.3 Interactions with particles in the gas phase

As shown in the previous chapter, the transfer of DEHP from the emission source to the sink (e.g. dust) is a long-term process. However, these findings are not matching with published results about the concentrations of DEHP in < 14 days-old dust. The explanation of this fact is given by airborne particles in the air of real rooms. The previously used emission test chambers are supplied with particle-free air which establishes a compound-distribution solely by the gas phase. Under real room conditions airborne particles are present which feature a large surface area and high mobility. The theoretical and experimental determination of the distribution of the considered two phthalates will be shown in the following.

Regarding the analytics of phthalate distribution between airborne particles and gas phase several problems exist. The parallel measurement of a compound's particle-phase concentration and gas phase concentration by separation is associated with high analytical effort and high uncertainty. Therefore, the mathematical modeling of expected changes in concentration and emission rate of the material basing on known particle properties can provide useful information. However, the model has to be validated against real data. In the following the impact of particles on the emission behavior of a material is illustrated using the model by Xu and Little (2006) for a model room.

Particles in indoor air increase the export of absorbable compounds from the system additional to the air exchange rate. Thus, they decrease the maximum reachable concentration of this compound in air. The additional mass-flow from the system causes an increase in emission rate of the material. In principle, an increase in particle concentration causes the same effect as the increase of the air exchange rate. In the following observation the deposition of particles is not considered. The comparison of modeled data to experimental data showed the minor influence of diffusion on the emission from a pure liquid.

In the following a simulation basing on the model by Xu and Little (2006) is used to predict the air concentrations under the conditions of the Danish standard room (Danish Standard, 1994). The emission source is chosen to be pure liquid DBP. The initial particle concentration as well as the inlet particle concentration is set to zero.

Table 28: Modeling parameter of the model room simulation

	Danish Standard room
V [m³]	17.4
Q [m³ h^{-1}]	8.7
$A_{Chamber}$ [m²]	31.2
A_{Sample} [m²]	0.0064
C_0 [µg m^{-3}]	10^{12}
L_P [µm]	2000
h_m [m h^{-1}]	12.79
y_0 [µg m^{-3}]	160
D_m [m² h^{-1}]	1
K [ ]	$6.12 \cdot 10^9$
K_s [ ]	11
n_F [ ]	1
K_p [m³ µg^{-1}]	0.0059

After 4 days the inlet particle concentration is set to 20 µg TSP m^{-3} (C in Figure 28). The sorption coefficient was taken from the publication of Weschler et al. (2008) who reported a value of 0.0059 m³ µg^{-1} for K_p. This value is calculated from the vapor pressure of the compound given by the Antoine equation. Using the described model the impact on the air concentration of DBP (A in Figure 28) is predicted. The modeling parameters are summarized in Table 28.

The uptake of DBP by the aerosol causes a decrease in gas phase concentration of ~0.15 µg m^{-3}. The simulated system needs less than 2 days to reach equilibrium concentrations for DBP after changing of the inlet particle concentration in air at day 4. The equilibrium of the particle concentration is reached much faster. In equilibrium, the mass-flow of DBP from the system increases by ~ 0.3 µg d^{-1} (D in Figure 28). Without particles present in air the predicted concentration of DBP is 1.4917 µg m^{-3}. Due to the increase in emission rate the total amount of DBP in air (particle bound and gas phase concentration) increases. The total concentration can be calculated using equation (4.2).

$$y_{a,P} = y(\infty)\left(1 + K_P TSP(\infty)\right) \tag{4.2}$$

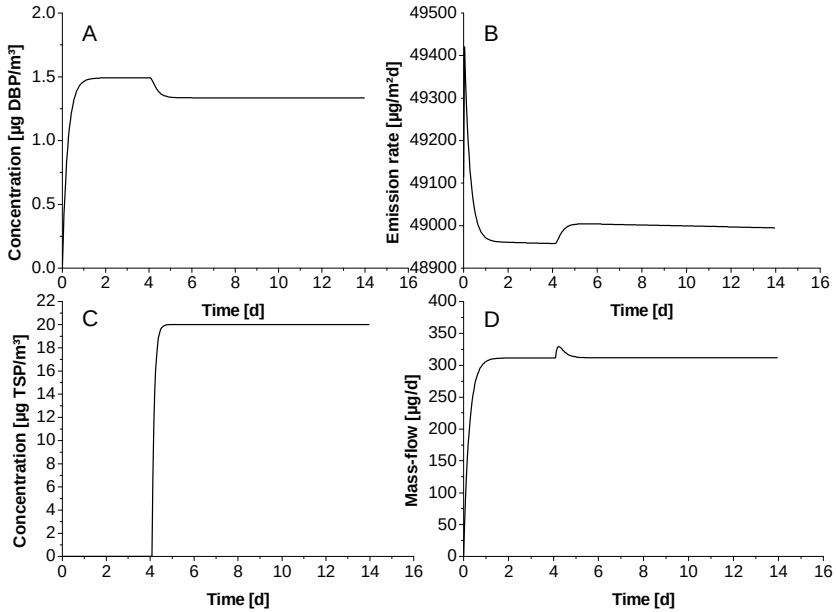

Figure 28: Development of air concentrations (A), emission rate of the material (B), TSP-concentration (C), and DBP-mass-flow (D) from the system in a Danish standard room at different particle concentrations.

In this case the predicted total concentration of DBP in air (gas phase and particle phase) is 1.4927 µg m^{-3}. The high capacity of some sorbents to retain airborne particles is described later in this chapter. As a consequence, the sum of gas phase concentration and particle phase concentration is measured. However, the predicted increase (+0.001 µg m^{-3}) would not be reliably detectable with the analytical devices of this study. If the partition coefficient is larger, the impact on the mass-flow from the system can increase. Weschler et al. (2008) report a ten times higher K_P for DBP if the basis of calculation is the octanol-water partition coefficient. Anyhow, even at worst case conditions the determination of the emission rate increase is associated with a high uncertainty and, thus, the impact of particles on a real room scenario is difficult to identify. The connection of equilibrium DBP gas phase concentration and particle concentration can be described mathematically by equating the mass-flow from the system and the emission rate (4.3).

$$Lh_m(y_0 - y(t)) = ny(t) + nK_P y(t)TSP(t) \quad (4.3)$$

The relation between y and TSP yields an exponential decrease of the gas phase concentration with linear increasing particle concentration (4.4).

$$y(t) = \frac{h_m L y_0}{h_m L + n + K_P n TSP(t)} \quad (4.4)$$

In principle, an aerosol with high K_P can increase the emission rate near to the maximum SER of the material. This is equal to the infinite increase of the air exchange rate but the determination of the particle phase concentration is still possible. Theoretically, this allows the direct determination of the maximum emission rate of a material.

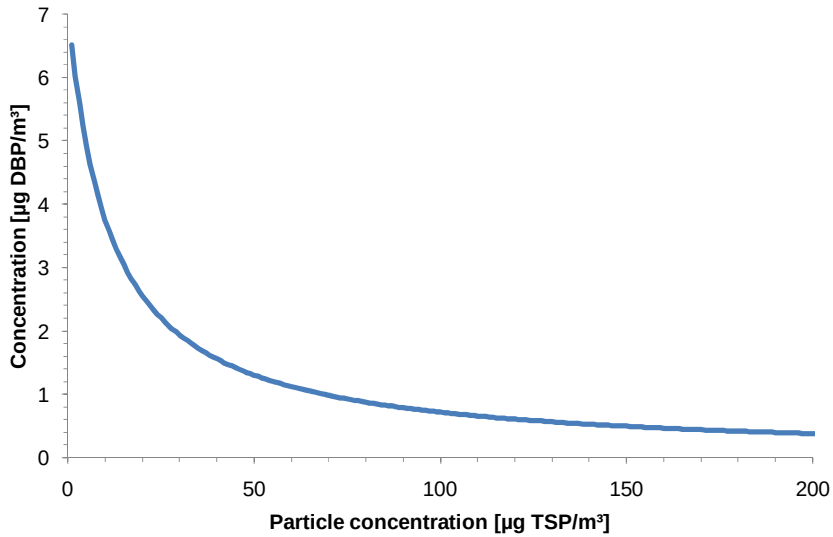

Figure 29: Relation between TSP-concentration and DBP-concentration under equlibrium conditions in the Danish standard room (K_P = 0.091 m³ µg^{-1}).

To experimentally determine the interaction between phthalates in the gas phase and bound to airborne particles two experimental specifications are necessary: a) a chamber with a high phthalate concentration in air and b) particles of known composition, size distribution, and sorption behavior. To achieve an elevated air

concentration of phthalates after an applicable time, the sinks of the chamber have to be reduced. Additionally, the air flow over the emitting surface has to be laminar and oriented to use the correlation equations by Axley (1991). A tube chamber thats interior is fully lined with the sample provides all the mentioned necessities. The loading factor is very high while the only present sink is the sample itself. The flow through the chamber determines the air velocity as well as the air exchange rate and thus establishes a certain emission rate. The used tube chamber was made of PVC and loaded with endowed wall paint (~ 1 m%) on ingrain wall paper.

Regarding the interaction between airborne particles and phthalates in the gas phase of the tube the drop in emission rate should be attenuated if particles are present. This is illustrated in Figure 30 for the last sub unit of the tube. The sorption coefficient $K_P = 5.7 \cdot 10^{-8}$ m² µg^{-1} was derived from a publication that measured the interactions of gasoline SOA with phthalate esters (Liang, et al., 1997). In the present case, the calculation of K_P bases on the vapor pressure provided by the Antoine equation ($p = 1.12 \cdot 10^{-5}$ Torr (Weschler, et al., 2008)) If the sum of gas phase concentration and particle phase concentration at the end of the tube is monitored with and without particles present in the chamber the influence on the emission rate can be measured directly.

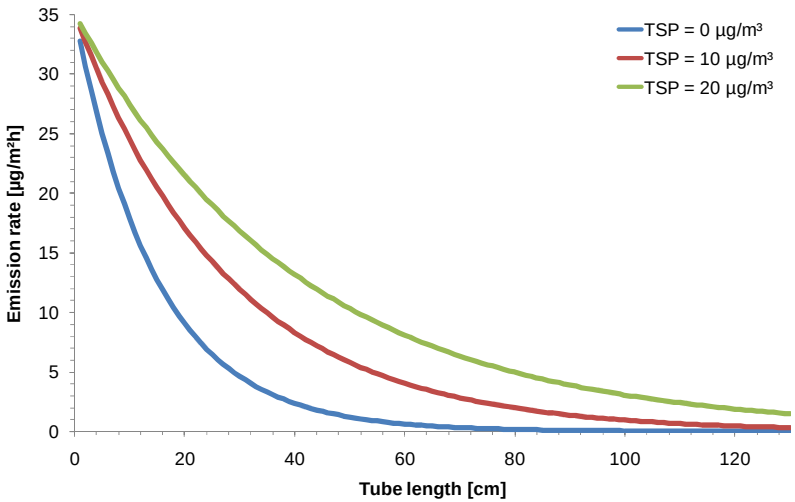

Figure 30: Predicted change in emission rate over tube length without and with airborne particles present in the chamber.

The experiment was performed using carbon particles which were purchased from Aldrich and evaporated using a TSI aerosol generator. The obtained aerosol consists of two particle size modes. The first mode ranges between 5 and 20 nm (nucleation mode) while the second mode has a medium diameter of ~ 50 nm. The first mode results from small contaminations of the evaporated water (e.g. H_2SO_4, NH_3, org. acids) that are known to react with water to form particles between 3 and 10 nm (Korhonen, et al., 1999; Kulmala, et al., 2001). The size distribution of the particles is shown in Figure 31. The results of the air analysis are summarized in Table 29. The experiment was performed twice to ensure the low concentrations and possible breakthrough of substance through the sorbent.

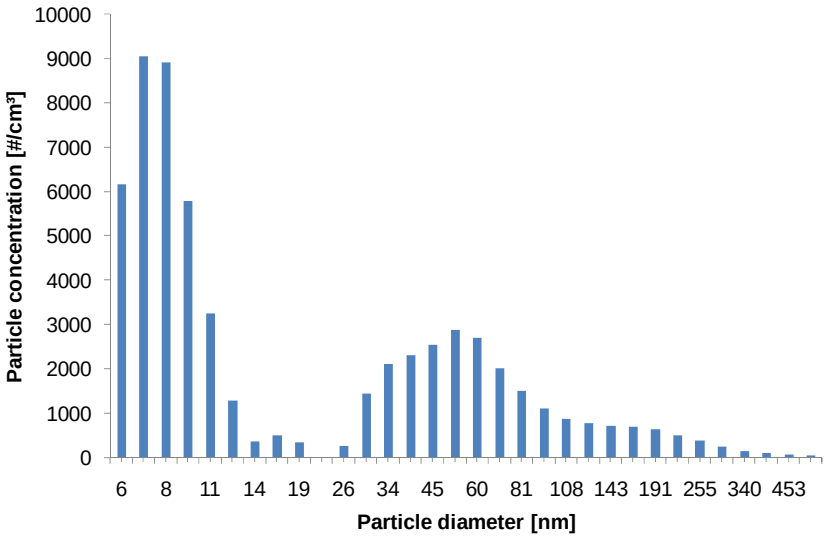

Figure 31: Particle size distribution of the generated carbon aerosol.

From the literature (Jamriska and Uhde, 2003) the high retention capacity of Tenax TA for ultra-fine particles is known (~90 % of 20 – 700 nm particles). As expected from the modeled results the emission rate should increase if particles are present. The present results illustrate that the mass-removal from the chamber increases strong enough to measure a concentration above the saturation concentration in air. This proves the transfer of DEHP, that is bound to the particle matrix, from the

system. Basing on the data shown in Figure 31 and a particle density of 2.25 g cm^{-3} (graphite) the TSP-concentration is ~ 70 µg m^{-3}.

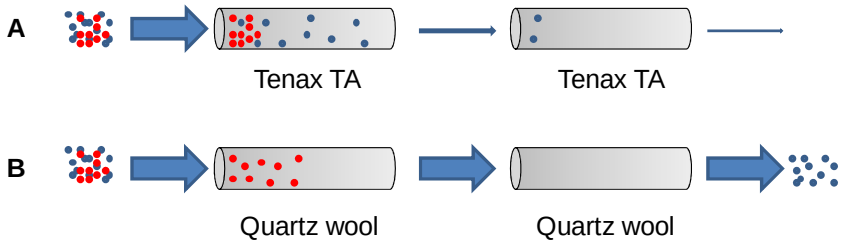

Figure 32: Scheme of the expected rentention capacity of a strong adsorbent (A) and a weak adsorbent (B) against DEHP (red) and particles/DEHP (blue) in the present experiment.

The breakthrough of the Tenax sorbent was determined by measuring the backup tube (second tube in a row) for the case of particles present in the sampled air (Figure 32). The results in Table 29 prove the transport of DEHP through the sorbent via the particle phase. This results from the incomplete retention of particles by the first Tenax tube. In both experiments the quartz wool was not able to retain the particles and thus contains very low DEHP concentration. Within the second measurement the direct Tenax sampling from the aerosol generator without the tube chamber assures that the additional DEHP does not originate from contaminations by the generator.

Table 29: Results of measurements in a tube chamber without and with carbon particles present in the chamber.

Adsorbent	Particles	[DEHP] [µg m^{-3}]	
		First measurement	Second measurement
Tenax	-	< 0.2	1
Quartz wool	-	< 0.2	1
Quartz wool (breakthrough)	-	< 0.2	< 0.2
Tenax	x	5	5
Tenax (breakthrough)	x	n.d.	3
Quartz wool	x	< 0.2	< 0.2
Quartz wool (breakthrough)	x	< 0.2	< 0.2
Tenax without chamber	x	n.d.	< 0.2

The performed experiment proves the sorption of DEHP on particle surfaces in an air flow and the resulting, principal, increase in emission rate. In the present case, the emission rate decrease over the length of the tube is lowered by the reduced air concentration. In the indoor environment these particles tend to deposit on all surfaces by diffusion and improve the mobility of the compound considerably.

5. Conclusions

This work showed the pathways of the indoor distribution of the phthalic acid esters DBP and DEHP. Furthermore, techniques for the characterization of the distribution have been applied and evaluated. The main aspects were the prediction of the air concentration development of DBP and DEHP basing on material properties, the mass-transfer from an emission source into settled dust, and the impact of airborne particles on the emission rate of a material.

During the emission tests of materials in two different emission test chambers (glass and stainless-steel) the air concentration development of DBP and DEHP has been recorded. The chambers had known environmental conditions and the samples were prepared with a known amount of plasticizer. An emission model should be able to predict the emission profile of a compound under these known conditions. Anyhow, the sorption of the compound on the chamber wall cannot be predicted and is difficult to measure. Therefore, this parameter was determined by fitting the predicted concentration to the experimental results. In principle, this undermines the modeling approach of predicting the concentration development in a system from known environmental conditions and material characteristics (“ab initio approach”). The application of the model on the obtained experimental results showed a high uncertainty in prediction even in a system with reduced complexity. As a consequence, an expansion of the application on a real room scenario is doubtful. This problem does not originate from the mathematical approach of the model because it bases on the governing physical aspects of emission, but follows from the complexity of a non-idealized real system. The experiment, that was used to simulate an indoor environment in a large climate chamber, illustrated these findings. Regarding real room simulation, the sorption of the different surfaces in a room (wall covering, ceiling, furniture, objects) and the influence of the inhabitants are impossible to predict without widespread measurements. In principle, a rough prediction for a large scale population might be possible this way but will be affected with a high uncertainty. This outcome is also outlined by Xu et al. (2009a; 2009b) regarding the exposure analysis basing on modeled data.

The applied emission model by Xu and Little (2006) was found to be the most flexible of the discussed models because it needs limited presumptions on the system. This

flexibility leads to a collective of parameters, which have to be determined separately. As shown in chapter 2, the determination of some modeling parameters bases on published correlation equations. The applicability of these equations for the system under observation is not given in every case. For example, the determination of the mass-transfer-coefficient via the Axley-correlations (Axley, 1991) for the walls in the simulated indoor environment is complicated by the fact that direction and velocity of the air are different for each wall. However, the experimental derivation of the mass-transfer-coefficient for a certain system needs time and effort. Here, the simulation approach is falsified by the experimental characterization of the measuring environment and not just the emission source.

The experiments illustrate that DBP can reach high concentrations in indoor air depending on the characteristics of the source (diffusion hinderance, free emitting surface) while DEHP reaches concentrations below 1 µg m^{-3}. Nevertheless, reported residential dust concentrations of DEHP are considerably higher than the concentrations of the more volatile phthalates. The experiments in the 0.5 m^3 stainless-steel emission test chambers prove low dust concentrations of DEHP if no particles are present in the air. This finding was found to be independent on the organic carbon content of the adsorbing dust.

As a result of these experiments two principle pathways of DEHP-transfer into dust in the real indoor environment remain:

A) direct contamination of the dust sample (e.g. by abrasion of plasticizer- containing polymers or cleaning agents)

B) airborne particle-bound transport of DEHP from source into dust.

Both pathways are expected to be present in a real room but one will dominate the results if the dust concentration is determined. In the first case small amounts of the emitting source can have a vast influence on the analytical results. If no phthalate-containing polymer is present in the room the usage of cleaning agents may be also increase the dust concentration artificially (see Kolarik et al. (2008a)).

The experiments in the PMMA and PVC tube chambers forced the contact of strong adsorbing particles and a strong emission source of DEHP. As a result, the particles were loaded with the plasticizer and would establish an air/particle phase-

concentration above the maximum concentration of DEHP solely in the gas phase. Carbon particles are often present in the indoor environment due to formation indoors (e.g. candles, frying) or external entry (e.g. exhaust emissions). These particles are very mobile and stay in air depending on their particle size. Especially carbonaceous particles from different indoor sources are suitable for the transport of organic compounds indoors due to their strong sorption capacity. These micron- and submicron particles are known to deposit on furnishings (Thatcher, et al., 2002; Thatcher and Layton, 1995) and other rough surfaces (El Hamdani, et al., 2008). The particles improve the mass-transfer of the SVOC into the sink and, thus, the source of the detected plasticizers does not have to be near the place of sampling inevitably.

This study showed that the gas phase transfer of DEHP is not a main contamination pathway of indoor dust which complicates the assessment of measured dust concentration for exposure analysis. The different mentioned mass-transfer mechanisms from the emission source to available sinks are of high importance for the exposure analysis of phthalates. Airborne particles have a different depth of penetration in the human lung. If the diameter of the particles is larger than 3 µm they are deposited in the upper respiratory part while particles < 1 µm can penetrate nearly every cell type of the human respiratory tract (Marquardt and Schäfer, 1997). If the particles are in the range of 10 nm, most of them are exhaled immediately (Asgharian and Price, 2007) but particles from indoor sources in the range between 10 nm and 350 nm are considerably deposited in the human lung (Mitsakou, et al., 2007). In this case, the DEHP incorporation via the particle phase is possible. If DEHP is bound to settled dust the incorporation usually happens orally. Consequently, a difference regarding the bioavailability of DEHP is expected for these two pathways.

Appendix A – Determination of plasticizers using PTR-MS

In the following an experiment is described that tested the applicability of a proton-transfer-reaction-mass-spectrometer (PTR-MS) for the online determination of the concentration of plasticizers in air.

The PTR-MS uses a soft ionization technique to reduce fragmentation of the target compound and features a detection limit of ~ 5 ppt for some VOC (according to the manufacturer). The instrument is only able to measure compounds with a higher proton affinity than water which excludes the permanent gases (e.g. N_2, CO_2, Ar) from the analysis. Furthermore, alkanes, ethene, ethine, H_2S, and HCN are also not detectable. Oxygen is partly ionized depending on the ionization parameters. The technique and applications are described in detail by Lindinger et al. (1998).

The PTR-MS consist of four main parts: ion source, reaction chamber, mass filter, and detector. Within the ion source water is ionized at voltages between 50 and 500 V. The necessary ionization energy is 12.6 eV. This reaction yields also other ions like H_2^+, H^+, and O^+. Due to the reaction of ionized water with non-ionized water protonated water is formed.

$$H_2O + H_2O^+ \rightarrow H_3O^+ + OH$$

To increase the amount of available primary ions a reaction chamber follows the ion source. The voltage applied to this chamber (“drift voltage”) controls the grade of fragmentation. High impact energy increases compound fragmentation while low energy increases the amount of molecular clusters. The most common cluster is $H_2O*H_3O^+$ (m/z 37). The promotion of cluster formation can be used to soften the energy transfer to the target compound because the water cluster has a lower proton affinity (197 kcal mol^{-1}) than H_3O^+ (167 kcal mol^{-1}). After the reaction chamber the ions are filtered using a quadrupol mass filter. The detection is performed by a secondary electron amplifier. Usually, the measurement time for a certain mass is 100 ms. The concentration of the compound is calculated from the reference mass m/z 21. This reference is the isotopic water containing ^{18}O and ^{2}D.

The experiment was performed using a high-sensitivity proton-transfer-reaction-mass-spectrometer (hsPTR-MS) by Ionicon GmbH (Innsbruck, Austria). The inlet was heated to 120 ℃ to provide a fast transfer of the compound to the reaction chamber.

The spectra of the used compound were measured between 50 and 300 amu (200 ms amu^{-1}). The concentration vs. time measurements were also performed at 200 ms amu^{-1}.

Six phthalic acid esters (DBP, DEHP, DCHP, DIDP, DMP, DEP) were inserted into headspace vials and tempered in a water bath at 70°. After measurement of the laboratory background spectrum the inlet tube was attached to the vial. A second opening in the lid prevents assembling of a vacuum. After identification of m/z values that showed an increase in intensity, the concentration vs. time development was recorded for these masses. Objective of the experiment was the determination of specific m/z values for the analyzed compounds.

The normalized PTR-MS-spectra of the six compounds are displayed in Figure 33. Specific values for only one plasticizer were only detected for m/z with a low intensity (~ 1 cps). When validating these values using a time depending measurement only one obtained m/z could be verified. The small peaks in the spectra might result from contamination or fluctuations of the instrument.

The specific mass m/z 137 could be related to the presence of DMP, which is the most volatile phthalate in this experiment. The fragmentation pattern of plasticizers in the PTR-MS is not known momentarily. In the case of m/z 137 protonated methoxybenzaldehyde might be the measured fragment. This assumption cannot be assured. A contamination of the standard with a small amount of a volatile compound is also possible.

To reliably measure a compound in chamber air using the PTR-MS the used m/z has to be specific and high in intensity. Both conditions are not the case for the phthalic acid esters. Volatile phthalates like DMP are easy to detect using the PTR-MS while high-boiling compounds like DEP show huge delays between sampling and detection. This results from the tubing of the inlet that cannot be heated completely and might serve as a sink for high-boiling compounds. For VOC this design issue is not of importance due to the small surface area and high air flow. In the case of SVOC such a sink reduces the low air concentration even more which increases the limit of detection. Additionally, if a strong SVOC source is present the compound contaminates the system and disturbs the following measurements. For example DEP could be detected for the following 2 hours after removing the heated flask.

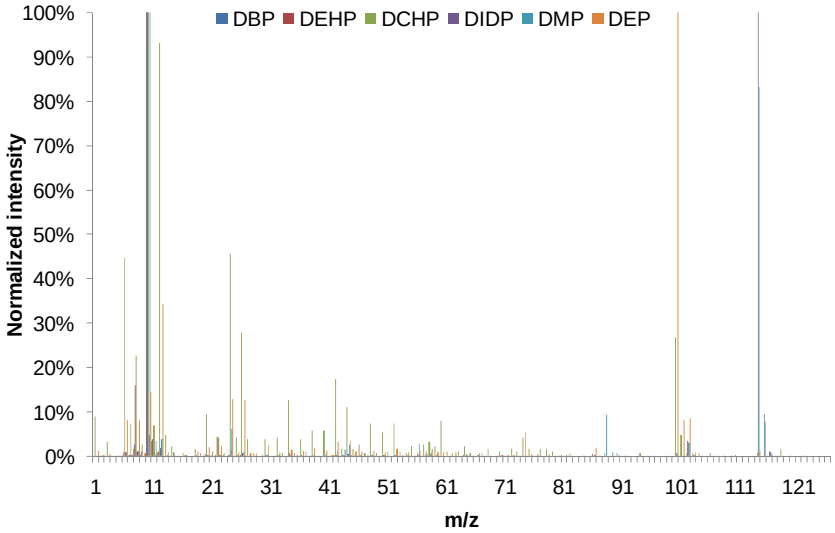

Figure 33: Comparison of PTR-MS spectra of 6 different phthalates

Basing on the presented results the PTR-MS online measurement technique is not feasible for the reliable and specific measurement of phthalates in air without prior modifications on the system. If the fragmentation pattern of phthalates under the given conditions is known and the inlet system has been modified using higher temperatures this instrument might be able to measure these compounds in the future. However, actual results showed that the artifact-free analysis of a limited amount of volatile compounds in chamber air is complicated by the fragmentation of the compounds and the overlap of fragmentation spectra (Schripp, et al., 2009). This effect is expected to hinder the analysis of plasticizers in a mixture of several compounds in air due to the low concentration of the target compound.

References

Adibi, J. J.,Perera, F. P.,Jedrychowski, W.,Camann, D. E.,Barr, D.,Jacek, R.,Whyatt, R. M., 2003. Prenatal Exposure to Phthalates among Women in New York City and Krakow, Poland. Environmental Health Perspectives 111, 1719-1722.

Afshari, A.,Gunnarsen, L.,Clausen, P. A.,Hansen, V., 2004. Emission of phthalates from PVC and other materials. Indoor Air 14, 120-128.

Asgharian, B.,Price, T. O., 2007. Deposition of Ultrafine (NANO) Particles in the Human Lung. Inhalation Toxicology 19, 1045-1054.

ATSDR, 2002. Toxicological Profile for di(2-ethylhexyl)phthalate.

Austen, I., 2008. Bottle Maker to Stop Using Plastic Linked to Health Concerns. The New York Times.

Axley, J. W., 1991. Adsorption Modelling for Building Contaminant Dispersal Analysis. Indoor Air 1, 147-171.

Baerns, M.,Behr, A.,Brehm, A.,Gmehling, J.,Hofmann, H.,Onken, U., 2006. Technische Chemie, Wiley-VCH, Weinheim.

BASF, 2005. Technisches Merkblatt M 6117 d, Petrochemikalien, Palatinol® 11P-E (DUP). 1-4.

BASF, 2007. Technisches Merkblatt M 2204 d, Petrochemikalien, Palatinol® IC. 1-4.

Becker, K.,Seiwert, M.,Angerer, J.,Heger, W.,Koch, H. M.,Nagorka, R.,Rokamp, E.,Schluter, C.,Seifert, B.,Ullrich, D., 2004. DEHP metabolites in urine of children and DEHP in house dust. International Journal of Hygiene and Environmental Health 207, 409-417.

Becker, K.,Seiwert, M.,Kaus, S.,Krause, C.,Schulz, C.,Seifert, B., 2002. German Environmental Survey 1998 (GERES III): Pesticides and other pollutants in house dust. Proceedings of the 9th International International Conference on Indoor Air Quality and Climate, Monterey, CA, 4, 883-887.

Begley, T.,Castle, L.,Feigenbaum, A.,Franz, R.,Hinrichs, K.,Lickly, T.,Mercea, P.,Milana, M.,O'Brien, A.,Rebre, S.,Rijk, R.,Piringer, O., 2005. Evaluation of migration models that might be used in support of regulations for food-contact plastics. Food Additives and Contaminants 22, 73 - 90.

Beratung und Analyse Verein für Umweltchemie, 1992. Analyse und Bewertung der in Raumluft und Hausstaub vorhandenen Konzentrationen der Weichmacherbestandteile Diethylhexylphthalat (DEHP) und Dibutylphthalat (DBP). Sachbericht B.A.U.C.H.

Bornehag, C. G.,Lundgren, B.,Weschler, C. J.,Sigsgaard, T.,Hagerhed-Engman, L.,Sundell, J., 2005. Phthalates in Indoor Dust and Their Association with Building Characteristics. Environmental Health Perspectives 113, 1399-1404.

Bornehag, C. G.,Sundell, J.,Weschler, C. J.,Sigsgaard, T.,Lundgren, B.,Hasselgren, M.,Hägerhed-Engman, L., 2004. The Association between Asthma and Allergic Symptoms in Children and Phthalates in House Dust: A Nested Case-Control Study. Environmental Health Perspectives 112, 1393-1397.

Brandsch, J.,Mercea, P.,Rüter, M.,Tosa, V.,Piringer, O., 2002. Migration modelling as a tool for quality assurance of food packaging. Food Additives and Contaminants 19, 29 - 41.

Brasche, S.,Bischof, W., 2005. Daily time spent indoors in German homes - Baseline data for the assessment of indoor exposure of German occupants. International Journal of Hygiene and Environmental Health 208, 247-253.

Bundesinstitut für Risikobewertung, 2003. Stellungnahme des BFR - Diisooctylphthalat in Ohrstöpseln.

Butte, W.,Heinzow, B., 2002. Pollutants in house dust as indicators of indoor contamination, in: Whitacre, D. M. (Eds.), Reviews of Environmental Contamination and Toxicology, Springer, 1-46.

Butte, W.,Hostrup, O.,Walker, G., 2008. Phthalate im Hausstaub und in der Luft: Assoziationen und mögliche Quellen in Wohnräumen. Gefahrstoffe - Reinhaltung der Luft 68, 79-81.

Butte, W.,Schenke, H.,Heinzow, B., 2006. Herbizide im Hausstaub. Proben aus Anrainerwohnungen von Baumschulen im Vergleich zu Kontrollen. Gefahrstoffe - Reinhaltung der Luft 66, 112-115.

Butte, W.,W., H.,Hostrup, O.,Schmidt, A.,Walker, G., 2001. Endocrine disrupting chemicals in house dust: results of a representative monitoring. Gefahrstoffe - Reinhaltung der Luft 61, 19-23.

Butte, W.,Walker, G., 1994. Sinn und Unsinn von Hausstaubuntersuchungen - das Für und Wider. Hausstaub als Messparameter zum Erkennen einer Innenraumbelastung mit Permethrin, Pentachlorphenol und Lindan. VDI-Bericht 1122, 535-546.

Cadogan, D. F.,Howick, C. J., 1996. Plasticisers, in: Kirk, R. E.; Othmer, D. F. (Eds.), Kirk-Othmer encyclopedia of chemical technology (4th Ed.), Wiley-VCH, New York,

Cammenga, H., 1967. Untersuchung über die Verdampfungsgeschwindigkeit von Flüssigkeiten und Festkörpern im Bereich kleiner Dampfdrücke, Technische Universität Braunschweig, PhD thesis,

Clark, K.,Cousins, I. T.,Mackay, D., 2003a. Assessement of Critical Exposure Pathways, in: Staples, C. A. (Eds.), The Handbook of Environmental Chemistry Vol. 3 Part Q, Springer Verlag, Berlin, Heidelberg,

Clark, K.,Cousins, I. T.,Mackay, D.,Yamada, K., 2003b. Observed Concentrations in the Environment, in: Staples, C. A. (Eds.), The Handbook of Environmental Chemistry Vol. 3, Part Q, Springer Verlag, Berlin, Heidelberg, 125-177.

Clausen, P.,Hansen, V.,Gunnarsen, L.,Afshari, A.,Wolkoff, P., 2002. Emission of Phthalates from PVC flooring in two very different test chambers. Proceedings of the 9th International Conference on Indoor Air Quality and Climate, Monterey, California, 2, 932-937.

Clausen, P. A.,Hansen, V.,Gunnarsen, L.,Afshari, A.,Wolkoff, P., 2004. Emission of Di-2-ethylhexylphthalate from PVC Flooring into Air and Uptake in Dust: Emission and Sorption Experiments in FLEC and CLIMPAQ. Environmental Science and Technology 38, 2531-2537.

Cousins, I. T.,Mackay, D., 2000. Correlating the physical-chemical properties of phthalate esters using the "three solubility" approach. Chemosphere 41, 1389-1399.

Cousins, I. T.,Mackay, D.,Parkerton, T. F., 2002. Physical-Chemical Properties and Evaluative Fate Modelling of Phthalate Esters, in: (Eds.), The Handbook of Environmental Chemistry Vol. 3 Part Q, Springer Verlag, Berlin, Heidelberg, 57-84.

Crank, J., 1975. The Mathematics of Diffusion, 2nd ed., Oxford University Press, Oxford, New York.

Danish Standard, 1994. Direction for determination and evaluation of the emission from building products. Dansk Standard, DS/INF 90, 1-38.

Deng, B.,Kim, C. N., 2004. An analytical model for VOCs emission from dry building materials. Atmospheric Environment 38, 1173-1180.

DIN 75201, 1992. Bestimmung des Foggingverhaltens von Werkstoffen der Kraftfahrzeug-Innenausstattung, Beuth Verlag, City.

Dobbs, A. J.,Cull, M. R., 1982. Volatilisation of chemicals - relative loss rates and the estimation of vapour pressures. Environmental Pollution 3, 289-298.

Dobbs, A. J.,Hart, G. F.,Parsons, A. H., 1984. The determination of vapour pressures from relative volatilization rates. Chemosphere 13, 687-692.

Dunn, J. E., 1987. Models and statistical methods for gaseous emission testing of finite sources in well-mixed chambers. Atmospheric Environment (1967) 21, 425-430.

Dunn, J. E.,Tichenor, B. A., 1988. Compensating for sink effects in emissions test chambers by mathematical modeling. Atmospheric Environment (1967) 22, 885-894.

El Hamdani, S.,Limam, K.,Abadie, M. O.,Bendou, A., 2008. Deposition of fine particles on building internal surfaces. Atmospheric Environment 42, 8893-8901.

Endo, S.,Grathwohl, P.,Schmidt, T. C., 2008. Absorption or Adsorption? Insights from Molecular Probes n-Alkanes and Cycloalkanes into Modes of Sorption by Environmental Solid Matrices. Environmental Science and Technology 42, 3989-3995.

EPA, 1993. Integrated Risk Information System (IRIS) on Di(2-ethylhexylphthalate.

European Commission, 2003. European Union Risk Assessment Report 1,2-benzenedicarboxylic acid, di-C8-10-branched alkyl esters, C9-rich and di-“isononyl” phthalate (DINP). 35.

Frissel, W. J., 1955. Volatility of vinyl plasticisers. Industrial & Engineering Chemistry Research 18, 1096-1099.

Fromme, H.,Lahrz, T.,Piloty, M.,Gebhart, H.,Oddoy, A.,Ruden, H., 2004. Occurrence of phthalates and musk fragrances in indoor air and dust from apartments and kindergartens in Berlin (Germany). Indoor Air 14, 188-195.

Fuller, E.,Schettler, P.,Giddings, J. C., 1966. New Method for Prediction of Binary Gas-Phase Diffusion Coefficients. Industrial & Engineering Chemistry Research 58, 18-27.

Glückel, W.,Kästel, R.,Lewerenz, J.,Synnatschke, G., 1982. A method for determining the volatility of active ingredients used in plant protection Part III: The temperature relationship between vapour pressure and evaporation rate. Pesticide Science 13, 161-168.

Greubel, D.,Herlyn, J. W.,Meinlschmid, P., 2001. Application and limits of weathering simulation for the maintenance of monuments. Internationale Zeitschrift für Bauinstandsetzen und Baudenkmalpflege 7, 655-674.

Hansen, D.,Volland, G.,Krause, G.,Zöltzer, D., 2001. Bestimmung und Vorkommen von phosphor-organischen Verbindungen in Hausstaub und Raumluft. Gefahrstoffe - Reinhaltung der Luft 61, 13-17.

Harnisch, M.,Möckel, H. J.,Schulze, G., 1983. Relationship between Log Pow shake-flask values and capacity factors derived from reversed phase high-perfomance liquid chromatography for n-alkylbenzenes and some OECD reference substances. Journal of Chromatography 282, 315-332.

Hauser, R.,Duty, S.,Godfrey-Bailey, L.,Calafat, A. M., 2004. Medications as a source of human exposure to phthalates. Environmental Health Perspectives 112, 751-753.

Heudorf, U., 2008. Phthalate und Kindergesundheit. Umweltmedizin in Forschung und Praxis 13, 358-372.

Heudorf, U.,Mersch-Sundermann, V.,Angerer, J., 2007. Phthalates: Toxicology and exposure. International Journal of Hygiene and Environmental Health 210, 623-634.

Hinckley, D. A.,Bidleman, T. F.,Foreman, W. T., 1990. Determination of Vapor Pressures for Nonpolar and Semipolar Organic Compounds from Gas Chromatographic Retention Data. Journal of Chemical Engineering Data 35, 232-237.

Hinrichs, K.,Piringer, O., 2002. Evaluation of migration models to used under Directive 90/128/EEC - Final report contract SMT4-CT98-7513. Report-EUR 20604EN.

Howard, P. H.,Banerjee, S.,Robillard, K. H., 1985. Measurement of water solubilities octanol/water partition coefficients and vapour pressures of commercial phthalate esters. Environmental Toxicology and Chemistry 4, 653-661.

Huang, H.,Haghighat, F., 2002. Modelling of volatile organic compounds emission from dry building materials. Building and Environment 37, 1349-1360.

ISO 16000-9, 2006. Indoor Air - Part 9: Determination of the emission of volatile organic compounds from building products and furnishing - Emission test chamber method, Beuth Verlag, City.

Jamriska, M.,Uhde, E., 2003. Particle collection efficiency of sorbent tubes. Proceedings of Healthy Buildings, Singapore, 2, 129-133.

Kersten, W.,Reich, T., 2003. Schwer flüchtige organische Umweltchemikalien in Hamburger Hausstäuben. Gefahrstoffe - Reinhaltung der Luft 63, 85-91.

Knudsen, M., 1909. Die Molekularströmung der Gase durch Öffnungen und die Effusion. Annalen der Physik 333, 999-1016.

Kolarik, B.,Bornehag, C.-G.,Naydenov, K.,Sundell, J.,Stavova, P.,Nielsen, O. F., 2008a. The concentrations of phthalates in settled dust in Bulgarian homes in relation to building characteristic and cleaning habits in the family. Atmospheric Environment 42, 8553-8559.

Kolarik, B.,Naydenov, K.,Larsson, M.,Bornehag, C. G.,Sundell, J., 2008b. The Association between Phthalates in Dust and Allergic Diseases among Bulgarian Children. Environmental Health Perspectives 116, 98-103.

Korhonen, P.,Kulmala, M.,Laaksonen, A.,Viisanen, Y.,McGraw, R.,Seinfeld, J. H., 1999. Ternary nucleation of H2SO4, NH3 and H2O in the atmosphere. Journal of Geophysical Research 104, 349-353.

Kulmala, M.,Dal Maso, M.,Mäkelä, J. M.,Pirjola, L.,Väkevä, M.,Aalto, P.,Miikkulainen, P.,Hämeri, K.,O'Dowd, C. D., 2001. On the formation, growth and composition of nucleation mode particles. Tellus Series B: Chemical and Physical Meteorology 53, 479-490.

Kumar, D.,Little, J. C., 2003. Single-Layer Model To Predict the Source/Sink Behavior of Diffusion-Controlled Building Materials. Environmental Science and Technology 37, 3821-3827.

Latini, G.,Vecchio, A. D.,Massaro, M.,Verrotti, A.,Felice, C. D., 2006. Phthalate exposure and male infertility (Review). Toxicology 226, 90-98.

Le, H. H.,Carlson, E. M.,Chua, J. P.,Belcher, S. M., 2008. Bisphenol A is released from polycarbonate drinking bottles and mimics the neurotoxic actions of estrogen in developing cerebellar neurons. Toxicology Letters 176, 149-156.

Liang, C.,Pankow, J. F.,Odum, J. R.,Seinfeld, J. H., 1997. Gas/Particle Partitioning of Semivolatile Organic Compounds To Model Inorganic, Organic, and Ambient Smog Aerosols. Environmental Science and Technology 31, 3086-3092.

Lide, D. R., 2007. Handbook of Chemistry and Physics, 88th Ed., CRC, New York.

Lindinger, W.,Hansel, A.,Jordan, A., 1998. On-line monitoring of volatile organic compounds at pptv levels by means of proton-transfer-reaction mass spectrometry (PTR-MS) medical applications, food control and environmental research. International Journal of Mass Spectrometry and Ion Processes 173, 191-241.

Little, J. C.,Hodgson, A. T.,Gadgil, A. J., 1994. Modeling emissions of volatile organic compounds from new carpets. Atmospheric Environment 28, 227-234.

Little, J. C.,Kumar, D.,Cox, S. S.,Hodgson, A. T., 2002. Barrier materials to reduce contaminant emissions from structural insulated panels. Proceedings of International Conference on Advances in Building Technology, Hong Kong, China, 113-120.

Little, J. C.,Xu, Y.,Hubal, E. C.,Clausen, P. A., 2008. Exposure to phthalate emitted from vinyl flooring and sorbed to interior surfaces, dust, airborne particles and human skin. Proceedings of the 11th International Conference on Indoor Air Quality and Climate, Copenhagen,

Lorz, P. M.,Towae, F. K.,Enke, W.,Jäckh, R.,Bhargava, N., 2002. Phthalic Acids and Derivatives, in: Pelc, H. (Eds.), Ullmann's Encyclopedia of Industrial Chemistry, Wiley-VCH, Weinheim,

Lugg, G. A., 1968. Diffusion coefficients of some organic and other vapors in air. Analytical Chemistry 40, 1072-1077.

Lyman, W. J.,Reehl, W. F.,Rosenblatt, D. H., 1982. Handbook of chemical properties estimation methods - Environmental behavior of organic compounds, McGraw-Hill Book Company, New York.

Marquardt, H.,Schäfer, S. G., 1997. Lehrbuch der Toxikologie, Spektrum Akademischer Verlag, Berlin.

Martin, N. A.,Barber, N. L. A. S.,Black, J. K.,Lipscombe, R. P.,Taig, C. A., 2007. A comparison of gas- and liquid-loaded sorbent standards for the calibration of measurements of volatile organic compounds. Atmospheric Environment 41, 7666-7671.

Massold, E., 2002. Determination of volatile organic compounds in air by GC/MS - Method development and validation. PhD.

Mehrer, H., 2005. Diffusion: Introduction and Case Studies in Metals and Binary Alloys, in: Heitjans, P.; Kärger, J. (Eds.), Diffusion in condensed matter: methods, materials, models, Springer, Berlin, New York, 3-65.

Mercea, P., 2000. Models for diffusion in polymers, in: Piringer, O.; Baner, A. L. (Eds.), Plastic Packaging Materials for Food : Barrier Function, Mass Transport, Quality Assurance, and Legislation, Wiley-VCH, Weinheim, New York, 125-157.

Mitsakou, C.,Housiadas, C.,Eleftheriadis, K.,Vratolis, S.,Helmis, C.,Asimakopoulos, D., 2007. Lung deposition of fine and ultrafine particles outdoors and indoors during a cooking event and a no acitivity period. Indoor Air 17, 143-152.

Möhlmann, C., 2005. Staubmesstechnik - damals bis heute. Gefahrstoffe - Reinhaltung der Luft 65, 191-194.

National Libary of Medicine ChemIDplus Advanced, 1981. OECD Guidelines for Testing of Chemicals, Partition coefficient (n-octanol-water) flask shaking method, Section 107.

Niederer, C.,Goss, K. U.,Schwarzenbach, R. P., 2006. Sorption Equilibrium of a Wide Spectrum of Organic Vapors in Leonardite Humic Acid: Modeling of Experimental Data. Environmental Science and Technology 40, 5374-5379.

O'Brien, A.,Cooper, I., 2001. Polymer additive migration to foods-a direct comparison of experimental data and values calculated from migration models for polypropylene. Food Additives and Contaminants 18, 343 - 355.

Official Journal of the European Communities, 2002. Commision Directive 2002/72/EC - relating to plastic materials and articles intended to come into contact with foodstuffs, City.

Otake, T.,Yoshinaga, J.,Yanagisawa, Y., 2001. Analysis of Organic Esters of Plasticiser in Indoor Air by GC-MS and GC-FPD. Environmental Science and Technology 35, 3099-3102.

Pankow, J. F., 1994. An absorption model of gas/particle partitioning of organic compounds in the atmosphere. Atmospheric Environment 28, 185-188.

Piringer, O., 2000a. Prediction of diffusion coefficients in gases, liquids, amorphous solids and plastic materials using an uniform model, in: Piringer, O.; Baner, A. L. (Eds.), Plastic Packaging Materials for Food : Barrier Function, Mass Transport, Quality Assurance, and Legislation, Wiley-VCH, Weinheim, New York, 159-181.

Piringer, O., 2000b. Transport equations and their solutions, in: Piringer, O.; Baner, A. L. (Eds.), Plastic Packaging Materials for Food : Barrier Function, Mass Transport, Quality Assurance, and Legislation, Wiley-VCH, Weinheim, New York, 183-219.

Piringer, O. G.,Baner, A. L., 2000. Plastic Packaging Materials for Food : Barrier Function, Mass Transport, Quality Assurance, and Legislation, Wiley-VCH, Weinheim, New York.

Qian, K.,Zhang, Y.,Little, J. C.,Wang, X., 2007. Dimensionless correlations to predict VOC emissions from dry building materials. Atmospheric Environment 41, 352-359.

Quackenbos jr, H. M., 1954. Plasticisers in vinyl chloride resins. Industrial & Engineering Chemistry Research 46, 1335-1349.

Ritter, E. J.,Scott, W. J. J. R., J.L.,Ritter, J. M., 1987. Teratogenicity of di(2-ethylhexyl)phthalate, 2-ethylhexanol, 2-ethylhexanoic acid, and valproic acid, and potentiation by caffeine. Teratology 35, 41-46.

Rohac, V.,Musgrove, J. E.,Ruzicka, K.,Ruzicka, V.,Zabransky, M.,Aim, K., 1999. Thermodynamic properties of dimethyl phthalate along the (vapour + liquid) saturation curve. Journal of Chemical Thermodynamics 31, 971-986.

Rohac, V.,Ruzicka, K.,Ruzicka, V.,Zaitsau, D. H.,Kabo, G. J.,Diky, V.,Aim, K., 2004. Vapour pressure of diethyl phthalate. Journal of Chemical Thermodynamics 36, 929-937.

Roth, C. M.,Goss, K. U.,Schwarzenbach, R. P., 2005a. Sorption of a Diverse Set of Organic Vapors To Diesel Soot and Road Tunnel Aerosols. Environmental Science and Technology 39, 6632-6637.

Roth, C. M.,Goss, K. U.,Schwarzenbach, R. P., 2005b. Sorption of a Diverse Set of Organic Vapors To Urban Aerosols. Environmental Science and Technology 39, 6638-6643.

Rudel, R. A.,Camman, D. E.,Spengler, J. D.,Korn, L. R.,Brody, J. D., 2003. Phthalates, Alkylphenols, Pesticides, Polybrominated Diphenyl Ethers, and Other Endocrine-Disrupting Compounds in Indoor Air and Dust. Environmental Science and Technology 37, 4543-4553.

Růžička, K.,Roháč, V.,Fulem, M.,Růžička, V.,Zaitsau, D. H.,Kabo, G. J.,Diky, V.,Aim, K., 2004. Vapour pressure of diethyl phthalate. Journal of Chemical Thermodynamics 36, 929-937.

Salthammer, T.,Fuhrmann, F.,Kaufhold, S.,Meyer, B.,Schwarz, A., 1995. Effects of Climatic Parameters on Formaldehyde Concentrations in Indoor Air. Indoor Air 5, 120-128.

Salthammer, T.,Meinlschmid, P.,Schripp, T.,Fauck, C., 2007. Final Report of UBA Research Project: Investigation of interaction of formation mechanisms of the BMD phenomenon via emission chamber tests.

Sander, R., 1999. Compilation of Henry's Law Constants for Inorganic and Organic Species of Potential Importance in Environmental Chemistry, Version 3.

Santos, Emília M. G.,Araújo, Alberto N.,Couto, Cristina M. C. M. M.,Montenegro, Conceição B. S. M., 2005. Use of Tin (IV) Porhyrins as Ionophores for the Construction of Phthalate-Selective Electrodes: Influence of the Structure and Membrane Composition on their Response Properties. Electroanalysis 17, 1945-1951.

Schripp, T.,Fauck, C.,Markewitz, D.,Salthammer, T., 2009. Application of the PTR-MS for the emission test of building products. Proceedings of the 4th International Conference on Proton Transfer Reaction Mass Spectrometry and its Applications, Obergurgl, Austria, 1, 284-288.

Schripp, T.,Nachtwey, B.,Toelke, J.,Salthammer, T.,Uhde, E.,Wensing, M.,Bahadir, M., 2007. A microscale device for measuring emissions from materials for indoor use. Analytical and Bioanalytical Chemistry 387, 1907-1919.

Sigma-Aldrich, 2007. Aldrich Katalog 2007/2008.

Sparks, L. E.,Tichenor, B. A.,Chang, J.,Guo, Z., 1996. Gas-Phase Mass Transfer Model for Predicting Volatile Organic Compound (VOC) Emission Rates from Indoor Pollutant Sources. Indoor Air 6, 31-40.

Staples, C. A.,Peterson, D. R.,Parkerton, T. F.,Adams, W. J., 1997. The Environmental Fate of Phthalate Esters: A Literature Review. Chemosphere 35, 667-749.

Stoffers, N. H.,Brandsch, R.,Bradley, E. L.,Cooper, I.,Dekker, M.,Störmer, A.,Franz, R., 2005. Feasibility study for the development of certified reference materials for specific migration testing. Part 2: Estimation of diffusion parameters and comparison of experimental and predicted data. Food Additives & Contaminants 22, 173 - 184.

Stoffers, N. H.,Störmer, A.,Bradley, E. L.,Brandsch, R.,Cooper, I.,Linssen, J. P. H.,Franz, R., 2004. Feasibility study for the development of certified reference materials for specific migration testing. Part 1: Initial migrant concentration and specific migration. Food Additives & Contaminants 21, 1203 - 1216.

Swan, S. H.,Main, K. M.,Liu, F.,Stewart, S. L.,Kruse, R. L.,Calafat, A. M.,Mao, C. S.,Redmon, J. B.,Ternand, C. L.,Sullivan, S.,Teague, J. L.,The Study for Future Families Research Team, 2005. Decrease in Anogenital Distance among Male Infants with Prenatal Phthalate Exposure. Environmental Health Perspectives 113, 1056-1061.

Teil, M. J.,Blanchard, M.,Chevreuil, M., 2006. Atmospheric fate of phthalate esters in an urban area (Paris-France). Science of The Total Environment 354, 212-223.

Thatcher, T. L.,Lai, A. C. K.,Moreno-Jackson, R.,Sextro, R. G.,Nazaroff, W. W., 2002. Effects of room furnishings and air speed on particle deposition rates indoors. Atmospheric Environment 36, 1811-1819.

Thatcher, T. L.,Layton, D. W., 1995. Deposition, resuspension, and penetration of particles within a residence. Atmospheric Environment 29, 1487-1497.

Thio, A. P.,Kornet, M. J.,Ali, K.,Tompkins, D. H., 1988. In-Block Derivatization of Herbicidal Carboxylic Acids by Pentafluorobenzyl Bromide. Analytical Letters 21, 477 - 489.

Tichenor, B. A.,Guo, Z.,Dunn, J. E.,Sparks, L. E.,Mason, M. A., 1991. The Interaction of Vapour Phase Organic Compounds with Indoor Sinks. Indoor Air 1, 23-35.

Uhde, E.,Bednarek, M.,Fuhrmann, F.,Salthammer, T., 2001. Phthalic Esters in the Indoor Environment - Test Chamber Studies on PVC-Coated Wallcoverings. Indoor Air 11, 150-155.

VDI, 2001. Messen von Innenraumluftverunreinigungen - Probenahme von Hausstaub, Beuth Verlag, City.

VDI, 2007. Measurement of indoor air pollution - Measurement of flame retardants and plasticizers based on phosphor organic compounds - Phosphoric acid ester, Beuth Verlag, City.

Walker, G.,Hostrup, O.,Hoffmann, W.,Butte, W., 1999. Biozide im Hausstaub. Ergebnisse eines repräsentativen Monitorings in Innenräumen. Gefahrstoffe - Reinhaltung der Luft 59, 33-41.

Werner, A. C., 1952. Vapor pressures of phthalate esters. Industrial & Engineering Chemistry Research 44, 2736-2740.

Weschler, C. J.,Nazaroff, W. W., 2008. Semivolatile organic compounds in indoor environments. Atmospheric Environment 42, 9018-9040.

Weschler, C. J.,Salthammer, T.,Fromme, H., 2008. Partitioning of phthalates among the gas phase, airborne particles and settled dust in indoor environments. Atmospheric Environment 42, 1449-1460.

White, F. M., 1988. Heat and Mass Transfer, Addison-Wesley, Reading (MA).

WHO, 1989. Indoor Air Quality: Organic Pollutants.

Wormuth, M.,Scheringer, M.,Vollenweider, M.,Hungerbühler, K., 2006. What are the Sources of Exposure to Eight Frequently Used Phthalic Acid Esters in Europeans? Risk Analysis 26, 803-824.

Xu, Y.,Hubal, E. C.,Clausen, P. A.,Little, J. C., 2009a. Prediciting Residential Exposure to Phthalate Plasticizer Emitted from Vinyl Flooring: A Mechanistic Analysis. Environmental Science and Technology 43, 2374-2380.

Xu, Y.,Hubal, E. C.,Little, J. C., 2009b. Predicting Residential Exposure to Phthalate Plasticizer Emitted from Vinyl Flooring - Sensitivity, Uncertainty, and Implications for Biomonitoring. Environmental Health Perspectives submitted for publication.

Xu, Y.,Little, J. C., 2006. Predicting Emissions of SVOCs from Polymeric Materials and Their Interaction with Airborne Particles. Environmental Science and Technology 40, 456-461.

Xu, Y.,Park, J.,Clausen, P. A.,Kofoed-Sorensen, V.,Little, J. C., 2008. Characterizing emissions of phthalate plasticizer from vinyl flooring in a specially-designed chamber. Proceedings of the 11th International Conference on Indoor Air Quality and Climate, Copenhagen, Paper ID 688.

Xu, Y.,Zhang, Y., 2003. An improved mass transfer based model for analyzing VOC emissions from building materials. Atmospheric Environment 37, 2497-2505.

Yang, X.,Chen, Q.,Zhang, J. S.,An, Y.,Zeng, J.,Shaw, C. Y., 2001. A mass transfer model for simulating VOC sorption on building materials. Atmospheric Environment 35, 1291-1299.

Zhang, L. Z.,Niu, J. L., 2003. Laminar fluid flow and mass transfer in a standard field and laboratory emission cell. International Journal of Heat and Mass Transfer 46, 91-100.

Lebenslauf

Name	Tobias Schripp	
Geburtsname	Tobias Grzyb	
Geburtsdatum	28.01.1980	
Geburtsort	Braunschweig	
Staatsangehörigkeit	Deutsch	
Familienstand	Ledig	
Anschrift	Joseph-Fraunhofer-Straße 6B 38104 Braunschweig Tel. 0531/8789237	
Schulbildung	1986 – 1990	Grundschule
	1990 – 1992	Orientierungsstufe
	1992 – 1996	Realschule
	1996 – 1999	Gymnasium
Hochschulstudium	2000 – 2003	Chemiestudium an der Technischen Universität Carolo-Wilhemina, Braunschweig (Bachelor of Science)
	2003 – 2005	Aufbaustudium an der Technischen Universität Carolo-Wilhelmina, Braunschweig (Master of Science)
	2006 – 2009	Promotionsstudium an der Technischen Universität Carolo-Wilhelmina, Braunschweig
Berufliche Tätigkeit	1999 – 2000	Anstellung am Herzogin-Elisabeth-Hospital, Braunschweig (Zivildienst)
	2004	Anstellung als Hilfswissenschaftler am Institut für Ökologische Chemie und Abfallanalytik (TU Braunschweig)
	2005 – 2009	Anstellung als Hilfswissenschaftler am Fraunhofer Wilhelm-Klauditz-Institut im Fachbereich Materialanalytik und Innenluftchemie
	Seit März 09	Anstellung als Wissenschaftlicher Mitarbeiter am Fraunhofer Wilhelm-Klauditz-Institut im Fachbereich Materialanalytik und Innenluftchemie

Tagungsbeiträge

Schripp T, Uhde E, Wensing M, Salthammer T. Comparison of a quick analytical method to test chamber measurements : Emission of plastic samples. Healthy Buildings. 4, Lisbon, 2006, pp. 23-28.

Hughes P, Schripp T, Wensing M, Woolfenden E. Recent advances in materials emission testing chamber technology. Healthy Buildings. 4, Lisbon, 2006, pp. 13-17.

Wensing M, Pinz G, Bednarek M, Schripp T, Uhde E, Salthammer T. Particle measurement of hardcopy devices. Healthy Buildings. 2, Lisbon, 2006, pp. 461-464.

Schripp T, Salthammer T. Distribution of semi volatile organic compounds in the indoor environment, The 17th Annual Conference of the International Society of Exposure Analysis. Durham, NC., 2007.

Salthammer T, Wensing M, Schripp T, Uhde E, Characterization of Ultra Fine Particles Emissions from Hardcopy Devices, The 17th Annual Conference of the International Society of Exposure Analysis. Durham, NC., 2007.

Schripp T., Mulakampilly S., Wensing M., Kreuzig R., Salthammer T.,Bahadir M. (2008) Comparison of ultra-fine particle release from active hardcopy devices in an emission test chamber and an office room. In: Proceedings of the 11th International Conference on Indoor Air Quality and Climate, Copenhagen, Paper ID 57.

Schripp T., Salthammer T., Clausen P. A.,Little J. C. (2008) Gas-particle partitioning of plasticizers in emission test chambers with minimized sink effect. In: Proceedings of the 11th International Conference on Indoor Air Quality and Climate, Copenhagen, Paper ID 76.

Schripp T., Fauck C., Meinlschmidt P., Wensing M., Moriske H. J.,Salthammer T. (2008) Relationship between indoor air particle pollution and the phenomenon of “Black Magic Dust” in housings. In: Proceedings of the 11th International Conference on Indoor Air Quality and Climate, Copenhagen, Paper ID 122.

Wensing M., Schripp T., Delius W., Uhde E.,Salthammer T. (2008) Ultra-fine particle release from hardcopy devices: influence of different parameters, sources, characterization and efficiency of filter accessories. In: Proceedings of the 11th International Conference on Indoor Air Quality and Climate, Copenhagen, Paper ID 179.

Schripp T., Fauck C., Markewitz D.,Salthammer T. (2009) Application of the PTR-MS for the emission test of building products. In: Proceedings of the 4th International Conference on Proton Transfer Reaction Mass Spectrometry and its Applications, Obergurgl, Austria, Vol.1, 284-288.

Veröffentlichungen

Scherer C., Schmohl A., Breuer K., Sedlbauer K., Salthammer T., Schripp T., Uhde E.,Wensing M. (2006) Practical experience with thermal extraction as quick measurement method for emission testing of building products and polymer materials. Gefahrstoffe - Reinhaltung der Luft, 66(3), 87-93.

Hughes P., Salthammer T., Schripp T., Wensing M.,Woolfenden E. (2007) Micro-chamber thermal extractor - the latest cost effective solution for rapid materials emissions testing. Journal of Harbin Institute of Technology, 14, 259-262.

Schripp T., Nachtwey B., Toelke J., Salthammer T., Uhde E., Wensing M.,Bahadir M. (2007) A microscale device for measuring emissions from materials for indoor use. Analytical and Bioanalytical Chemistry, 387(5), 1907-1919.

Schripp T., Wensing M., Uhde E., Salthammer T., He C.,Morawska L. (2008) Evaluation of Ultrafine Particle Emissions from Laser Printers Using Emission Test Chambers. Environmental Science and Technology, 42(12), 4338-4343.

Schripp T., Mulakampilly S., Delius W., Uhde E., Wensing M., Salthammer T., Kreuzig R., Bahadir M., Wang L.,Morawska L. (2009) Comparison of ultrafine particle release from hardcopy devices in emission test chambers and office rooms. Gefahrstoffe - Reinhaltung der Luft, 69(3), 71-76.

Wensing M., Schripp T., Uhde E.,Salthammer T. (2008) Ultra-fine Particles Release from Hardcopy Devices: Sources, Real room measurements and Efficiency of Filter Accessories. Science of the Total Environment, 15(1), 418-427.